SEISMIC SHEAR AMPLIFICATION IN STRUCTURAL WALLS

by

Emre Düzgün

B.S., Civil Engineering, Dokuz Eylül University, 2006

Submitted to the Kandilli Observatory and Earthquake Research Institute
for Graduate Studies in Earthquake Engineering in partial fulfillment of
the requirements for degree of
Master of Science

Graduate Program in Earthquake Engineering
Boğaziçi University
2009

ACKNOWLEDGEMENTS

First of all, I would like to express my sincere gratitude to my advisor Professor Nuray Aydınoğlu for honoring me by giving the chance to work with him. Working with such a great engineer and scientist provided me gaining such a discipline in many ways.

I would like to express my special thanks to Dr. Cüneyt Tüzün, Dr. Utku Celep and Dr. Göktürk Önem for helping me all the time during study and treating me as a brother. At this point I should express my appreciations to Tüzün Family for all their support since the day we first met.

I am grateful to Osman Müyesser for his patience, understanding and support during such a hard educational period.

I also would like to thank to my colleague Bahadır Şaylan for his support during preparation of data.

I would like to thank The Scientific and Technological Research Council of Turkey (TUBITAK) for their scholarship. It would be hard to do such a study without their support especially in Istanbul.

I also would like to thank to Cihan Başkır and Doğan Başkır with my deepest feelings for being closer to me like a brother than a friend.

I am grateful to İrem Erol for being with me and not hesitating to support me all the time.

Last but not least, great appreciations to my family Mustafa Düzgün, Vicdan Düzgün, Işıl Düzgün for their endless support and sacrifice during my life. It is a great feeling to be a member of such a family. Thank you all, whom I forgot, for giving me a lift when I am going down.

ABSTRACT

SEISMIC SHEAR AMPLIFICATION IN STRUCTURAL WALLS

Earthquake resistant design of structural walls involves inhibiting brittle shear failure that would develop with the formation of plastic hinge at the base of the walls. During seismic action, recent studies demonstrate that maximum wall shear responses, during an earthquake depending on characteristics of the walls, are generally higher than the conventional code procedures, namely elastic analysis procedures, which can be attributed to the contribution of higher mode effects subsequent to the formation of plastic hinge at the base of the wall. In light of findings from analyses of structural walls, shear amplification factors have been proposed in Eurocode 8 EN1998-1 (CEN, 2004) to inhibit brittle shear failure occurrence in structural walls. Proposed relationships mainly depend on first mode period of wall and strength reduction factors. However, in Turkish Seismic Design Code, this issue has been handled by considering a constant base shear amplification of 1.5 regardless of first mode period and ductility level of the structural walls. Generic structural walls having four, eight, twelve, sixteen stories with different sectional properties have been analyzed in order to evaluate the dynamic shear amplification phenomenon. Responses of structural walls have been obtained through non-linear analyses results such as base shear amplification factors, force and deformation responses.

This study can be treated as an initial investigation for developing a sound procedure for shear design of structural walls in current code applications.

ÖZET

PERDE SİSTEMLERDE DEPREM NEDENİYLE OLUŞAN KESME KUVVETİ BÜYÜTMESİ

Depreme dayanıklı perde duvar tasarımı, deprem sırasında perde duvarların tabanında oluşacak plastik mafsal ile birlikte meydana gelebilecek gevrek kesme kırılmasını engellemeyi amaçlar. Geçmişte yapılan çalışmalar göstermiştir ki; deprem sırasında perde duvarlarda, elemanların karakteristiklerine bağlı olarak meydana gelen kesme kuvvetlerinin, lineer yöntemlerle hesaplanan kesme kuvvetlerinden daha büyük olduğu gözlemlenmiştir. Bu oluşum perde duvarın tabanında plastik mafsal oluşumu ile ortaya çıkan yüksek mod etkilerinin katkısına atfedilebilir.

Yapılan analizler sonucunda elde edilen bulgulara bakılarak; perde duvarlarda gevrek kesme kırılmasının önlenmesi için Eurocode 8 EN1998-1 (CEN, 2004)'de kesme kuvveti büyütme katsayısı ilişkileri önerilmiştir. Ana olarak, bu ilişkiler yapının birinci mod periyoduna ve deprem yükü azaltma katsayına bağlı olmasına rağmen; Deprem Bölgelerinde Yapılacak Binalar Hakkında Yönetmelik (2007) bu katsayıyı yapının birinci mod periyoduna ve süneklik seviyesine bakılmaksızın 1.5 olarak belirtmiştir.

Bu yüksek lisans çalışmasında 4, 8, 12, 16 katlı farklı kesit özelliklerine sahip perde duvarlar dinamik kesme büyütmesi katsayısının değerlendirilmesi için analiz edilmiştir. Çalışma sonucunda, doğrusal olmayan analiz sonuçlarına bakılarak ele alınan elemanların kesme kuvveti büyütme katsayıları, kuvvet ve deformasyon diyagramları elde edilmiştir. Bu çalışmanın, mevcut yönetmeliklerde bulunan perde duvarların kesmeye karşı tasarımına yönelik maddelerin geliştirilmesine katkı sağlayacağı söylenebilir.

TABLE OF CONTENTS

LIST OF FIGURES

LIST OF TABLES

LIST OF SYMBOLS

b	Width of structural wall section
d	Length of the structural wall section
D_i	Storey drift of i^{th} storey of the wall
D_{i+1}	Storey drift of $i+1^{th}$ storey of the wall
D_{pi}	Plastic displacement of i^{th} storey
D_{pi+1}	Plastic displacement of $i+1^{th}$ storey
E	Modulus of elasticity $3x10^7$ kN/m^2
EI_{cr}	Cracked section stiffness
EI_{gross}	Gross section stiffness
H_w	Total wall height
h_i	Height of i^{th} frame member compound
h_{i+1}	Height of $i+1^{th}$ frame member compound
H_j	Height of j^{th} storey
I	Moment of inertia of cracked section stiffness
I_g	Gross section moment of inertia
m	Mass of each storey
$m_{(y)}$	Mass of the wall per unit length
M_i	Envelope base moment observed during time history analysis
$M_{b,e}$	Envelope base moment observed during linear time-history analysis
M_y	Yield moment of section
$Q_{inelastic}$	Maximum storey shear force observed during of non-linear time-history analysis
$Q_{inelastic}$	Maximum storey shear force observed during linear time-history analysis
R_y	Yield strength reduction factor
α	Secondary stiffness of moment curvature relationship
β	Dynamic shear amplification factor
$\delta_{(j)}$	Storey drift ratio of j^{th} storey
$\delta_{(j)\text{-Plastic}}$	Storey cumulative plastic drift ratio of j^{th} storey

χ_{Total}	Total curvature
χ_y	Yield curvature
$\chi_{Plastic}$	Plastic curvature
$\chi_{(i)^{-}Plastic}$	Plastic curvature of ith frame member compound
$\chi_{(i+1)^{-}Plastic}$	Plastic curvature of i+1th frame member compound
$\chi_{(i)^{-}Plastic}$	Plastic curvature of ith frame member compound
μ	Curvature ductility

1. INTRODUCTION

Structural wall systems have many advantages in structural design of reinforced concrete or other types of buildings. Structural wall systems have an advantage of being stiffer in comparison to moment resisting frames and they provide a better displacement control by limiting damage in internal partition walls and non structural elements. They also have benefit of being economical when other structural and architectural aspects are considered, in addition to the facts mentioned above.

In earthquake resistant design of multistory buildings to ensure economical needs, general design philosophy tolerates a certain amount of damage in structure, while accommodating displacement based design requirements. Thus, during severe earthquakes, structural walls are expected to exhibit inelastic flexural behavior, while other brittle deformation mechanisms, such as shear, remain elastic. In other words, to assure inelastic behaviour of walls it becomes vital to inhibit formation of shear failure, which would develop after the occurrence of plastic hinging at the base of a wall with the effect of higher modes of structure.

Main design philosophy in current seismic codes are based on applying strength reduction factors, which stand for acceptable damage in structural system in case of seismic action. Strength reduction factors proportionally reduce earthquake forces, such as bending moments and shear forces. However, during a dynamic action maximum wall shear responses during an earthquake are generally higher than the statically computed values. This is the basis of seismic shear amplification in structural walls, which corresponds to the fact that shear forces are not in proportion with moments. Although there is a certain consensus between researchers in literature on this subject; methodology for design is not clearly defined. In studies performed by different researchers and some of current seismic design codes, an empirical amplification factor for shear design of structural walls has been taken into account.

1.1. Aim and Scope of Study

Seismic shear amplification in structural walls is not fully integrated within the seismic design codes. Findings from the recent studies are not satisfactory to define an analytical procedure for design of all structural walls in terms of shear. In current Turkish Seismic Design Code, this issue has been handled by considering a base shear amplification of 1.5 regardless of first mode period and ductility level of the structural wall. In a recent study by Celep (2008) relationships for base shear amplification, shear force profile and moment profile along the wall height have been proposed for Turkish Seismic Design Code (2007).

This study involves the analysis of generic structural walls with different design properties in order to evaluate the dynamic shear amplification phenomena. This study can be treated as a initial investigation for developing a sound procedure for shear design of structural walls in code applications.

Literature survey on dynamic shear amplification has been covered in Chapter 2. Characteristics of the selected walls, analysis procedure and analysis results for representative wall are presented in Chapter 3.

2. LITERATURE SURVEY

Earthquake resistant design of multistory buildings containing reinforced concrete structural walls intends, inhibiting brittle shear failure that would develop with the formation of plastic hinge at the base of the walls. In the last couple of decades this issue has been investigated and included in national seismic codes. It has been stated that due to dynamic effects, maximum wall shear responses during an earthquake depending on characteristics of the walls, are generally higher than the conventional methods based on elastic analysis procedures.

Primarily in base shear amplification issue, Blakeley *et al.,*(1975) have pointed to the fact that actual base shear force is higher than the base shear force derived by a normal code lateral load distribution when plastic hinge occurs at the base of the wall. In Blakeley's study, elastic normal mode response spectrum analysis results of 10 storey building have been compared to step by step numerical integration dynamic analysis of cantilever wall structures in terms of shear forces to examine the change between the two methods. Authors also stated that, when plastic hinge occurs at the base of the wall, the center of lateral the inertial loading shifts downward resulting in higher forces than those derived by the lateral code load distribution. According to authors, plastic hinging could extend well above the base of a wall, up to half the height of a tall structure. A relationship for the base shear amplification factor has been proposed as follows,

$$\begin{aligned} w_n &= 0.9 + \frac{n}{10} && \text{n} \leq 6 \\ w_n &= 1.3 + \frac{n}{30} \leq 1.8 && \text{n} > 6 \end{aligned} \tag{2.1}$$

where, w_n represents the base shear amplification factor and n represents number of stories.

Derecho and Corley (1984) have presented an investigation about the force and deformation demands of isolated structural walls under earthquake effect. Authors have presented a relationship referring to the shear amplification as the outcome of the conducted analysis. Derecho and Corley proposed a shear coefficient α_v, which is defined as a function of the fundamental period and available ductility. Relation between shear design factor, fundamental period and ductility level has been set out in the Figure 2.1 below. The coefficient α_v represents the ratio of the calculated maximum dynamic shear to the lateral force V_T used in design for flexure. Values of α_v are remarkable which are generally greater than unity and can be as high as 3.5 for the longer period structures with available ductility of 4.0.

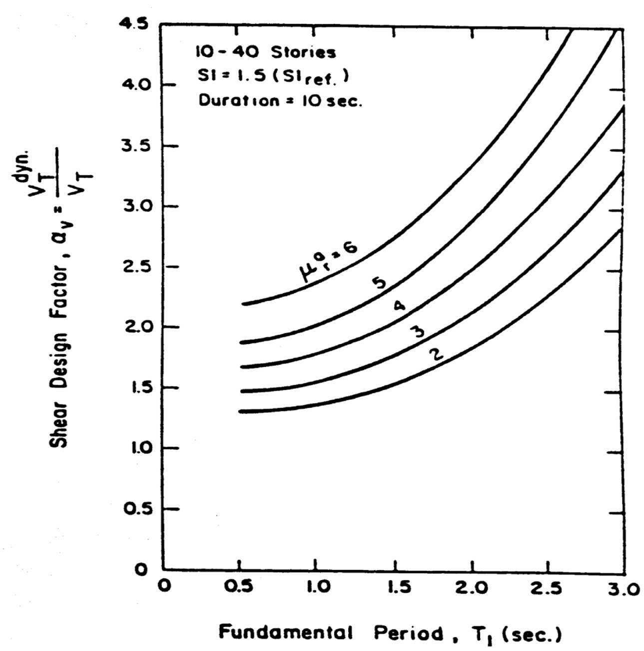

Figure 2.1. Base shear amplification factor relationship proposed by Derecho and Corley (1984)

It should be noted that Derecho and Corley's relation shows earthquake intensity equal to 1.5 times the reference intensity (SI_{ref}) which has been stated as spectrum intensity corresponding to the first 10 seconds of the N-S component of the 1940 El Centro record. μ_r^a has been stated as available ductility.

Kabeyasawa (1987) have stated that possible maximum dynamic wall shear could be estimated rationally as the modal sum of the first mode shear from static analysis and the higher mode shear estimated from the base acceleration level. A full scale seven storey reinforced concrete building has been analyzed in which structure is subjected to lateral loads of inverted triangular distribution.

Kabeyasawa observed that higher components of inertial force, calculated by response history analysis, varied approximately in phase with the ground motion. A modal decomposition method has been proposed to clarify characteristics of non-linear dynamic motion. In light of analysis results, Kabeyasawa have expressed the dynamic amplification factor as the function of the period of the higher modes and frequency components of the input base motion.

Relationship proposed by Kabeyasawa for maximum base shear have been presented below in Equation (2.2).

$$V_{\max} = V_n + c \times W \times PGA \tag{2.2}$$

in which, V_n is the base shear capacity for the structure calculated by ultimate limit state analysis assuming a triangular force distribution, *c is* a coefficient that stands for the higher mode effects varying between 0.25 and 0.30, *W* is the seismic weight of the wall and *PGA* is the design peak ground acceleration.

Eibl and Keintzel (1988) have presented a novel method for evaluation of the seismic shear forces in seismic regions which later formed the basis of Eurocode 8 EN1998-1 (CEN, 2004) base shear amplification provisions for high ductile walls. The proposed relation of shear amplification factor has been given below;

$$\varepsilon = q\sqrt{\left(\frac{\gamma_{rd}}{q}\frac{M_{rd}}{M_{Ed}}\right)^2 + 0.1\left(\frac{S_e(T_c)}{S_e(T_1)}\right)^2} \leq q \tag{2.3}$$

where, ε is the base shear amplification factor, q is the strength reduction factor, γ_{Rd} is the over strength factor, M_{Rd} is the design flexural strength at the wall base, M_{Ed} is the design moment at the wall base, T_c is the upper limit period of the spectral acceleration plateau in the design spectrum and $S_e(T)$ is the ordinate of the elastic response spectrum.

In the Equation (2.3), first term under the square root denotes the effect of capacity design and the second term emphasizes the effect of second mode contribution to shear amplification phenomena.

Ghosh and Markevicius (1990) have stated that there is a variable relation between the moment and shear in multi degree of freedom systems which are subjected to reversing loads due to the effects of different modes. Authors have proposed shear force relationship depending on yield moment capacity of the base section and intensity of the ground motion. It should be noted that maximum shear force relationship has no dependence to the first mode period of the system.

$$V_{\max} = 0.25W \times PGA/g + M_y/0.67H \tag{2.4}$$

where, W represents the seismic weight of the wall, PGA represents the design peak ground acceleration, M_y represents the yield moment capacity at the base of the wall and H represents the total wall height.

Eberhard and Sozen (1993) studied shear amplification phenomena for walls in medium rise, reinforced concrete buildings with a similar point of view in Kabeyasawa study (1987). In Eberhard and Sozen's study, dynamic tests have been conducted over nine small scale reinforced concrete structures that included walls on earthquake simulator. Results of experimental dynamic tests have shown that base shear demand for medium rise reinforced concrete buildings with earthquake resistant structural walls can be defined by a coefficient of 0.30 in the Equation (2.5) given below.

$$V_k = V_n + 0.30 \times W \times A_e \tag{2.5}$$

where, V_k is estimated peak base shear for the entire structure, V_n is the base shear capacity for the structure calculated by limit analysis assuming a triangular force distribution, W is the total weight of the structure and A_e is the effective peak acceleration coefficient.

Seneviratna and Krawinkler (1994) have pointed out in their study that base shear amplification phenomenon is dependent on both strength level reduction and the first mode period of the structural wall.

Shear force variation due to the fundamental first mode period and strength reduction factors has been presented in Figure 2.2. As it can be seen from the figure shear forces get higher values for longer periods and lower strength levels.

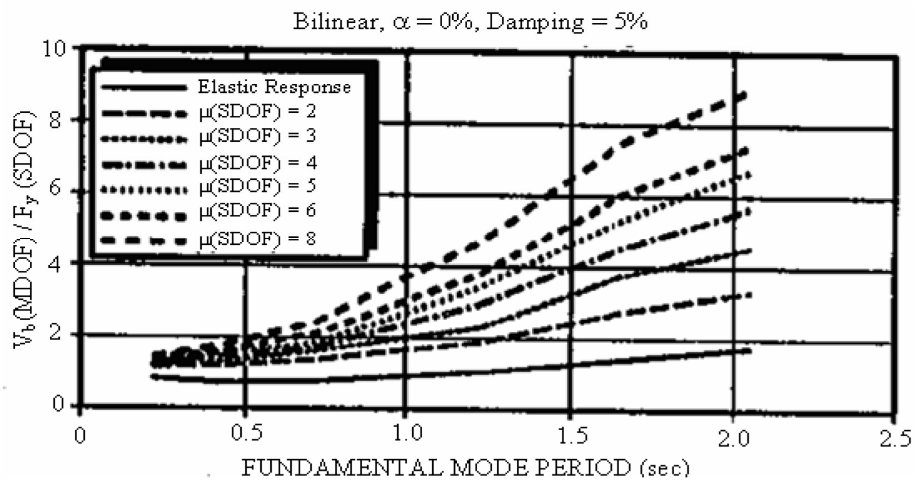

Figure 2.2. Base shear amplification factor relationship proposed by Seneviratna and Krawinkler (1994)

Filiatrault *et al.,*(1994) have presented an analytical investigation on the shear demand of ductile flexural walls which have been designed according to Canadian seismic provisions in which force reduction factor is applicable to both flexure and shear regardless of shear amplification phenomena. Five wall type buildings (3, 6, 10, 15 and 25 storey buildings), which had been designed for three different seismic zones, have been taken into account during analysis. In consequence of the conducted analysis, following the issue of higher mode effect contribution to shear, which is more significant in taller buildings, dynamic shear amplification between 1.0 and 1.5 has been proposed.

Rutenberg and Nsieri (2006) have pointed out that amplification factors specified in Eurocode 8 provisions, particularly for walls designed for medium and high ductility demands are in need of revision. Authors study has been focused on the seismic shear provisions of Eurocode 8 for ductile reinforced concrete single walls or a system comprising a number of equal length walls and a system comprising walls of different lengths.

Rutenberg and Nsieri have proposed following base shear amplification factor.

$$\varepsilon=0.75+0.22\times(T+q+Tq) \tag{2.6}$$

where, T is first mode fundamental period and q is strength reduction factor.

In a recent study, Celep (2008) has dealt with the dynamic shear force amplification and proposed a novel parametric design formula for shear to prevent shear failures not only at the base of the wall but also along the height of the structural wall. Five cantilever structural walls with 8, 12, 16, 20, 30 stories and with different section heights have been taken into account for five different strength reduction factors (R=2.0, 4.0, 6.0, 8.0, 10.0). Proposed relationship for dynamic shear amplification has been presented as,

$$\begin{gathered}\beta^b=1.0+(0.281\times T_{1-cr}+0.394)\times(R-1.5)^{0.553}\\ 1.0\leq\beta^b\leq R\end{gathered} \tag{2.7}$$

in which, β^b represents the base shear dynamic amplification factor, $T_{1\text{-}cr}$ represents the first mode period of wall corresponding to cracked section stiffness and R represents the strength reduction factor.

Relation between amplification factor and cracked section elastic first mode period has been presented in Figure 2.3..for different strength reduction factors.

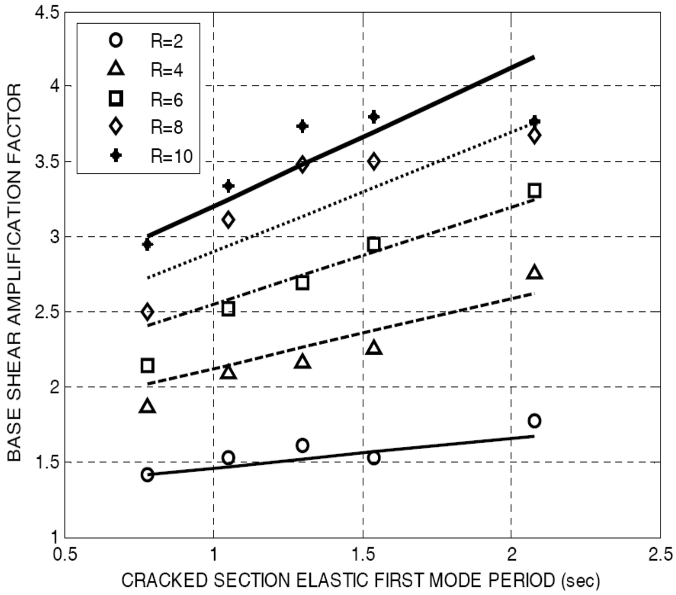

Figure 2.3. Base shear amplification factor relationship proposed by Celep (2008)

Author has stated that the proposed relationship is in good agreement with the mean amplification factors for strength reduction factors between 2.0 and 6.0, and overestimates the amplification factors for strength reduction factors 8.0 and 10.0.

3. METHODOLOGY AND MODELS USED IN STUDY

. This chapter covers the basic methodology carried out in this study for selected structural systems.

Four structural walls, having different heights and sectional properties, have been selected for numerical computations. A set of four, eight, twelve, sixteen storey structural walls with typical storey heights of 3.0 meters, representing multi-storey structural systems have been investigated in the analysis. Wall sections have been determined according to procedure defined by Celep (2008) in which shear amplification phenomenon studied for cantilever type structural walls.

Preliminary design of walls has been made with Equation (3.1) as given below:

$$0.05H_w^{3/4} = \frac{2\pi}{\frac{3.516}{H_w^2}\sqrt{\frac{EI_g}{m(y)}}} \tag{3.1}$$

where, H_w represents total wall height, I_g represents moment of inertia of gross section, $m_{(y)}$ represents mass of the wall per unit length and E (kN/m^2) has been taken as $3x10^7$ kN/m^2.

Wall sections have been given in Table 3.1 in line with the results of Equation (3.1).

Table 3.1. Geometrical properties of selected walls

WALL	H_w (m)	b(m)	d(m)	m(t)	T_{1cr} (s.)
4 STOREY	12	0.30	2.15	30.00	0.533
8 STOREY	24	0.30	4.00	30.95	0.749
12 STOREY	36	0.30	5.75	30.12	0.949
16 STOREY	48	0.30	7.50	29.68	1.101

Storey masses, given in Table 3.1, have been assumed to be lumped at the storey levels. Schematic drawing of selected walls have been given in the Figure 3.1 below.

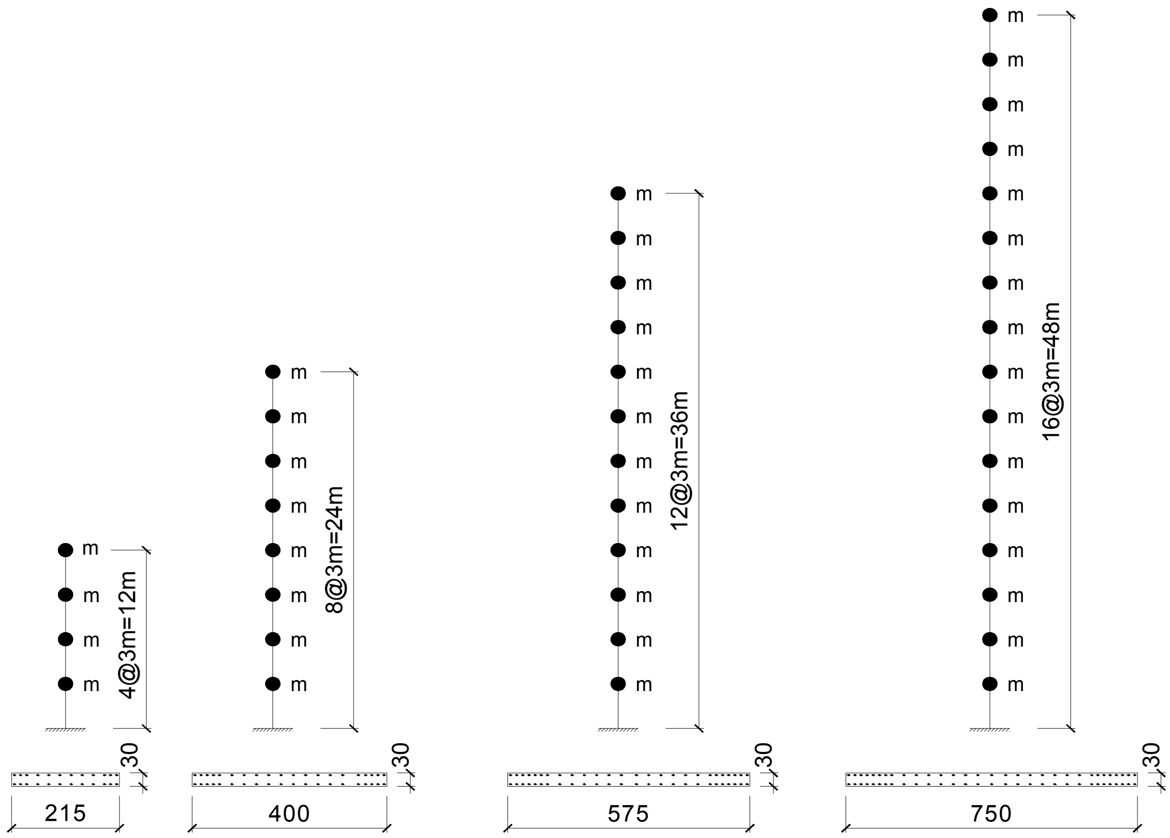

Figure 3.1. Schematic drawing for selected walls and section properties

In determining the sectional flexural capacities, linear time-history analyses have been carried out using a set of 10 strong ground motions. Analysis have been performed using PERFORM 3D structural analysis software (CSI, 2007) licensed to Department of Earthquake Engineering of Bogazici University.

Ground motion parameters used in the study, which had been obtained from PEER Strong Motion Database and Cosmos Virtual Data Center, have been given in Table 3.2.

Table 3.2. Ground motion parameters used in structural analysis

No.	Date	Earthquake Name	Magnitude (M_s)	Station Name	Station Number	NEHRP Site Class	Dist (km)	Comp (deg)	PGA (g)
1	02.09.1971	San Fernando	6.5	Lake Hughes Array Station 12	128	C	17	21	-0.353
2	02.09.1971	San Fernando	6.5	Lake Hughes Array Station 9	127	A/B	26.6	291	-0.112
3	10.01.1987	Whittier	6.1	Inglewood Union Oil Yard	14196	C	22.5	0	0.251
4	01.17.1994	Northridge	6.8	Los Angeles City Terrace	24592	A/B	37.1	90	0.263
5	10.17.1989	Loma Prieta	7.1	Coyote Lake Dam Downstream	57504	C	21.7	285	0.178
6	10.17.1989	Loma Prieta	7.1	Coyote Lake Dam Downstream	57504	C	30.9	195	0.158
7	02.09.1971	San Fernando	6.5	Pasadena CIT Cal Tech Seismo Lab	266	A/B	25.5	270	0.202
8	10.17.1989	Loma Prieta	7.1	Gilroy #6 San Ysidro Microwave Site	57383	C	19.9	90	0.170
9	10.17.1989	Loma Prieta	7.1	Gilroy #6 San Ysidro Microwave Site	57383	C	35.2	0	0.114
10	01.17.1994	Northridge	6.1	San Marino SW Academy	24401	C	39.3	90	0.125

Ground motions have been selected based on site classes, distances and moment magnitudes. Fault distances are chosen to be not closer than 15.0 km with A/B and C type NEHRP site classes and moment magnitudes in the range of 6.0 and 7.1. Effort has been made to gather ground motions with similar properties to have a consistency in between.

Acceleration response spectrum of ground motions have been given in Figure 3.2.

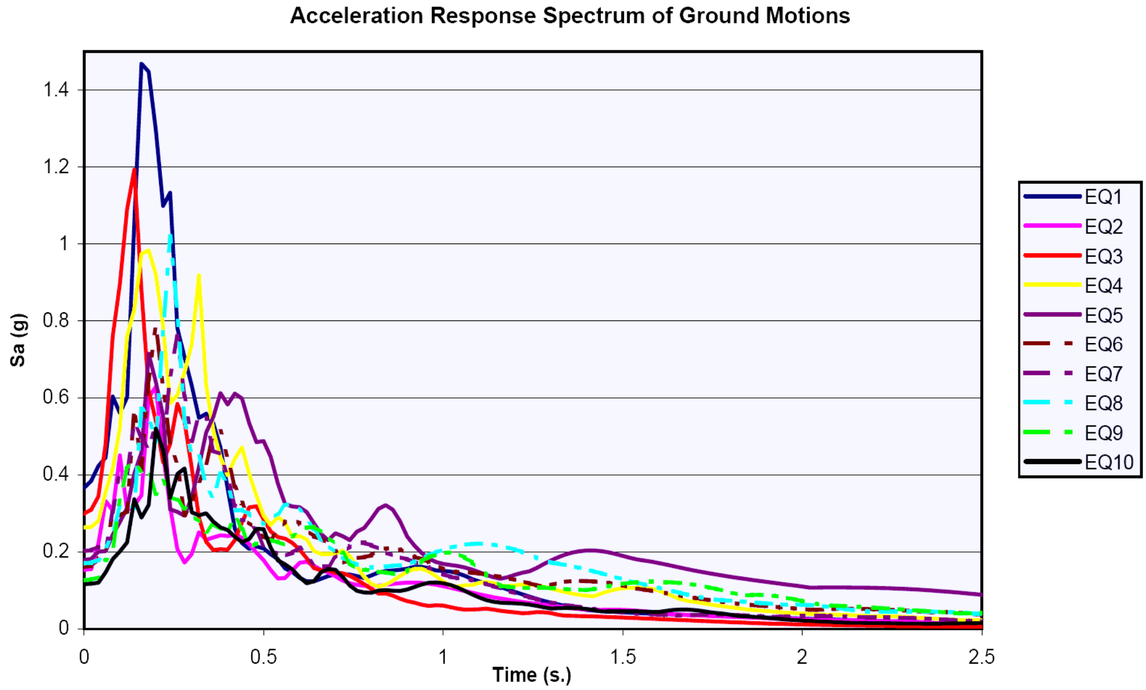

Figure 3.2. Acceleration Response Spectrum of Ground Motions

Depending on the results of analyses, flexural capacities of the sections have been determined as maximum moment value obtained from time-history analysis for each structure. Since the main concern in flexural design of structural walls is the bending moment occurring at the base; all ground motions are linearly scaled in order to have the same base moment yield value. By this approach structural wall under consideration has the same yield moment at the base level regardless of the ground motion. It has been intended to reduce the unknowns to ground motion amplitude and frequency as unique ground motion parameters affecting the analysis results Furthermore, it should be noted that number of ground motions and frequency contents affect the results and may lead to different shear amplification factors.

By using the design structural walls with the above mentioned properties, non-linear time-history analysis have been carried out for each wall with 5 different yield strength reduction factors.(R_y=2.0, 3.0, 4.0, 5.0, 6.0) For non-linear analysis, ground motion data have been factored in proportion with selected yield strength reduction factors (R_y =2.0, 3.0, 4.0, 5.0, 6.0). For each structural wall, shear amplification factors have been obtained and variation of these factors in relation to the yield strength reduction factor has been investigated. Likewise, variation of response profiles such as moment, shear force, displacement, plastic curvature and curvature ductility have been investigated. Mean values and standard deviations of results from the analyses for each parameter in concern have been calculated for observing the scatter in results. In order to examine the variation in each parameter, parameters have been plotted along the wall height.

3.1. Detailed Explanation of the Procedure

Main criteria for the selection of ground motions can be specified as follows,

1. Distance between source and target shall not be less than 15.0 km in order to avoid near field effect phenomena.
2. NEHRP Site Class shall be classified in AB or C Site Classes.
3. Ground motions with similar acceleration response spectrum patterns have been selected in order to reduce the effect of ground motion on scatter of the results.

Ground motion acceleration time histories of earthquakes have been given in Appendix A.

Structural walls have been modeled with frame ("Beam, RC" as defined in PERFORM 3D) compound elements. For a detailed investigation of non-linear structural behaviour, elements have been divided into segments, having length of 0.25 meters along the height of the wall. Masses of each storey have been lumped at storey levels which have been defined in typical storey heights of 3.0 meters. Illustration of subdivision of the frame members and elements forming a frame member compound have been given in Figure 3.3.

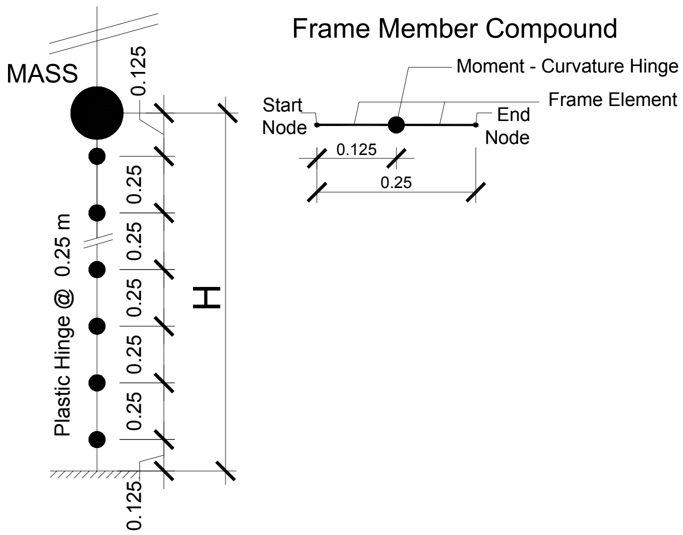

Figure 3.3. Illustration of frame member subdivision and frame member compound

Cracked section stiffness has been used for both linear analysis and non-linear analysis. Cracked section stiffness has been assumed as the half of the gross section stiffness. (EI_{cr}=0.50 EI_{gross})

Figure 3.3 shows lumped plasticity approach with zero length plastic hinges. Hysteresis rule for the moment curvature hinges have been assumed as elastic-perfectly plastic, in which secondary stiffness (α) is zero. This assumption has been made after observing a negligible change in shear responses with respect to results of analyses using plastic hinges with different hysteresis rules having different secondary stiffness. For moment curvature type hinges, in order to compute rotations, suitable tributary length has been selected which is defined in terms of element's proportional length. Properties of plastic hinge and tributary length concept have been shown in Figure 3.4.

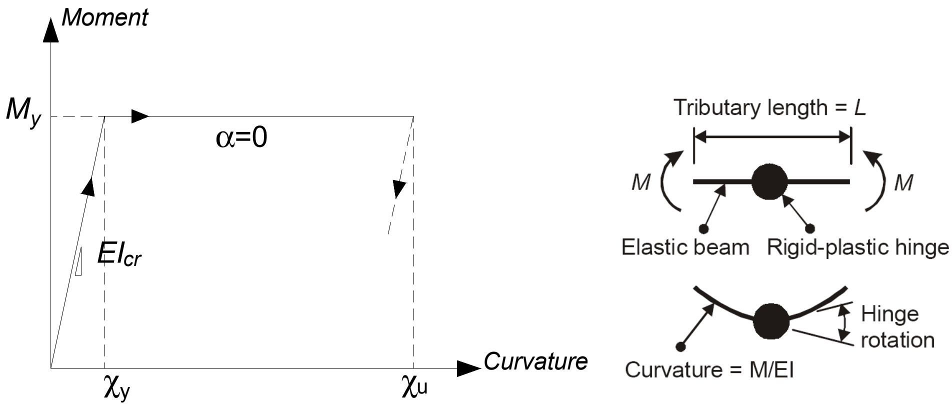

Figure 3.4. Moment - curvature hysteresis property and tributary length concept for plastic hinges (Moment - Curvature Hinge)

Structural walls with geometric characteristics given previously in this chapter have been analyzed with non-linear time-history analysis. In light of the statements in PERFORM 3D Manual (CSI, 2007), time-history analyses have been performed based on step-by-step integration, using “the constant average acceleration method”.

PERFORM 3D uses an event-to-event solution strategy in time-history analysis, in which the structure properties are re-formed each time when there is a change in the stiffness. Modal damping has been taken into account as 5 per cent for all modes of structural system in linear time-history analysis. Damping matrix has been formed with Rayleigh Damping method, which is assumed to be proportional to the stiffness and mass matrices of the systems.

Time-history analyses have been performed in two stages. First-stage analyses consist of linear time-history analysis by which flexural capacities of the walls have been determined. Depending on the results of linear time-history analysis, linear scaling procedure has been applied. Procedure steps are as follows,

1. Perform linear time-history analysis
2. Obtain maximum base moment from each time-history analysis.
3. Compute the scale factors to obtain the same base moment obtained from all earthquakes.

Scale factors for eight storey structural wall have been given in Table 3.3. Scale factors of other sections have been presented in Appendix A. Maximum moment value is shown bold at the table.

Table 3.3. Scale factors for earthquakes as result of linear scaling procedure for eight storey wall

EQ No.	**$M_{b,e}$ (*kN-m*)**	**Scale Factors**
1	4543	1.442
2	3404	1.925
3	5200	1.260
4	4790	1.368
5	**6551**	1.000
6	5223	1.254
7	6161	1.063
8	4525	1.448
9	4763	1.375
10	3309	1.980

Maximum base moment value has been observed at the base of the wall from earthquake no.5 (Table 3.2). Maximum base moment response for twelve and sixteen storey structural walls has been observed from earthquake no. 8 (Table 3.2).

Second-stage analyses consist of non-linear time-history analyses for structural wall sections given in Table 3.1 for yield strength reduction factors (R_y) of 2.0, 3.0, 4.0, 5.0 and 6.0. Time-history responses of structures have been averaged to obtain mean story forces and deformations as well as mean base shear amplification factors. In order to investigate variability of time-history responses, standard deviation of responses of each structure for each R_y value is determined and ± 1 standard deviation has been added to each mean response.

Since the number of non-linear time-history analysis is very high, all response profiles have been presented only for the eight storey structural wall with yield strength reduction factor of R_y = 4.0 as a representative example. The complete set of results of analyses of all structural types for all R_y values have been presented in Appendix B.

3.1.1. Storey Moments (R_y = 4.0)

Maximum storey moment diagrams for earthquakes in consideration and mean of these moment diagrams with ±1 standard deviation have been shown in Figures 3.5 and 3.6 respectively.

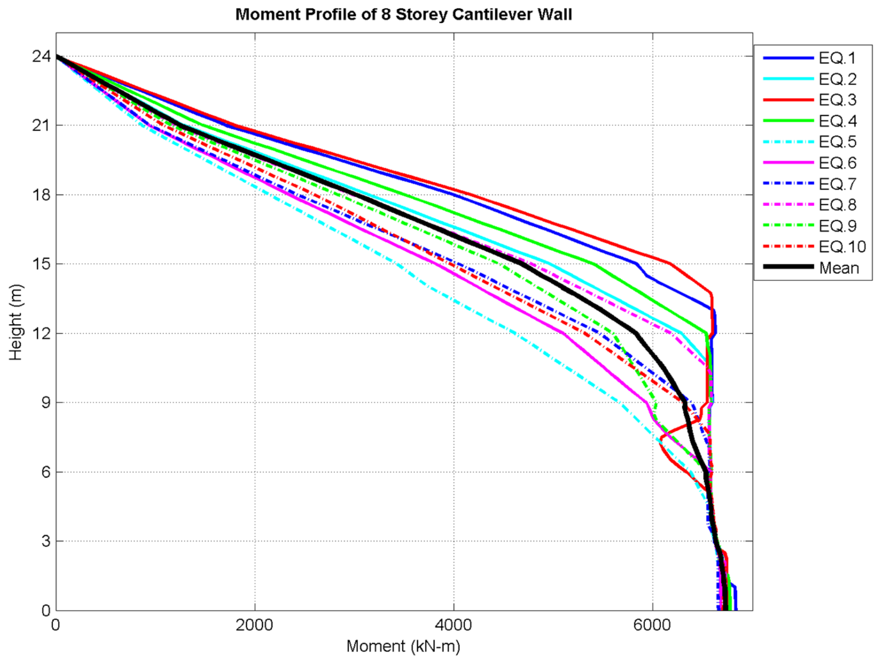

Figure 3.5. Storey moment diagrams of eight storey wall with strength level R_y = 4.0

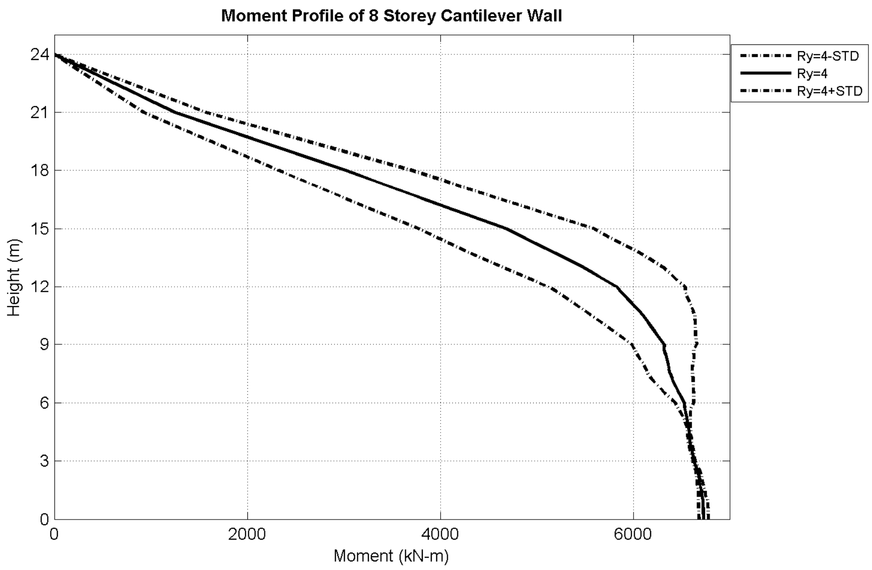

Figure 3.6. Storey mean moment diagram and ±1 standard deviation of eight storey wall R_y = 4.0

3.1.2. Storey Shears (R_y = 4.0)

Maximum storey shear forces and mean storey shear force diagrams with ±1 standard deviation have been presented in Figure 3.7 and Figure 3.8.

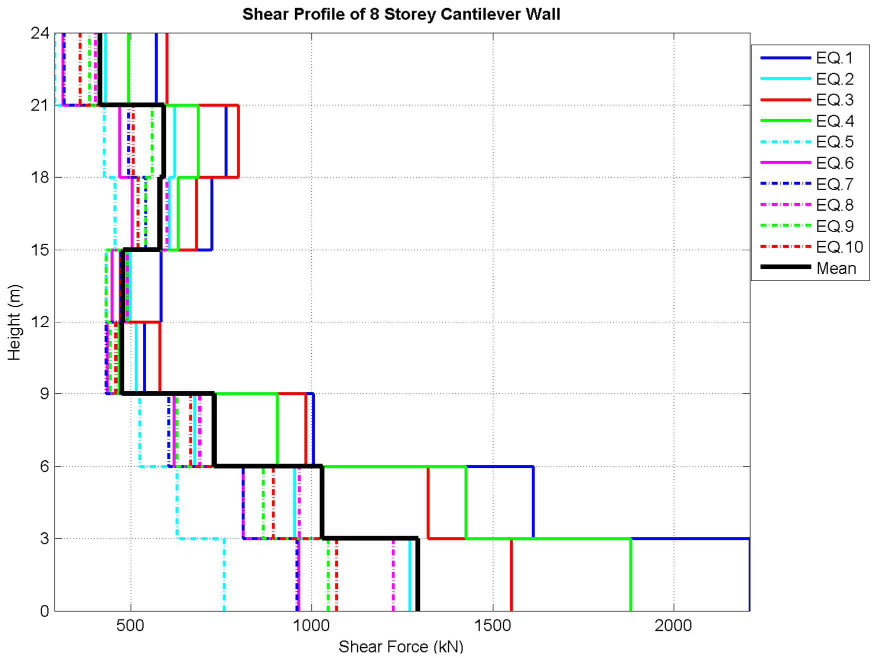

Figure 3.7. Storey shear force diagrams of eight storey wall with strength level R_y = 4.0

Figure 3.8. Storey mean shear diagram and ±1 standard deviation of eight storey wall

R_y = 4.0

3.1.3. Storey Plastic Curvatures (R_y = 4.0)

Plastic curvature values have been calculated as given below:

$$\chi_y = \frac{M_y}{EI} \tag{3.2}$$

$$\chi_{Plastic} = \chi_{Total} - \chi_y \tag{3.3}$$

where, χ_{Total} represents total curvature, χ_y represents yield curvature, $\chi_{Plastic}$ represents plastic curvature, M_y represents yield moment, I represents moment of inertia of cracked section stiffness and E (kN/m^2) represents modulus of elasticity (3x10^7 kN/m^2).

Plastic curvature is an informative parameter in order to determine the extent of plastic deformation along the height of the wall. Plastic curvature and storey mean plastic curvature diagrams with ±1 standard deviation have been presented in Figure 3.9 and 3.10.

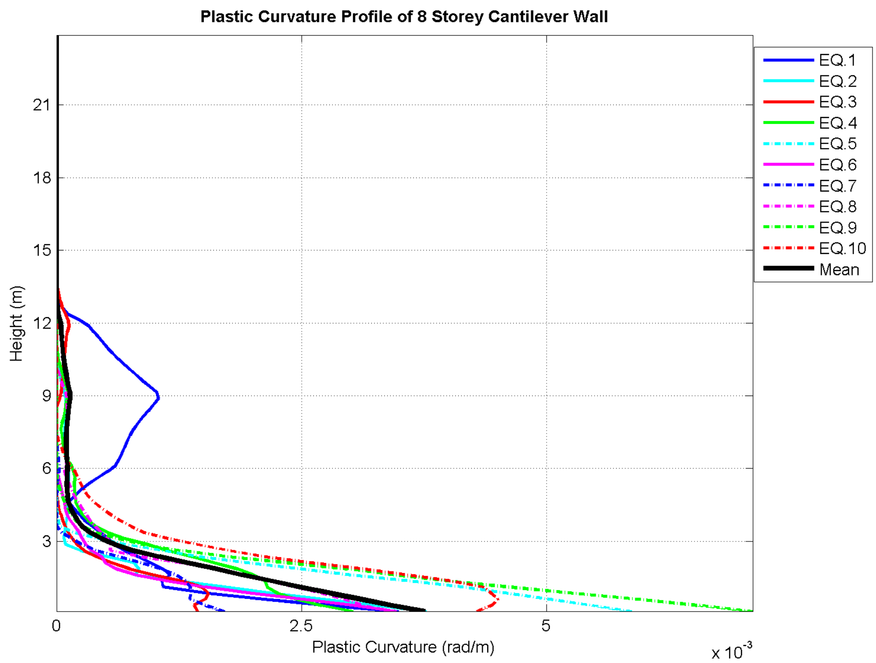

Figure 3.9. Storey plastic curvature diagrams of eight storey wall with strength level R_y = 4.0

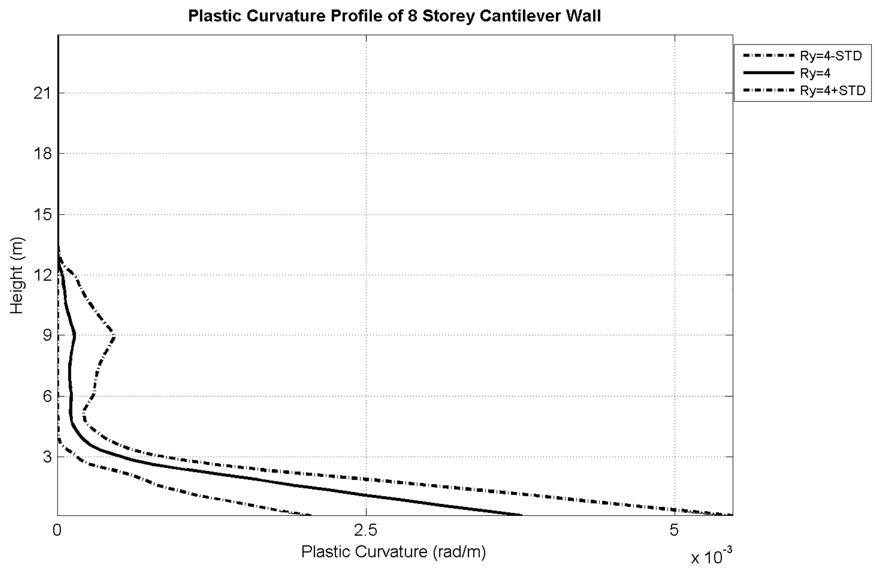

Figure 3.10. Storey mean plastic curvature diagram and ±1 standard deviation of eight storey wall R_y = 4.0

Curvature ductility value has been calculated as shown in Equation (3.4) and presented in Figure 3.11.

$$\mu = \frac{\chi_{Total}}{\chi_y} \tag{3.4}$$

where, χ_{Total} represents total curvature which is an output PERFORM3D software, χ_y represents yield curvature (Equation 3.2) and μ represents curvature ductility.

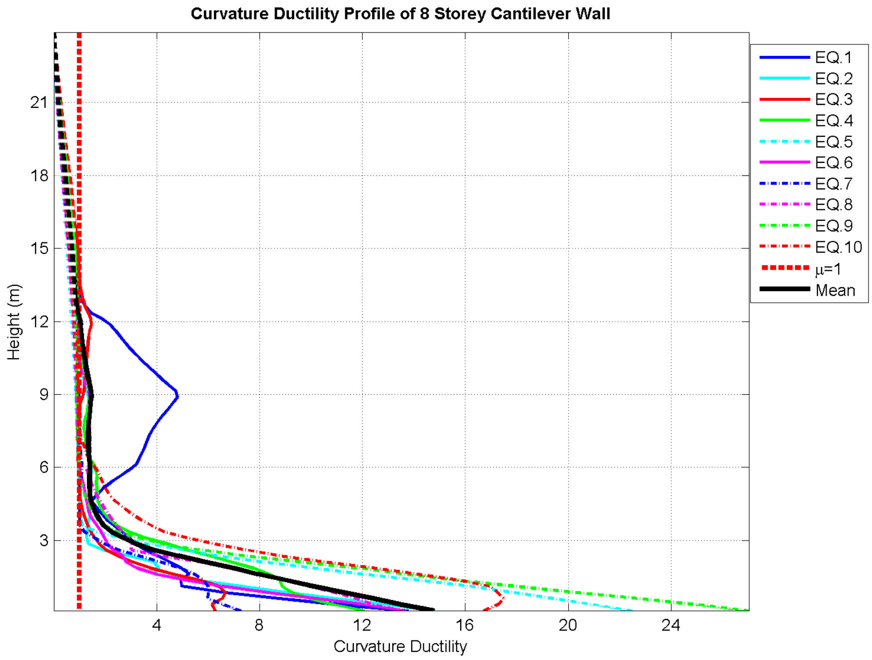

Figure 3.11. Storey curvature ductility diagrams of eight storey wall with strength level $R_y = 4.0$

3.1.4. Storey Displacements (R_y = 4.0)

Storey total displacements and mean displacements with ±1 standard deviation have been presented in Figure 3.12 and 3.13 respectively.

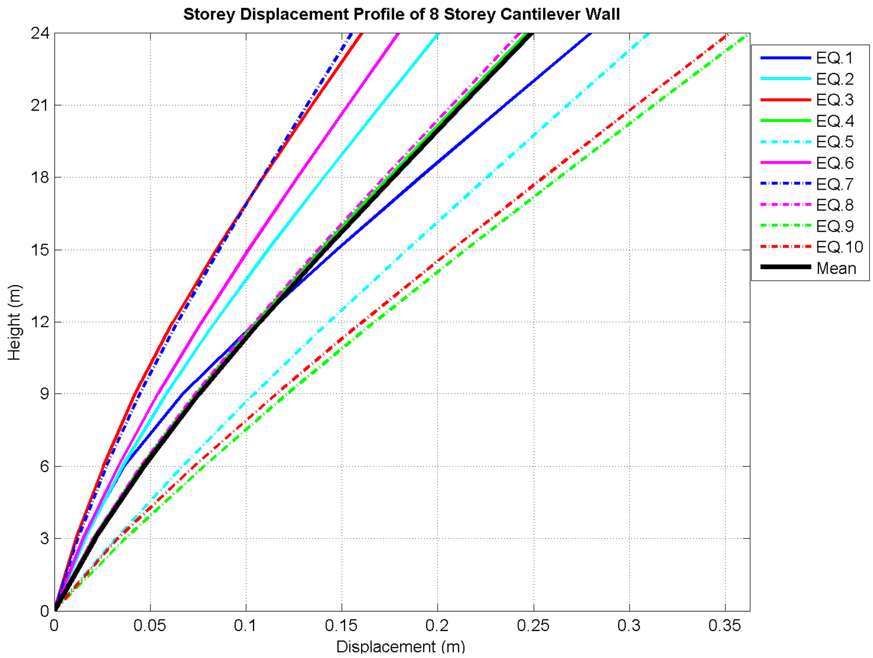

Figure 3.12. Storey displacement diagrams of eight storey wall with strength level R_y = 4.0

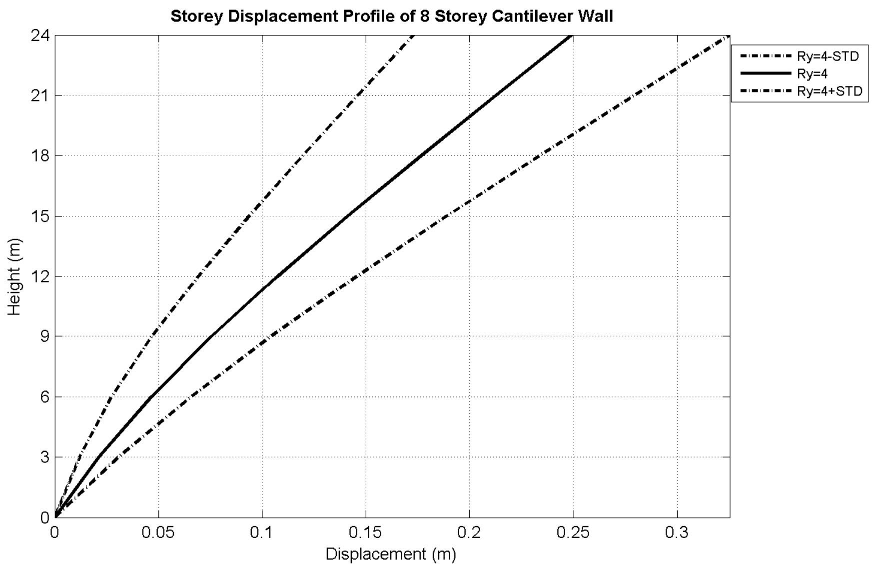

Figure 3.13. Storey mean displacement diagram and ±1 standard deviation of eight storey wall R_y = 4.0

Storey plastic displacement diagrams of structures have been derived using plastic curvature responses. Derivation of plastic displacement has been given in Equation (3.5) and (3.6).

$$\Delta_{(i)-Plastic} = \chi_{(i)-Plastic} \times h_i^{\,2} \tag{3.5}$$

$$\Delta_{(i+1)-Plastic} = \Delta_{(i)-Plastic} + \chi_{(i+1)-Plastic} \times h_{i+1}^{\,2} \tag{3.6}$$

$$D_{(j)-Plastic} = \sum_{i=1}^{n} \Delta_{(i)-Plastic} \tag{3.7}$$

where, $\Delta_{(i)\text{-}Plastic}$ represents plastic displacement of ith frame member compound, $\Delta_{(i+1)\text{-}Plastic}$ represents plastic displacement of i+1th frame member compound, $\chi_{(i)\text{-}Plastic}$ represents plastic curvature of ith frame member compound, $\chi_{(i+1)\text{-}Plastic}$ represents plastic curvature of i+1th frame member compound, h_i represents height of ith frame member compound (taken as 0.25 m), h_{i+1} represents height of i+1th frame member compound and $D_{(j)\text{-}Plastic}$ represents sum of plastic displacements along relevant storey .

Plastic displacement diagrams have been given in Figure 3.14.

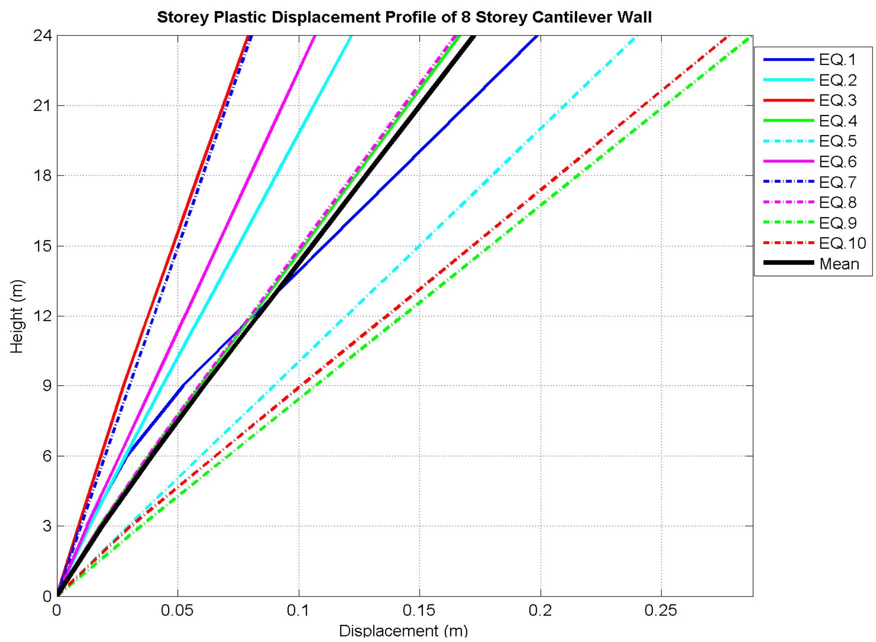

Figure 3.14. Storey plastic displacement diagrams of eight storey wall with strength level $R_y = 4.0$

3.1.5. Storey Drift Ratios (R_y = 4.0)

Storey drift ratio has been calculated as stated in Equation (3.8).

$$\delta_j = \frac{(D_{j+1} - D_j)}{H_j} \tag{3.8}$$

in which, δ_j represents storey drift ratio of j^{th} storey, D_{j+1} represents storey drift of $j+1^{th}$ storey of the wall, D_j represents storey drift of j^{th} storey of the wall and H_j represents storey height.

Storey drift ratio diagrams and mean storey drift ratio diagram with ±1 standard deviation have been presented in Figures 3.15 and 3.16 respectively.

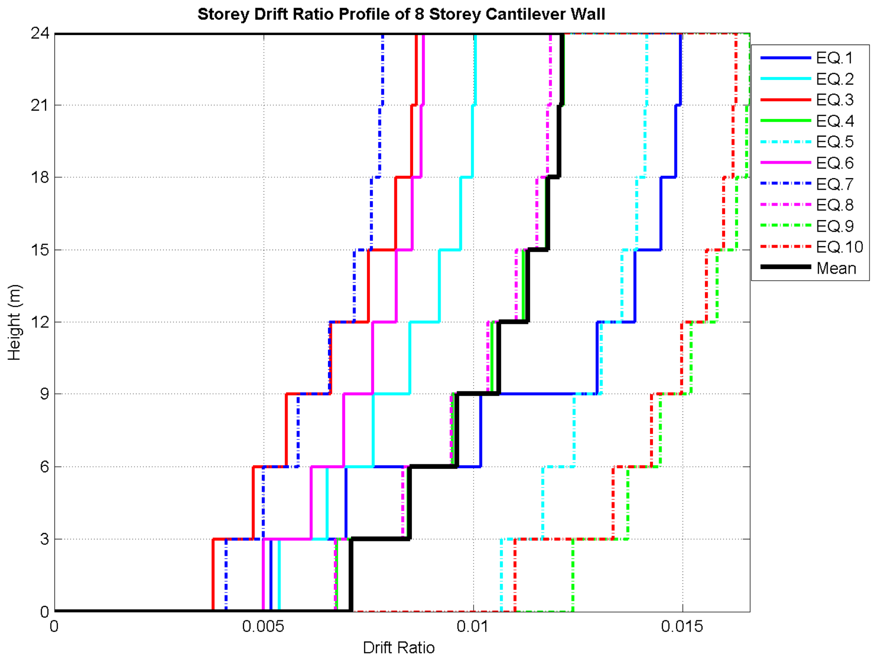

Figure 3.15. Storey drift ratio diagrams of eight storey wall with strength level R_y = 4.0

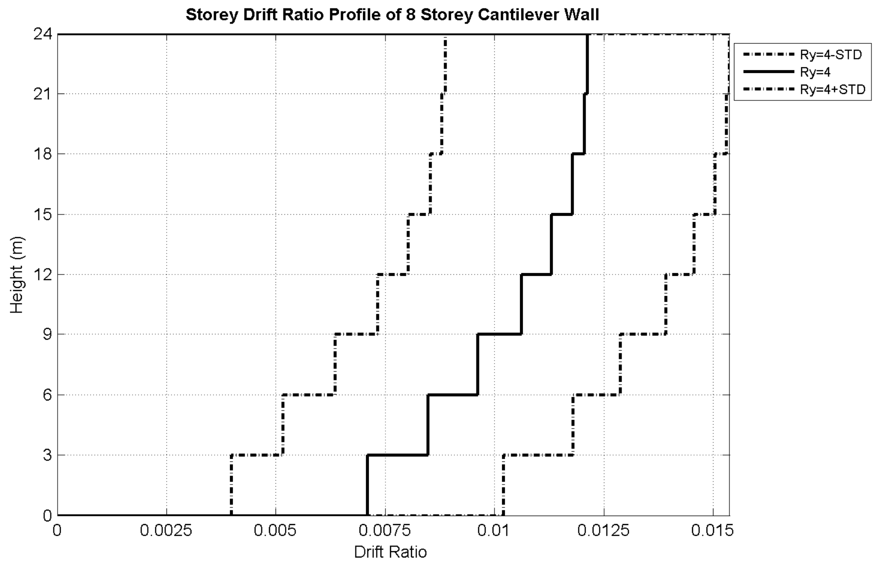

Figure 3.16. Storey mean drift ratio diagram and ±1 standard deviation of eight storey wall $R_y = 4.0$

Storey plastic drift ratio has been derived using the plastic storey displacements calculated by Equation (3.7). Storey plastic drift ratio can be calculated as follows:

$$\delta_{(j)-Plastic} = \frac{(D_{(j+1)-Plastic} - D_{(j)-Plastic})}{H_j} \tag{3.9}$$

in which, $\delta_{(j)-Plastic}$ represents cumulative plastic storey drift ratio of j^th^ storey, $D_{j+1-Plastic}$ represents plastic storey drift of j+1^th^ storey of the wall, $D_{j-Plastic}$ represents plastic storey drift of j^th^ storey of the wall and H_j represents storey height.

Storey plastic drift ratio diagrams have been given Figure 3.17.

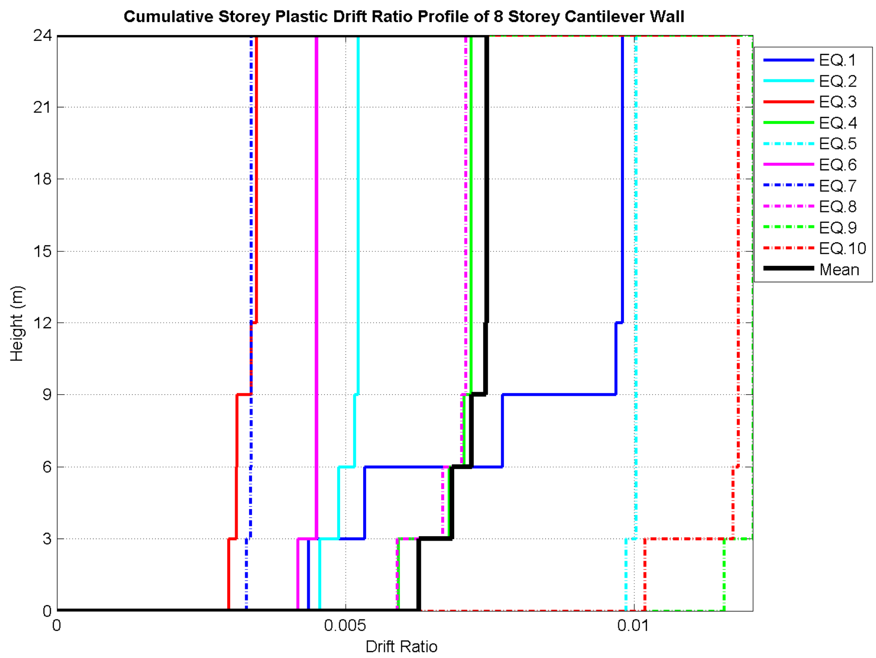

Figure 3.17. Storey cumulative plastic drift ratio diagrams of eight storey wall with strength level R_y = 4.0

3.1.6. Dynamic Shear Amplifications (R_y = 4.0)

Dynamic shear amplification factor has been calculated for each R_y value dividing inelastic shear response to elastic shear response as stated in following Equation (3.12)

$$\beta = \frac{Q_{inelastic}}{Q_{elastic}} \tag{3.10}$$

in which, $Q_{inelastic}$ represents maximum storey shear force obtained from non-linear time-history analysis, $Q_{elastic}$ represents maximum storey shear force obtained from linear time-history analysis and β represents dynamic shear amplification factor.

Mean dynamic shear amplification factor and mean dynamic shear amplification with ±1 standard deviation have been presented in Figures 3.19 and 3.20 respectively for R_y= 4.0.

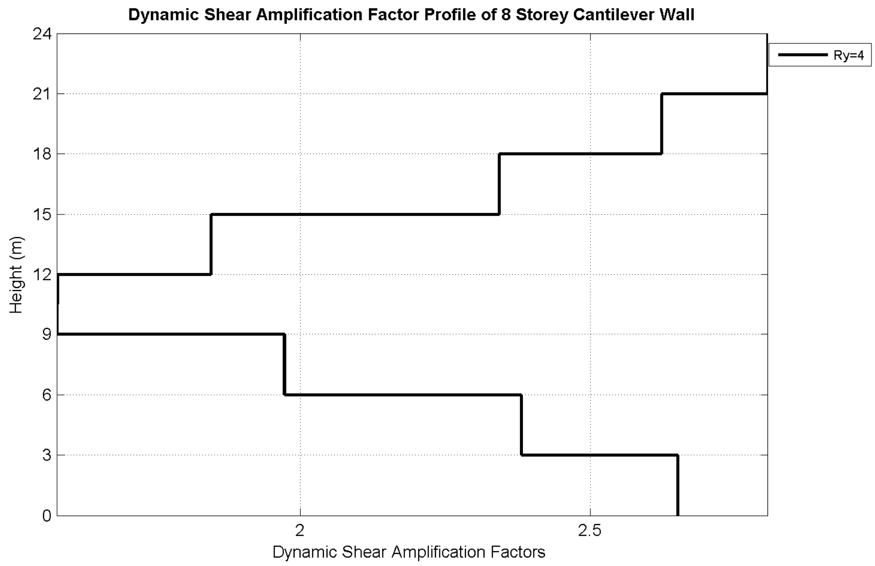

Figure 3.18. Storey mean dynamic shear amplification factor diagram of eight storey wall $R_y = 4.0$

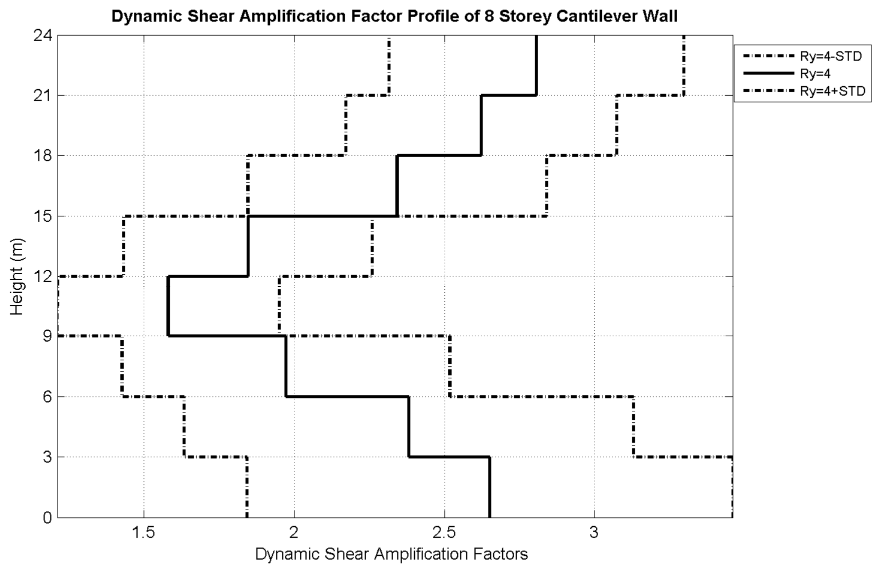

Figure 3.19. Storey mean dynamic shear amplification factor diagram and ±1 standard deviation of eight storey wall $R_y = 4.0$

3.1.7. Mean Response Results For All R_y Values

Mean response results of eight storey structural wall with R_y = 1.0, 2.0, 3.0, 4.0, 5.0, 6.are collectively presented in Figures 3.21 to 3.31.

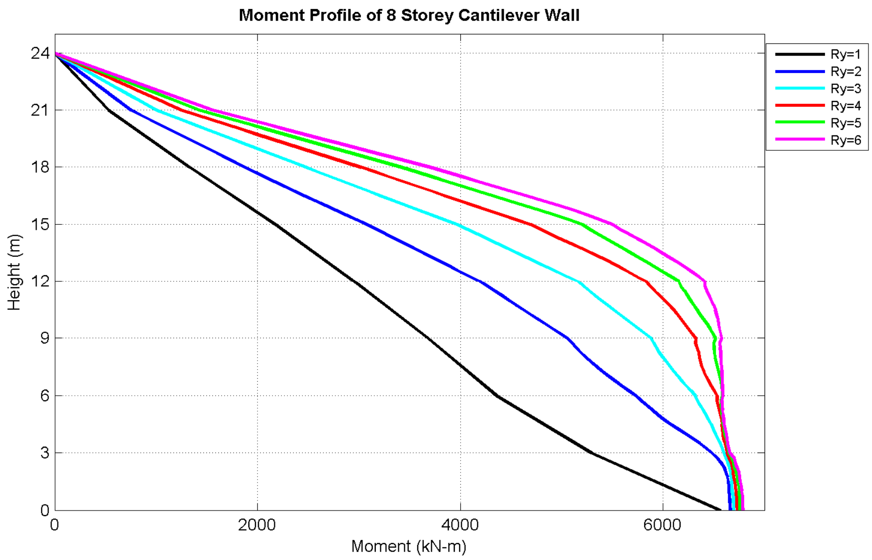

Figure 3.20. Storey moment diagrams of eight storey wall with strength level R_y = 1.0, 2.0, 3.0, 4.0, 5.0, 6.0

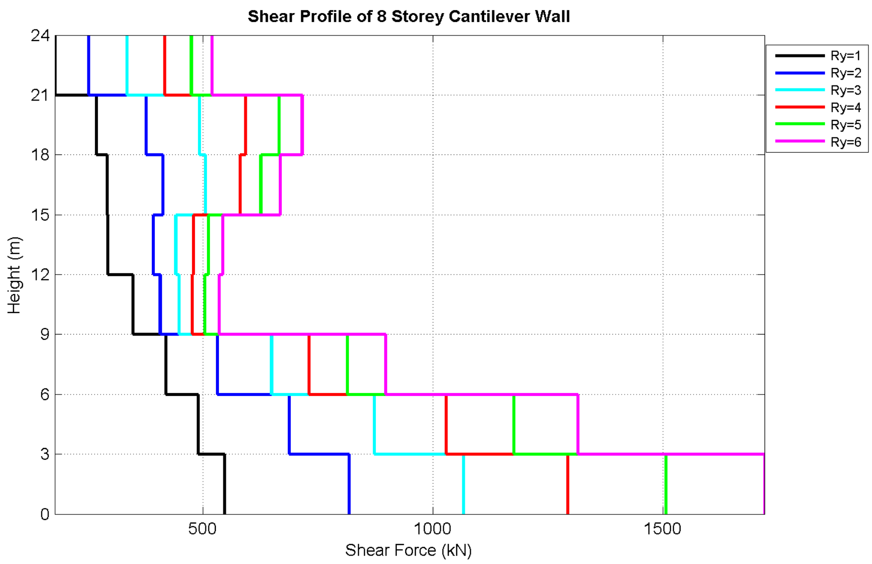

Figure 3.21. Storey shear force diagrams of eight storey wall with strength level R_y = 1.0, 2.0, 3.0, 4.0, 5.0, 6.0

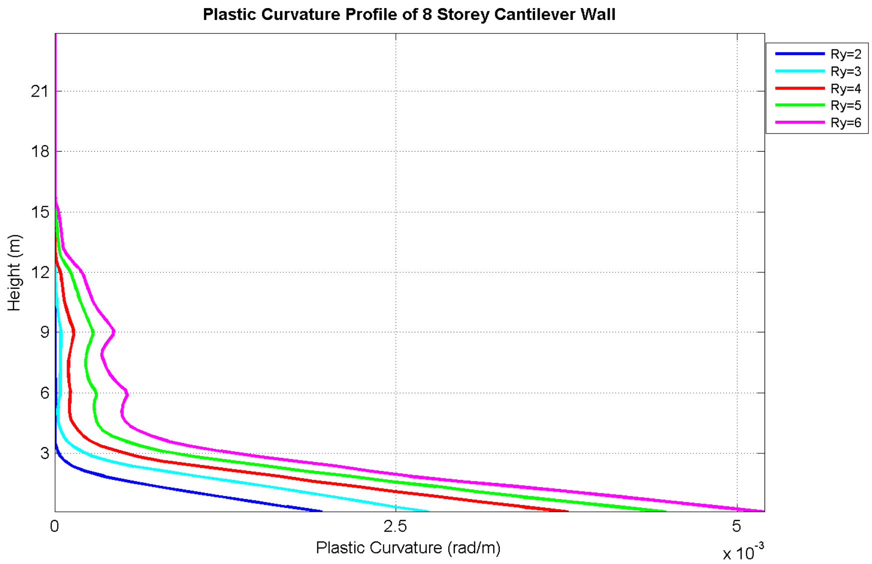

Figure 3.22. Storey plastic curvature diagrams of eight storey wall with strength level $R_y = 2.0, 3.0, 4.0, 5.0, 6.0$

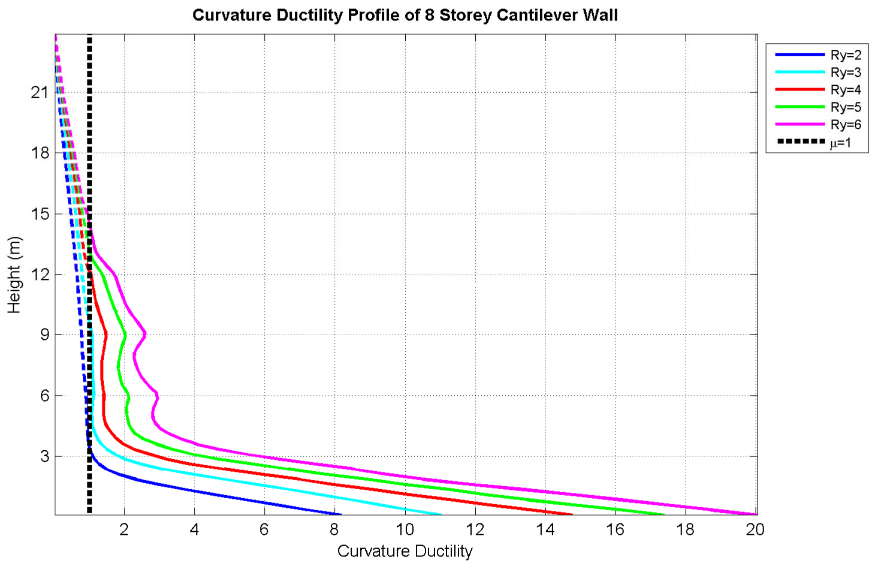

Figure 3.23. Storey curvature ductility diagrams of eight storey wall with strength level $R_y = 2.0, 3.0, 4.0, 5.0, 6.0$

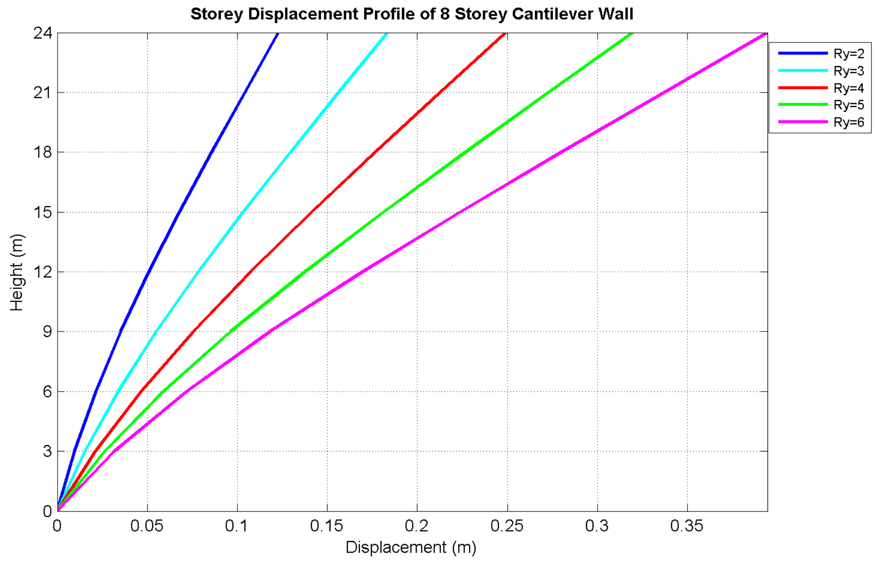

Figure 3.24. Storey displacement diagrams of eight storey wall with strength level $R_y = 2.0, 3.0, 4.0, 5.0, 6.0$

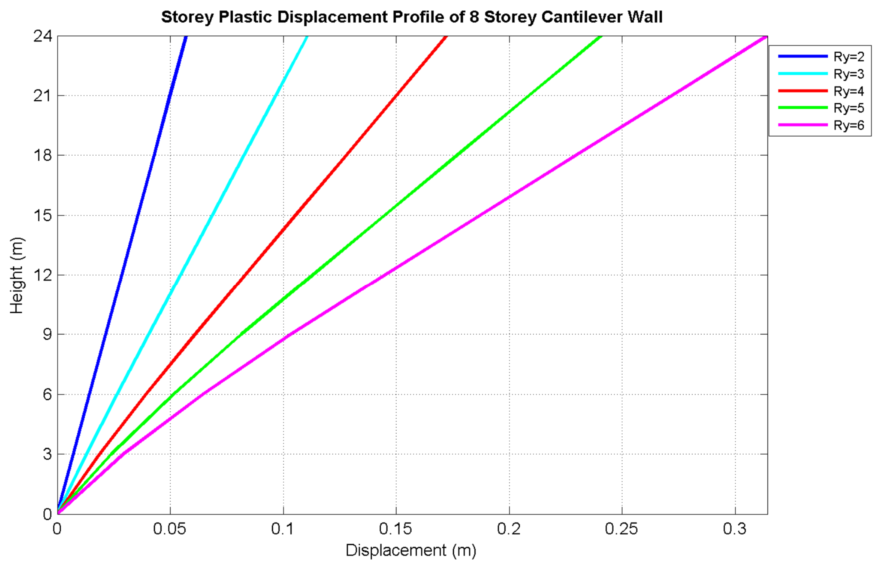

Figure 3.25. Storey plastic displacement diagrams of eight storey wall with strength level $R_y = 2.0, 3.0, 4.0, 5.0, 6.0$

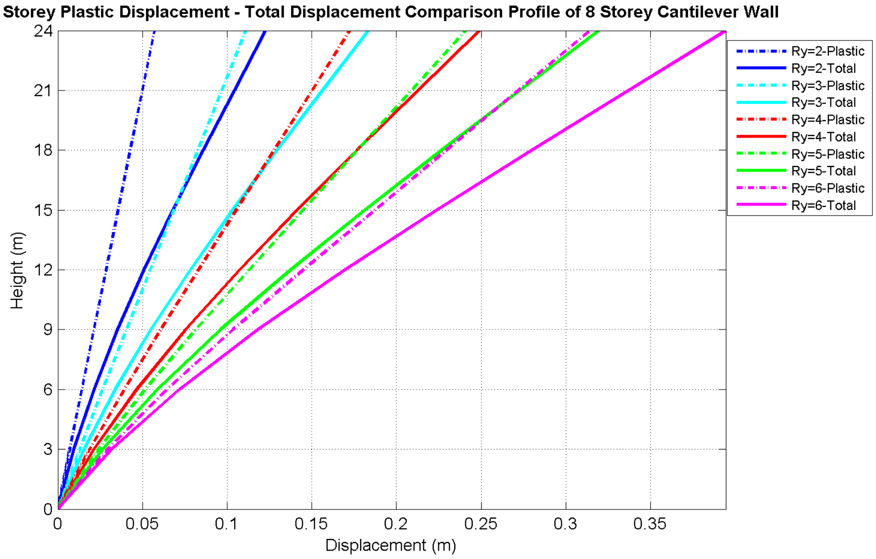

Figure 3.26. Storey total displacement - plastic displacement comparison diagrams of eight storey wall with strength level $R_y = 2.0, 3.0, 4.0, 5.0, 6.0$

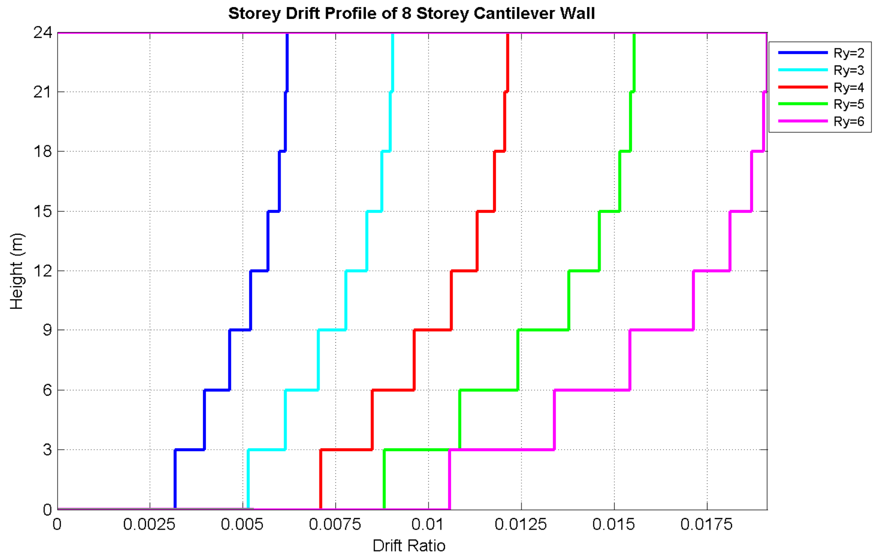

Figure 3.27. Storey drift ratio diagrams of eight storey wall with strength level $R_y = 2.0, 3.0, 4.0, 5.0, 6.0$

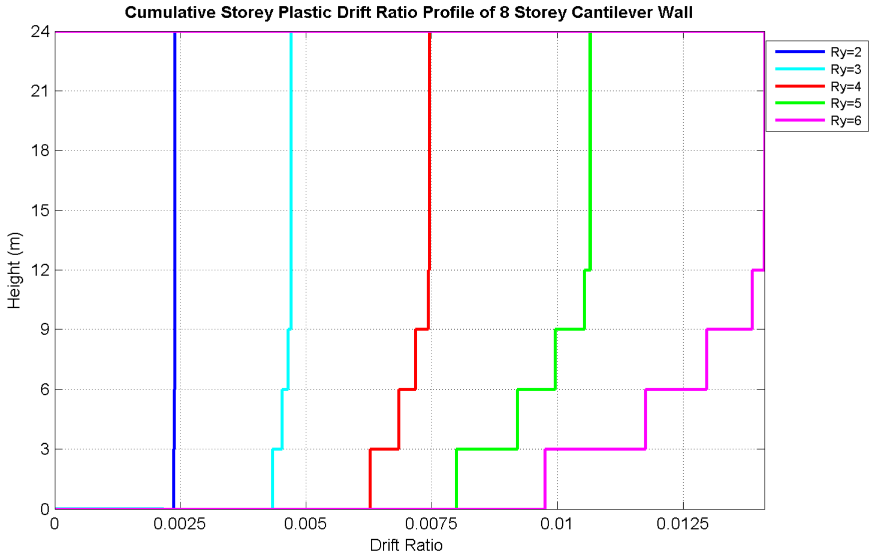

Figure 3.28. Storey cumulative plastic drift ratio diagrams of eight storey wall with strength level R_y = 2.0, 3.0, 4.0, 5.0, 6.0

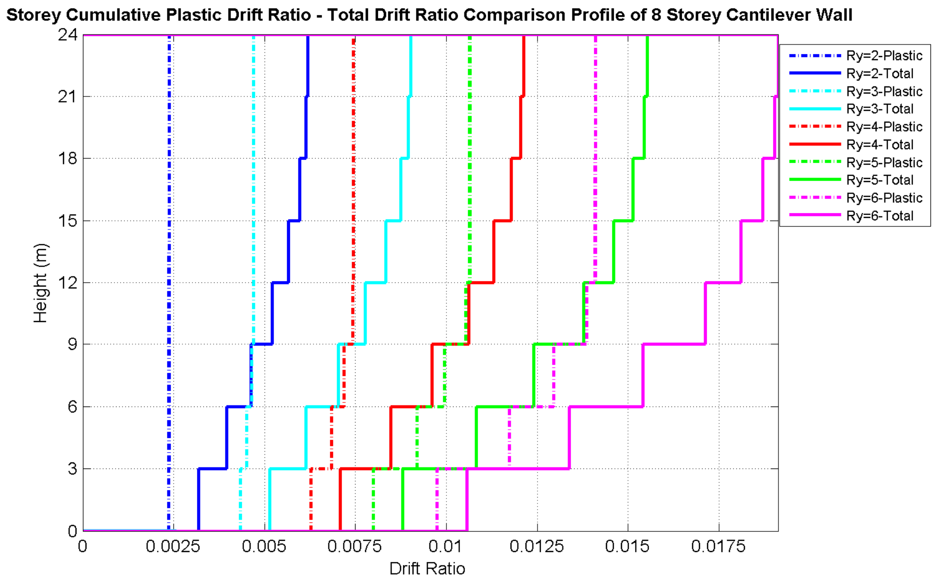

Figure 3.29. Storey drift ratio - cumulative plastic drift ratio comparison diagrams of eight storey wall with strength level R_y = 2.0, 3.0, 4.0, 5.0, 6.0

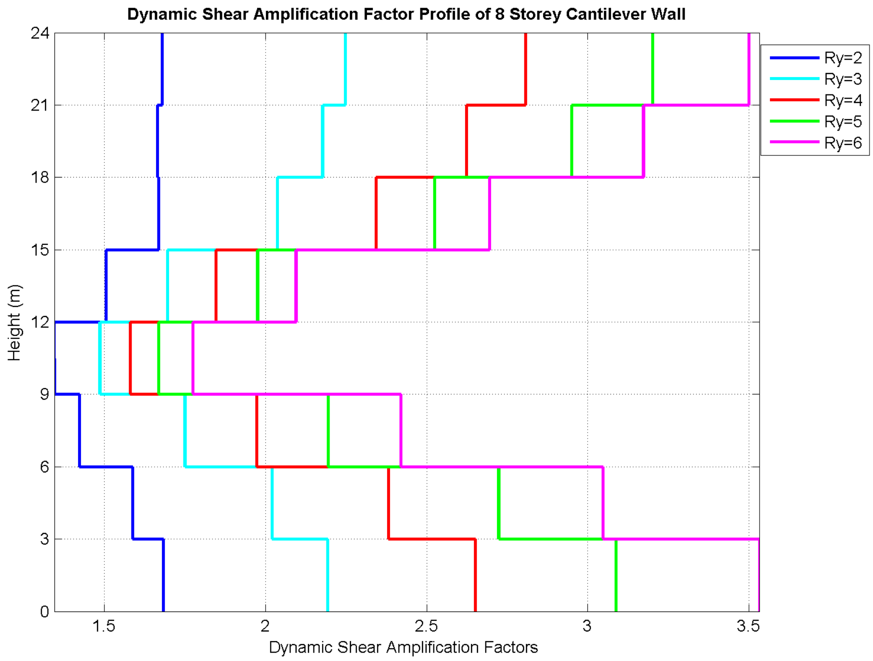

Figure 3.30. Storey dynamic shear amplification factor diagrams of eight storey wall with strength level R_y = 2.0, 3.0, 4.0, 5.0, 6.0

3.1.8. Dynamic Base Shear Amplification Factors

Dynamic base shear amplification factors in relation with wall height and yield strength reduction factors have been given in Table 3.4.

.

Table 3.4. Dynamic base shear amplification factors in relation with R_y and wall height

	β				
	R_y				
WALL	**2**	**3**	**4**	**5**	**6**
4 STOREY	1.49	1.76	2.00	2.43	2.82
8 STOREY	1.68	2.19	2.65	3.09	3.53
12 STOREY	1.58	2.02	2.44	2.84	3.20
16 STOREY	1.52	1.97	2.39	2.78	3.16

Dynamic shear amplification variations depending on cracked section elastic first mode period and yield strength reduction factors given in Table 3.4 have been presented in Figure 3.32.

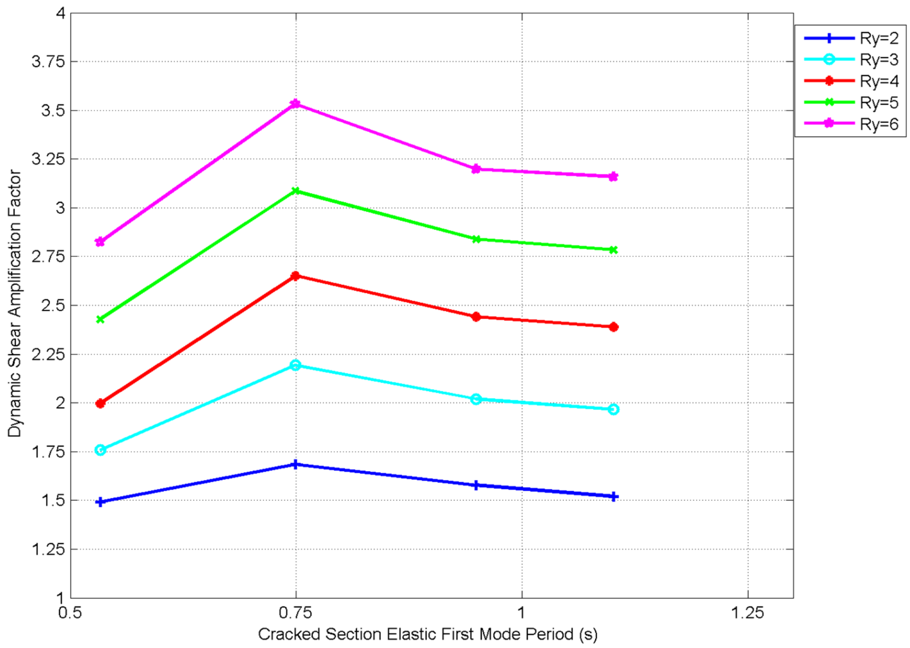

Figure 3.31. Storey dynamic shear amplification factor variation due to R_y and cracked section elastic first mode period

Numerical results obtained from the present study have been compared with the proposed dynamic shear amplification values by Celep (2008) and Rutenberg *et al.,* (2006) in Figure 3.33 and Figure 3.34. It is obvious that depending on major factors such as modeling procedure, selection of ground motions, ground motion scaling procedure; dynamic base shear amplification factors differ in various studies. Proposed relationship by Celep (2008) is in better agreement with amplification factors obtained in the present study for structures with longer cracked section elastic first mode periods compared to Rutenberg *et al.,* (2006) relationship.

Since yield strength reduction factors have been taken into account in the present study, an over strength factor of 1.5 has been considered for comparison with the relationships proposed by Celep (2008) and Rutenberg *et al.,*(2006), i.e. $R_y = R/1.5$ is assumed where R is the strength reduction factor considered by Celep(2008) and Rutenberg *et al.,* (2006).

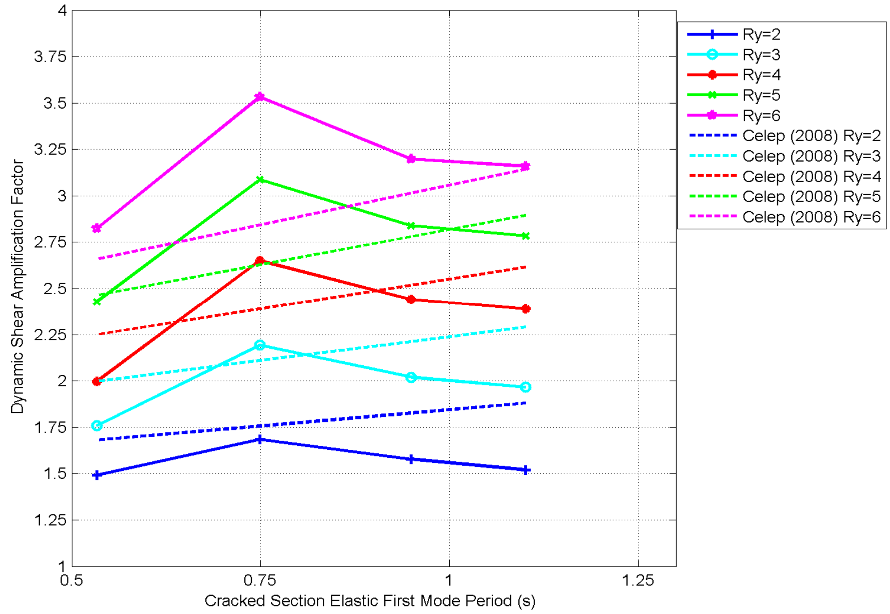

Figure 3.32. Comparison of storey dynamic shear amplification factor variation with Celep (2008) Study

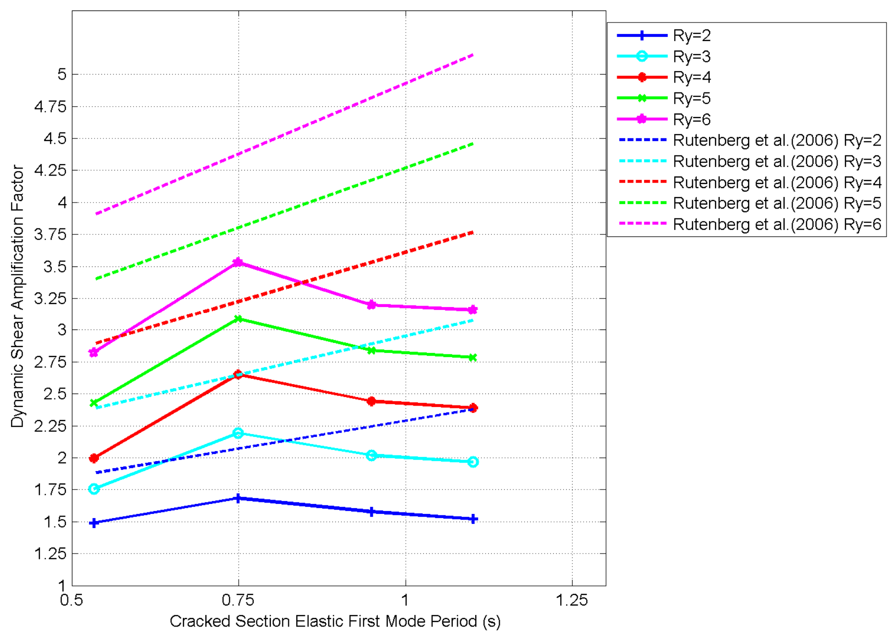

Figure 3.33. Comparison of storey dynamic shear amplification factor variation with Rutenberg *et al.,* (2006) study

3.2. Remarks on Results Obtained from Non-Linear Time-history Analyses

Following points have been observed through the information obtained from the non-linear time-history analyses results:

i) Maximum shear forces have been observed at the base of the wall as expected.

ii) Although storey moments tend to reach yield moments at higher stories extending approximately to half the wall height, significant plastic deformations have been observed to be limited to the first 4. meters from the base of the wall (~H_w/6). (Eight Storey Wall, $R_y = 4.0$)

iii) Maximum shear force profiles have a tendency of decreasing at the mid stories and re-increasing at the upper stories.

iv) Moment, shear, plastic curvature, total and plastic displacement, total and plastic drift ratios, shear amplification factor responses increase with increasing yield strength reduction factors.

v) Calculated base shear amplification factors not always increase with increasing period values as it has been stated in some of other studies.

vi) Dynamic base shear amplification factors obtained from the analyses of the present study are slightly greater than relationship results proposed by Celep (2008) relationship.

vii) Maximum value of the drift ratio agrees well with that defined in Turkish Seismic Design Code 2007 clause 2.10.1.3, $\frac{(\delta_i)_{\max}}{h_i} \leq 0.02$) with some exceptions observed for four storey walls.

4. CONCLUSIONS

Shear amplification phenomena in earthquake resistant design of multistory structures has been recently investigated and included in national seismic codes. Recent studies show that due to dynamic effects, maximum wall shear responses during an earthquake are generally higher than the conventional code procedures which can be attributed to contribution of higher mode effects subsequent to the formation of plastic hinge at base of wall.

It can be observed that current design codes have a weakness in shear design of structural walls. For compensating the needs of this issue, shear amplification factors have been proposed by design codes such as Turkish Seismic Design Code (2007) in which shear amplification factor has been taken as 1.5 regardless of first mode period and ductility of the structural wall.

Analyses in this study have shown that amplification factors have dependence on first mode periods and strength reduction factors of the structural walls. As stated in different studies amplification factors have the tendency to increase by increasing first mode periods and strength reduction factors. However, in the present study different results have been observed in terms of first mode periods, in which shear amplification factors tend to relatively decrease with higher periods.

It is observed that shear forces are augmented at upper part of the walls which can be attributed to higher mode effects as well. Therefore, amplification factors get high values.

It is observed that storey moments tend to reach yield moments at higher stories with small plastic deformation values. Significant plastic deformations have been observed to form approximately the bottom $H_w/6$ from the base of the. This finding fully supports the definition of critical wall height given by Turkish Seismic Design Code (2007).

Seismic shear amplification in structural walls is an open research area in need of further studies. There is still insufficient information about more complex structures such as dual systems (Structural walls plus frame systems) and coupled wall systems. Sophisticated non-linear modeling techniques such as fiber modeling techniques may improve the conclusion regarding dynamic shear amplification. Numerical studies should be carried out together with the laboratory tests for accomplishing a general methodology to represent a more realistic behaviour of reinforced concrete walls.

APPENDIX A: ACCELERATION TIME HISTORIES OF GROUND MOTIONS AND SCALE FACTORS FOR LINEAR SCALING OF GROUND MOTIONS

Ground motions used in the study are listed below in Table A.1 and presented in Figures A.1 to A.10.

Table A.1. Ground Motion Parameters Used In Structural Analysis

No.	**Date**	**Earthquake Name**	**Magnitude (M_s)**	**Station Name**	**Station Number**	**NEHRP Site Class**	**Dist (km)**	**Comp (deg)**	**PGA (g)**
1	02.09.1971	San Fernando	6.5	Lake Hughes Array Station 12	128	C	17	21	-0.353
2	02.09.1971	San Fernando	6.5	Lake Hughes Array Station 9	127	A/B	26.6	291	-0.112
3	10.01.1987	Whittier	6.1	Inglewood Union Oil Yard	14196	C	22.5	0	0.251
4	01.17.1994	Northridge	6.8	Los Angeles City Terrace	24592	A/B	37.1	90	0.263
5	10.17.1989	Loma Prieta	7.1	Coyote Lake Dam Downstream	57504	C	21.7	285	0.178
6	10.17.1989	Loma Prieta	7.1	Coyote Lake Dam Downstream	57504	C	30.9	195	0.158
7	02.09.1971	San Fernando	6.5	Pasadena CIT Cal Tech Seismo Lab	266	A/B	25.5	270	0.202
8	10.17.1989	Loma Prieta	7.1	Gilroy #6 San Ysidro Microwave Site	57383	C	19.9	90	0.170
9	10.17.1989	Loma Prieta	7.1	Gilroy #6 San Ysidro Microwave Site	57383	C	35.2	0	0.114
10	01.17.1994	Northridge	6.1	San Marino SW Academy	24401	C	39.3	90	0.125

Tables A.2 to A.5 contains numerical results obtained from linear scaling procedure. Maximum base moment value has been shown bold at all tables.

Table A.2. Scale factors for earthquakes in result of linear scaling procedure for 4 storey wall

EQ No.	$M_{b,e}$ (*kN-m*)	Scale Factors
1	1569	2.034
2	1182	2.700
3	2195	1.454
4	2155	1.481
5	**3191**	1.000
6	2017	1.582
7	1507	2.117
8	2331	1.369
9	1839	1.735
10	1495	2.134

Table A.3. Scale factors for earthquakes in result of linear scaling procedure for eight storey wall

EQ No.	$M_{b,e}$ (*kN-m*)	Scale Factors
1	4543	1.442
2	3404	1.925
3	5200	1.260
4	4790	1.368
5	**6551**	1.000
6	5223	1.254
7	6161	1.063
8	4525	1.448
9	4763	1.375
10	3309	1.980

Table A.4. Scale factors for earthquakes in result of linear scaling procedure for twelve storey wall

EQ No.	$M_{b,e}$ (*kN-m*)	Scale Factors
1	12160	1.096
2	7542	1.767
3	6334	2.105
4	10880	1.225
5	11480	1.161
6	12380	1.077
7	11100	1.201
8	**13330**	1.000
9	11530	1.156
10	8389	1.589

Table A.5. Scale factors for earthquakes in result of linear scaling procedure for sixteen storey wall

EQ No.	$M_{b,e}$ (*kN-m*)	Scale Factors
1	17390	1.345
2	13890	1.684
3	7812	2.994
4	17270	1.354
5	15900	1.471
6	16240	1.440
7	14500	1.613
8	**23390**	1.000
9	17200	1.360
10	8365	2.796

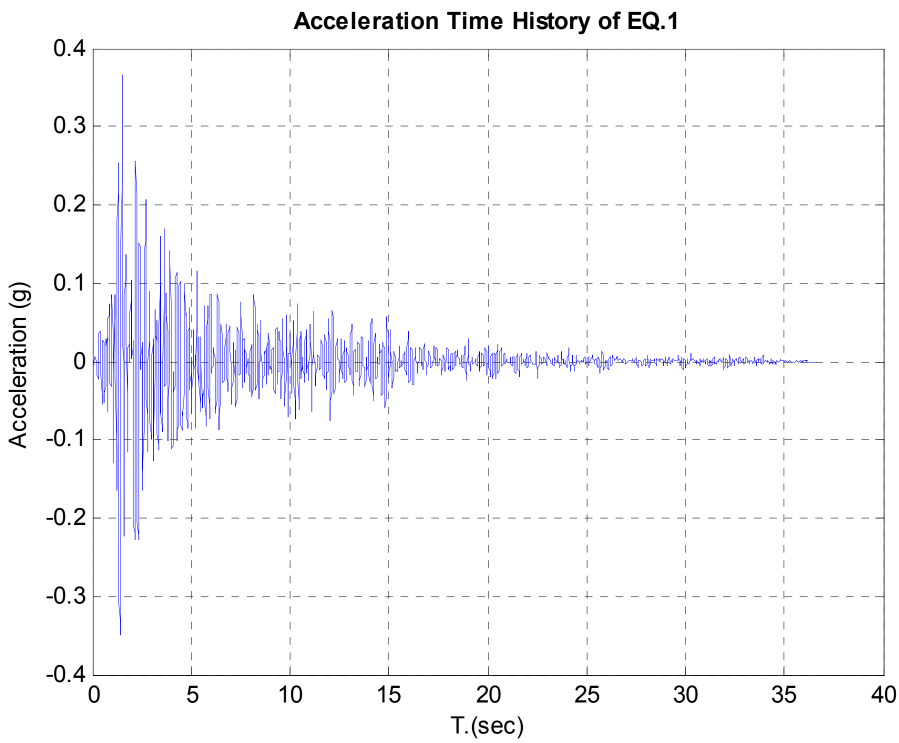

Figure A1. Acceleration time-history of earthquake 1

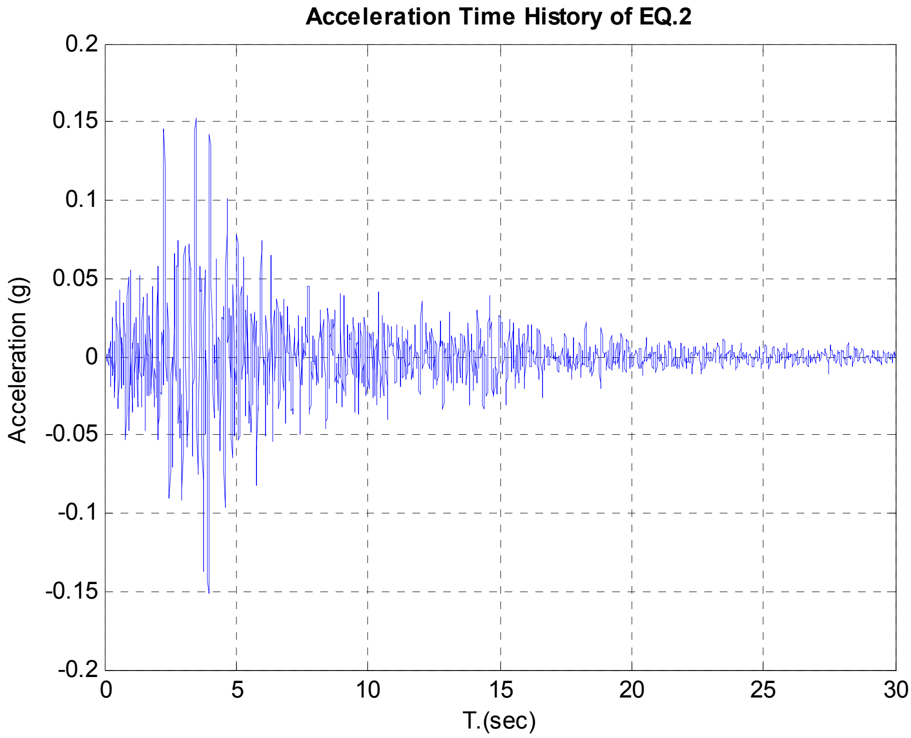

Figure A2. Acceleration time-history of earthquake 2

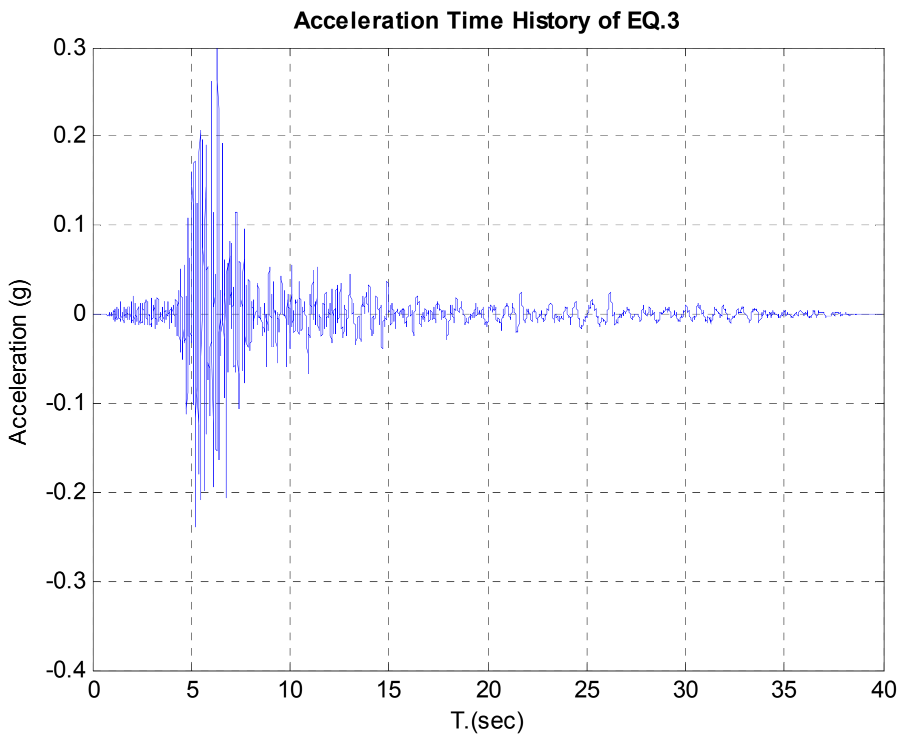

Figure A3. Acceleration time-history of earthquake 3

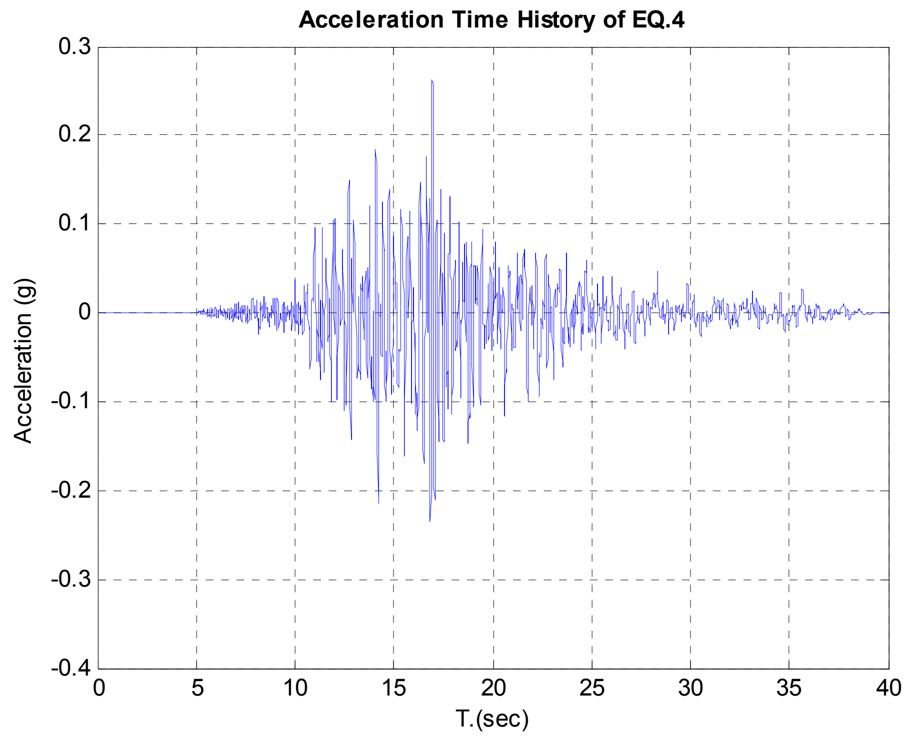

Figure A4. Acceleration time-history of earthquake 4

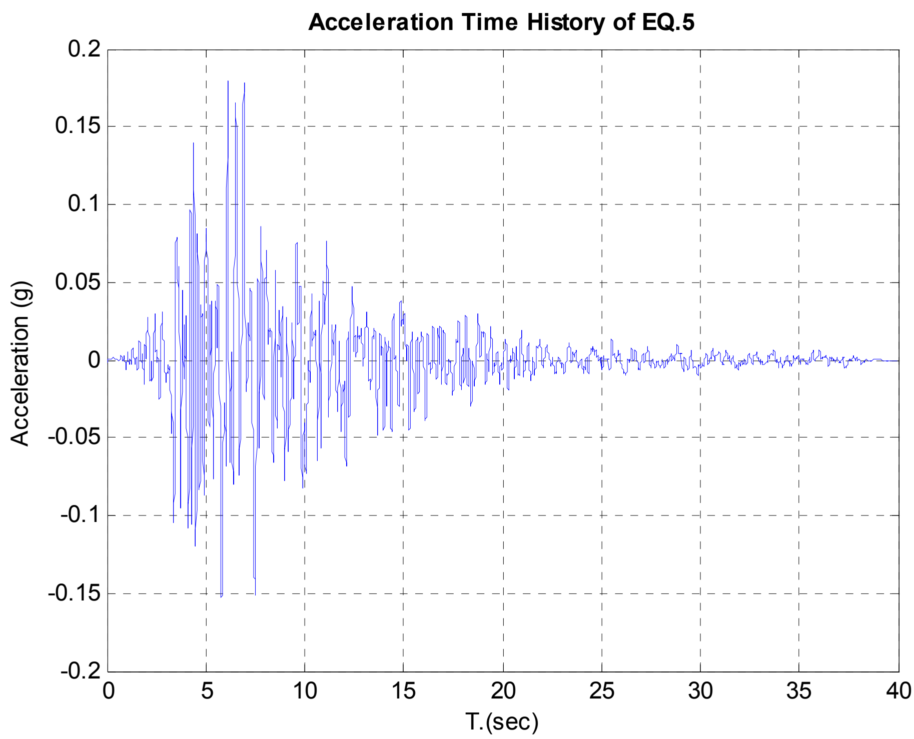

Figure A5. Acceleration time-history of earthquake 5

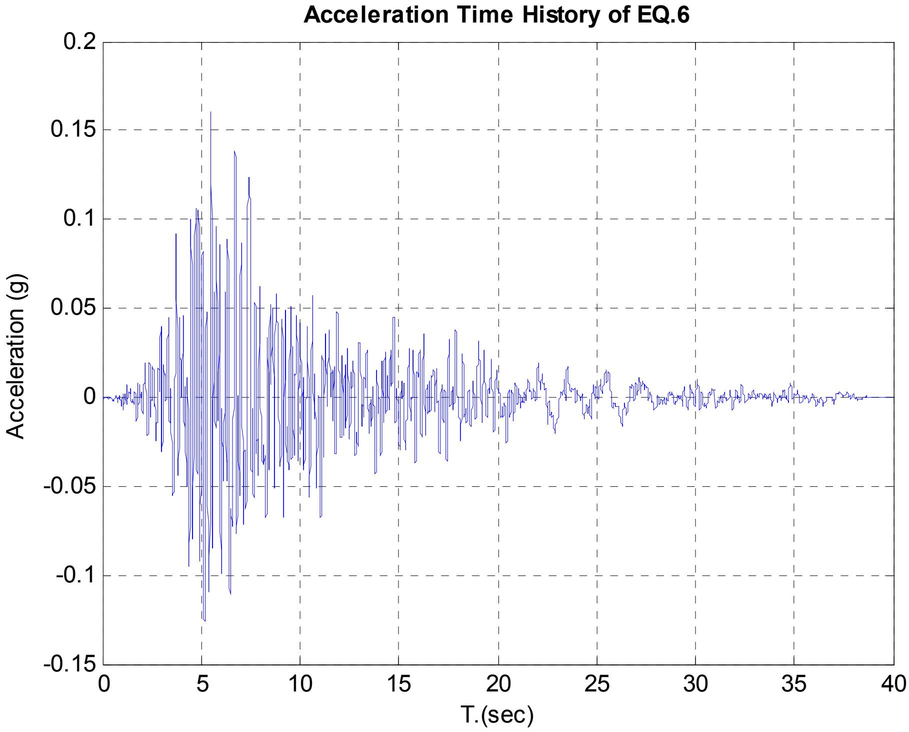

Figure A6. Acceleration time-history of earthquake 6

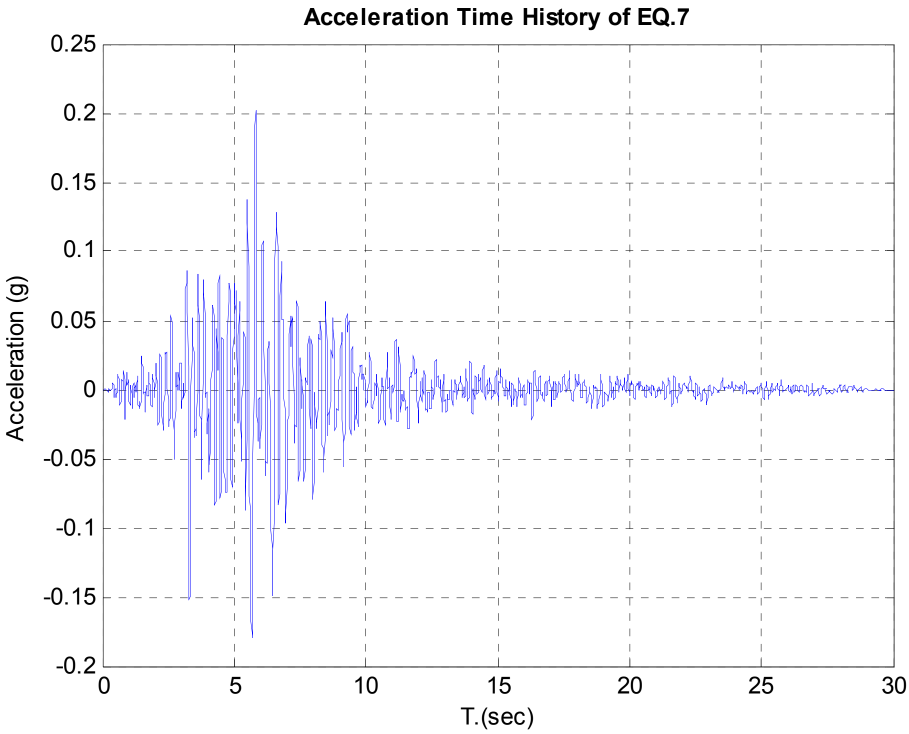

Figure A7. Acceleration time-history of earthquake 7

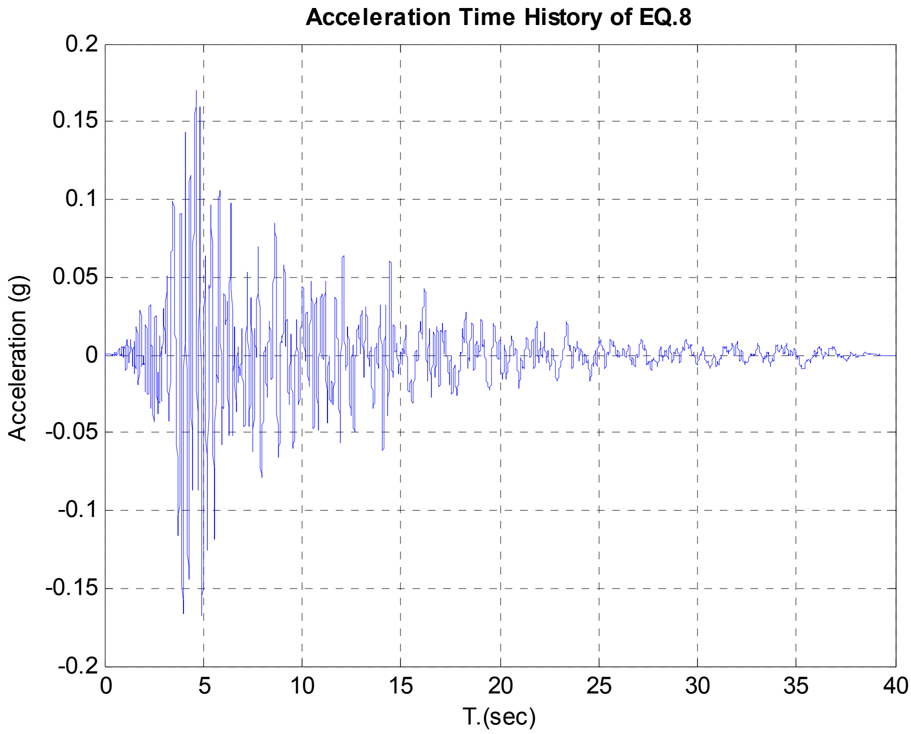

Figure A8. Acceleration time-history of earthquake 8

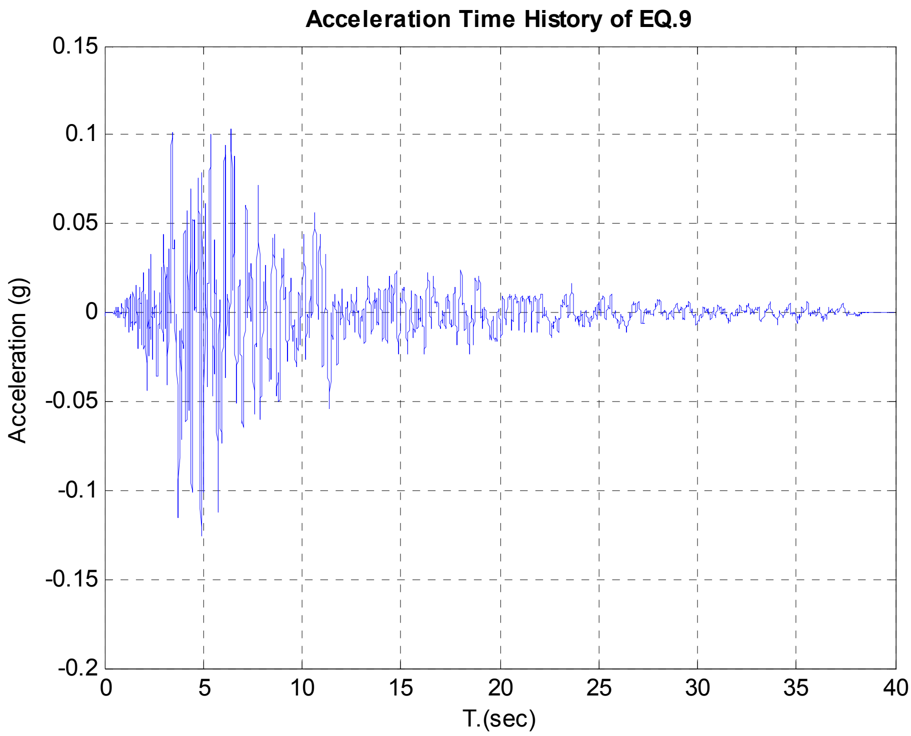

Figure A9. Acceleration time-history of earthquake 9

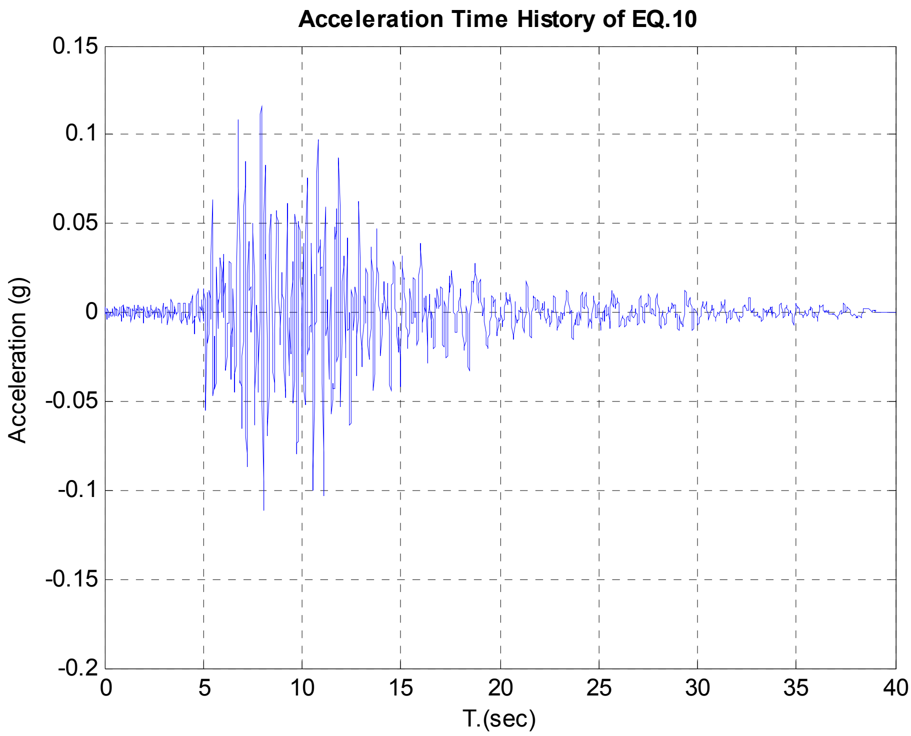

Figure A10. Acceleration time-history of earthquake 10

APPENDIX B: NON-LINEAR RESPONSES OF SELECTED STRUCTURAL WALLS

B.1.1 Four Storey Structural Wall (R_y = 2.0)

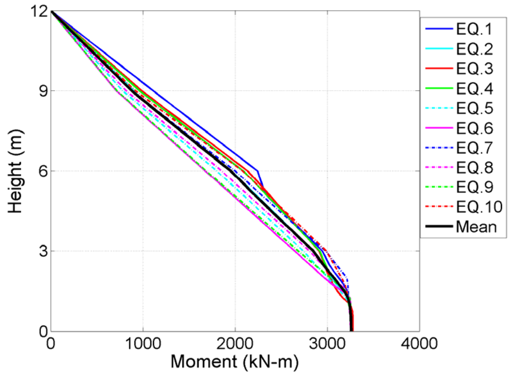

Figure B.1. Storey moment diagrams - four storey wall R_y = 2.0

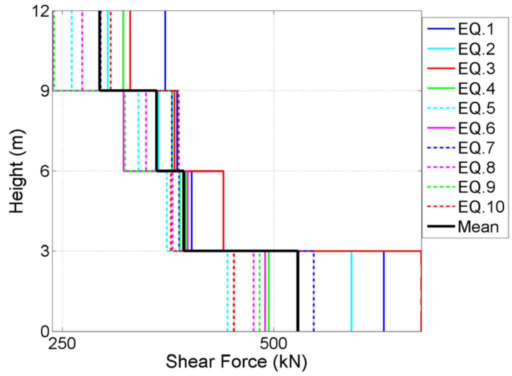

Figure B.3. Storey shear force diagrams - four storey wall R_y = 2.0

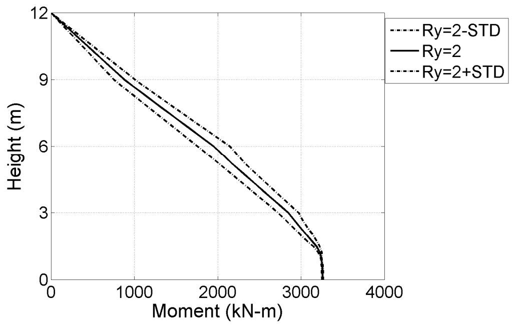

Figure B.2. Storey mean moment diagram and ±1 standard deviation of four storey wall R_y = 2.0

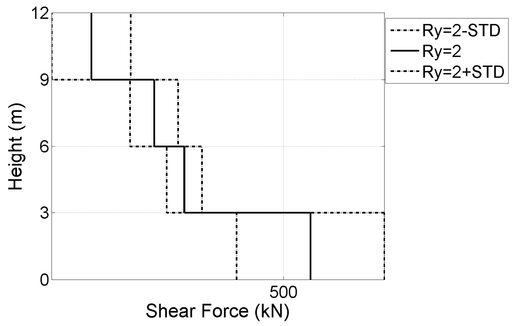

Figure B.4. Storey mean shear force diagram and ±1 standard deviation of four storey wall R_y = 2.0

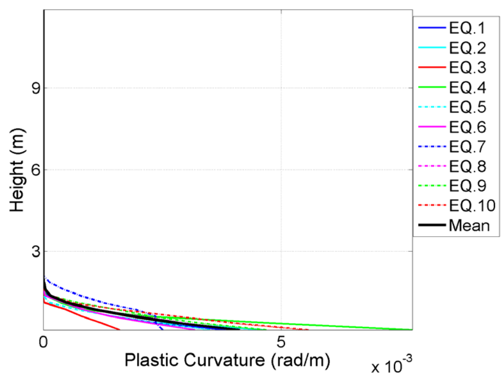

Figure B.5. Storey plastic curvature diagrams - four storey wall $R_y = 2.0$

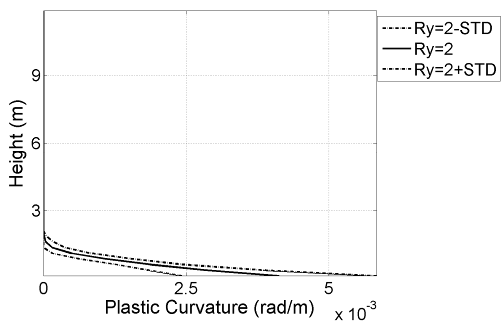

Figure B.6. Storey mean plastic curvature diagram and ±1 standard deviation of four storey wall $R_y = 2.0$

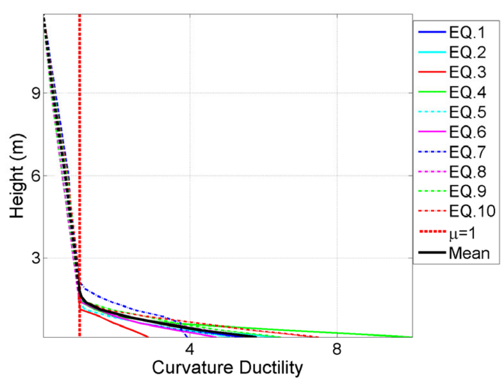

Figure B.7. Storey curvature ductility diagrams - four storey wall $R_y = 2.0$

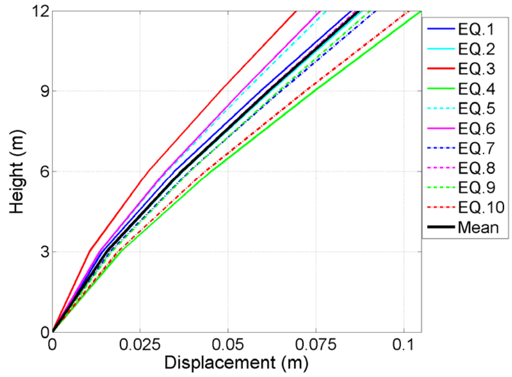

Figure B.8. Storey displacement diagrams - four storey wall $R_y = 2.0$

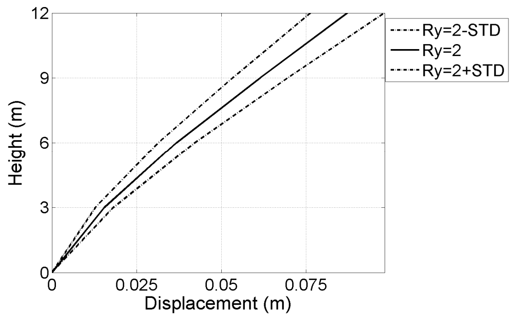

Figure B.9. Mean storey displacement diagram and ±1 standard deviation of four storey wall $R_y = 2.0$

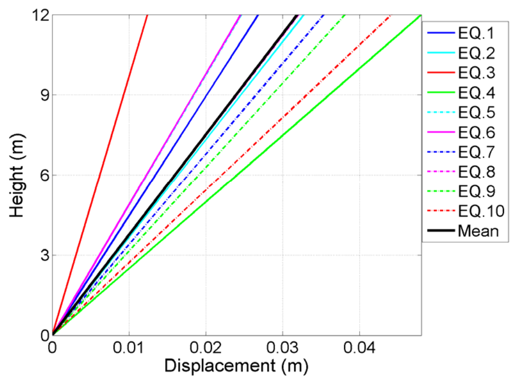

Figure B.10. Storey plastic displacement diagrams - four storey wall $R_y = 2.0$

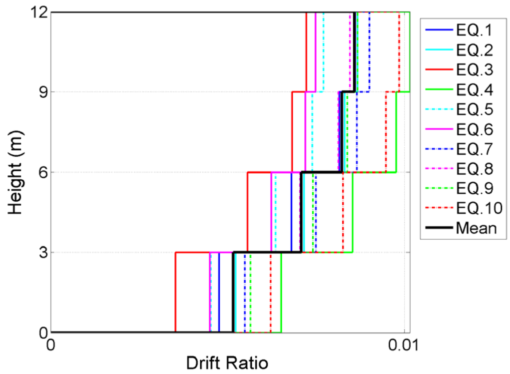

Figure B.11. Storey drift ratio diagrams - four storey wall $R_y = 2.0$

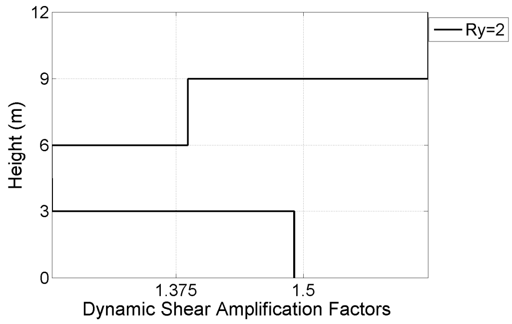

Figure B.14. Storey dynamic shear amplification factor diagrams - four storey wall $R_y = 2.0$

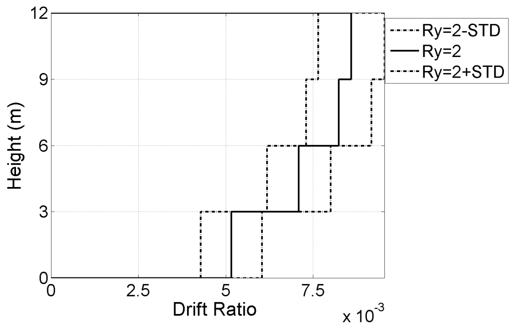

Figure B.12. Mean storey drift ratio diagram and ±1 standard deviation of four storey wall $R_y = 2.0$

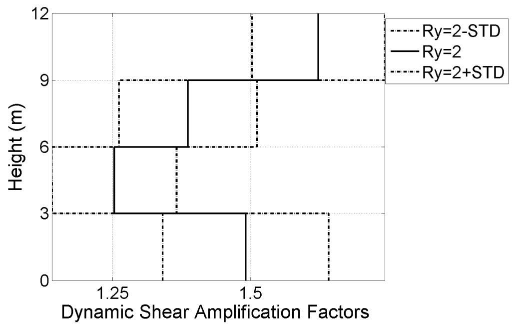

Figure B.15. Mean dynamic shear amplification factor diagram and ±1 standard deviation of four storey wall $R_y = 2.0$

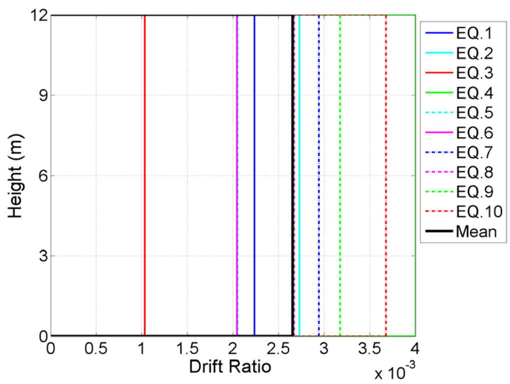

Figure B.13. Storey cumulative plastic drift ratio diagrams - four storey wall $R_y = 2.0$

B.1.2 Four Storey Structural Wall (R_y = 3.0)

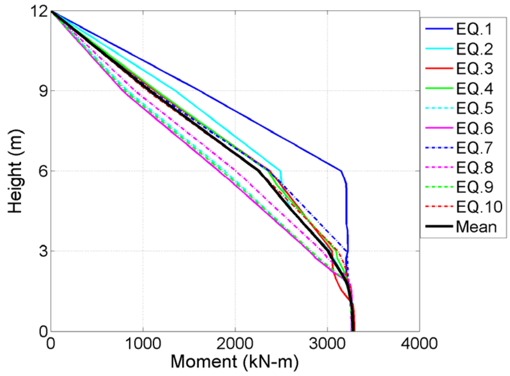

Figure B.16. Storey moment diagrams - four storey wall R_y = 3.0

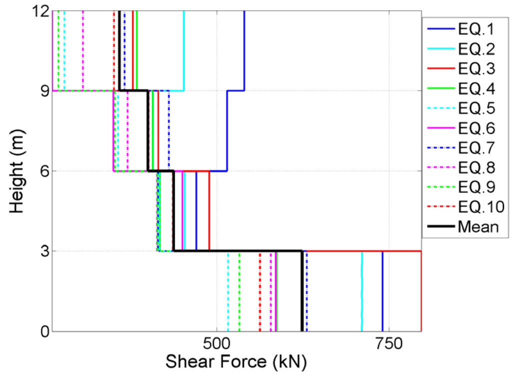

Figure B.18. Storey shear force diagrams - four storey wall R_y = 3.0

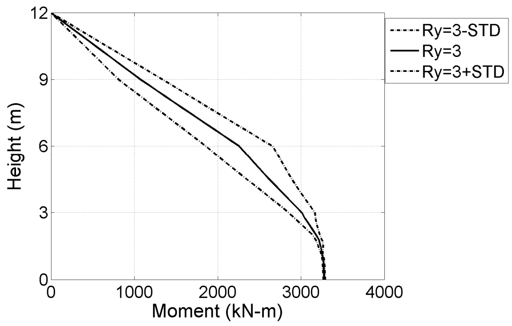

Figure B.17. Storey mean moment diagram and ±1 standard deviation of four storey wall R_y = 3.0

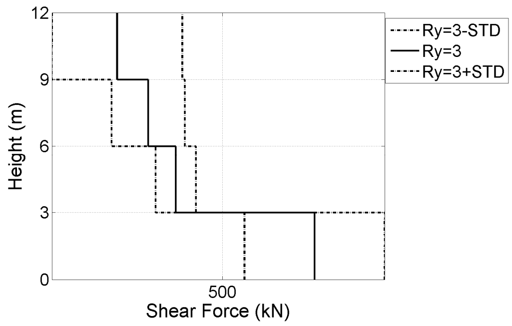

Figure B.19. Storey mean shear force diagram and ±1 standard deviation of four storey wall R_y = 3.0

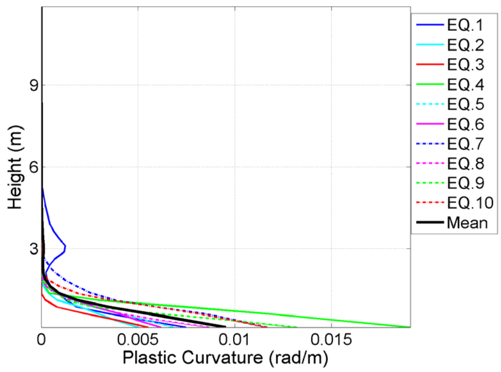

Figure B.20. Storey plastic curvature diagrams - four storey wall $R_y = 3.0$

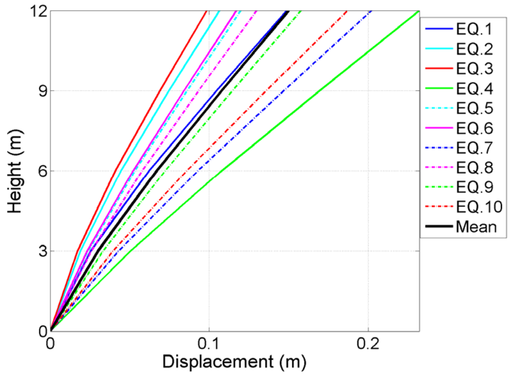

Figure B.23. Storey displacement diagrams - four storey wall $R_y = 3.0$

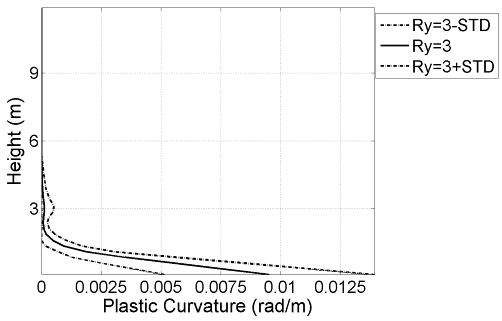

Figure B.21. Storey mean plastic curvature diagram and ±1 standard deviation of four storey wall $R_y = 3.0$

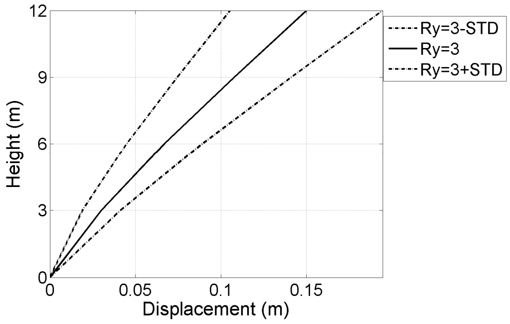

Figure B.24. Mean storey displacement diagram and ±1 standard deviation of four storey wall $R_y = 3.0$

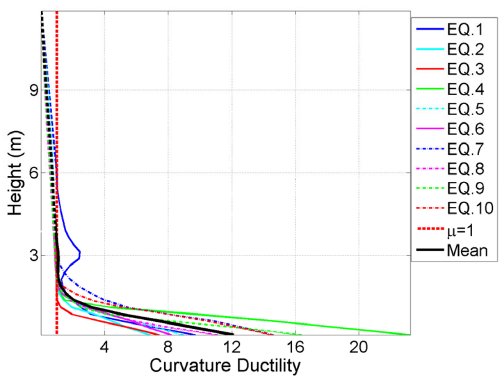

Figure B.22. Storey curvature ductility diagrams - four storey wall $R_y = 3.0$

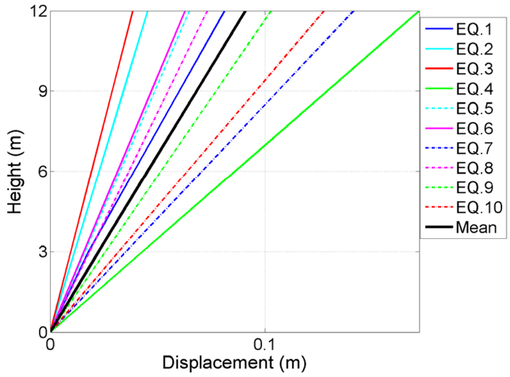

Figure B.25. Storey plastic displacement diagrams - four storey wall $R_y = 3.0$

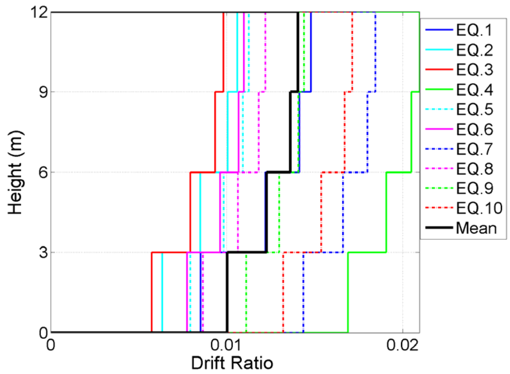

Figure B.26. Storey drift ratio diagrams - four storey wall $R_y = 3.0$

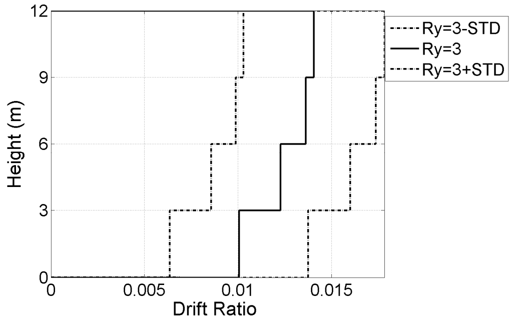

Figure B.27. Mean storey drift ratio diagram and ±1 standard deviation of four storey wall $R_y = 3.0$

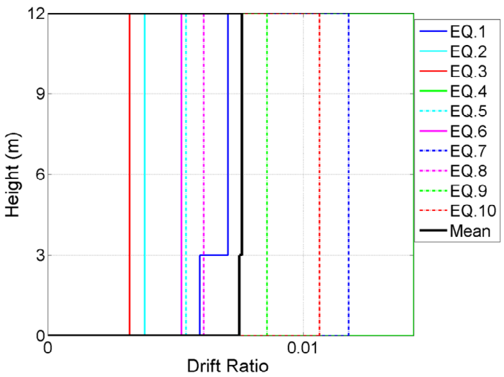

Figure B.28. Storey cumulative plastic drift ratio diagrams - four storey wall $R_y = 3.0$

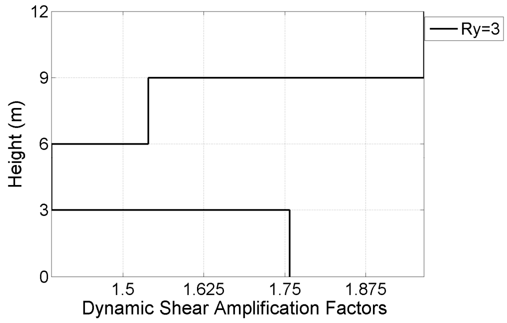

Figure B.29. Storey dynamic shear amplification factor diagrams - four storey wall $R_y = 3.0$

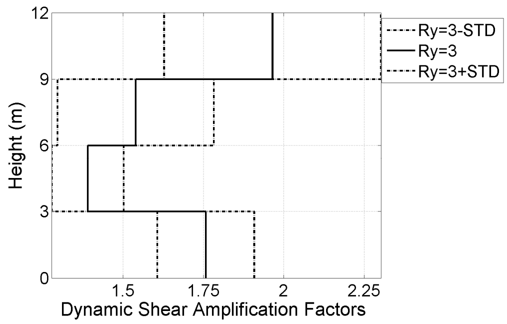

Figure B.30. Mean dynamic shear amplification factor diagram and ±1 standard deviation of four storey wall $R_y = 3.0$

B.1.3 Four Storey Structural Wall (R_y = 4.0)

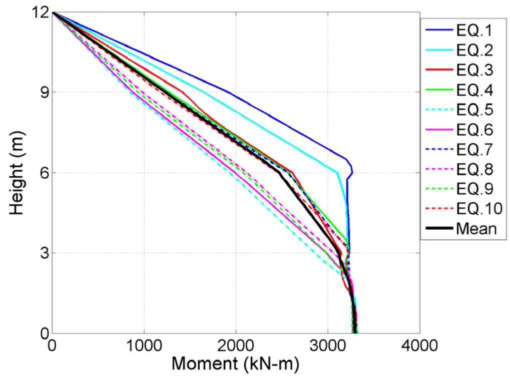

Figure B.31. Storey moment diagrams - four storey wall R_y = 4.0

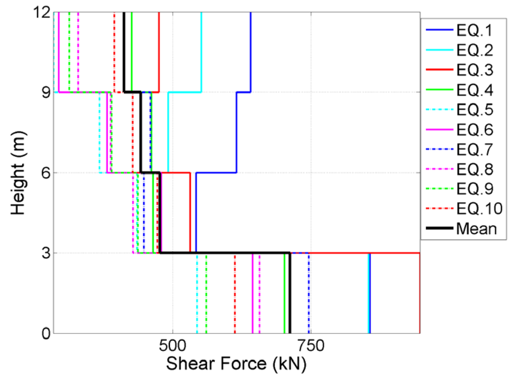

Figure B.33. Storey shear force diagrams - four storey wall R_y = 4.0

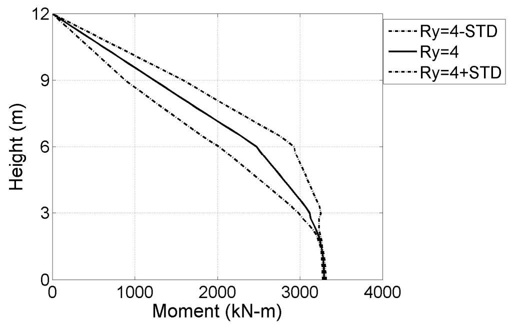

Figure B.32. Storey mean moment diagram and ±1 standard deviation of four storey wall R_y = 4.0

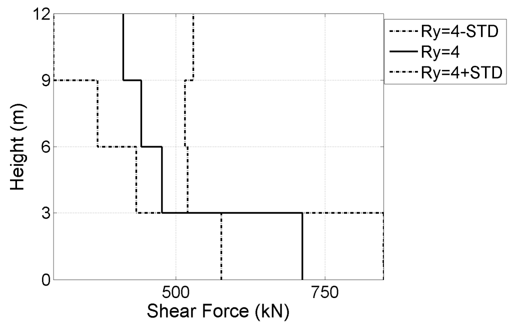

Figure B.34. Storey mean shear force diagram and ±1 standard deviation of four storey wall R_y = 4.0

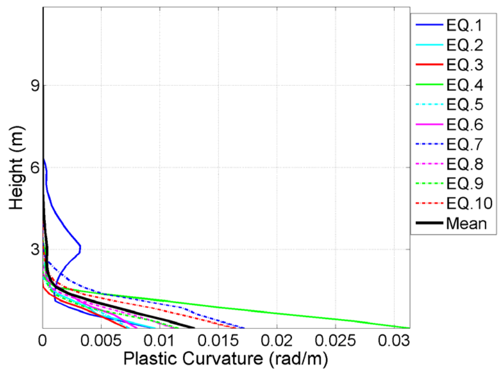

Figure B.35. Storey plastic curvature diagrams - four storey wall $R_y = 4.0$

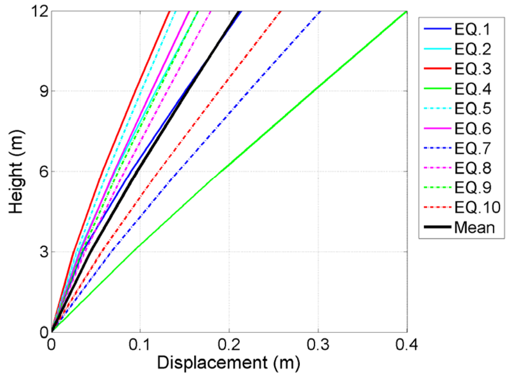

Figure B.38. Storey displacement diagrams - four storey wall $R_y = 4.0$

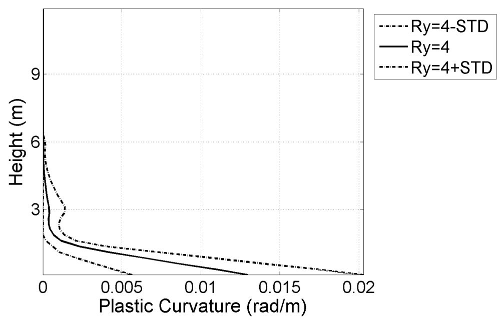

Figure B.36. Storey mean plastic curvature diagram and ±1 standard deviation of four storey wall $R_y = 4.0$

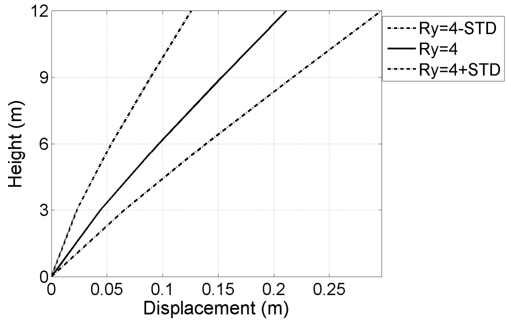

Figure B.39. Mean storey displacement diagram and ±1 standard deviation of four storey wall $R_y = 4.0$

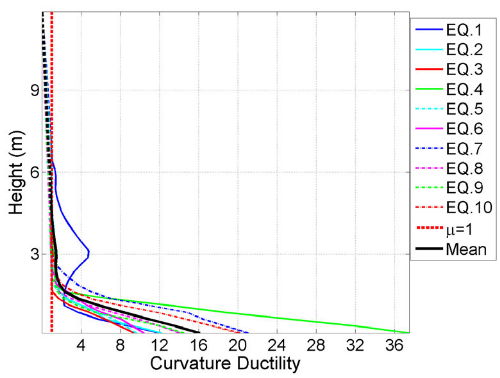

Figure B.37. Storey curvature ductility diagrams - four storey wall $R_y = 4.0$

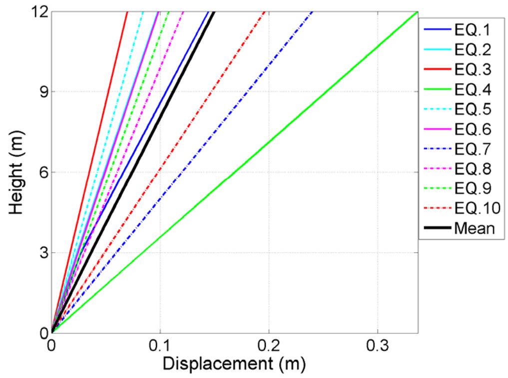

Figure B.40. Storey plastic displacement diagrams - four storey wall $R_y = 4.0$

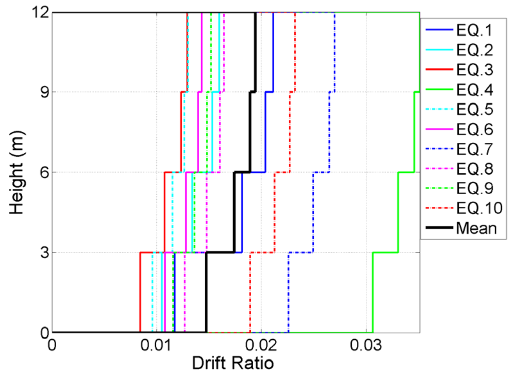

Figure B.41. Storey drift ratio diagrams - four storey wall $R_y = 4.0$

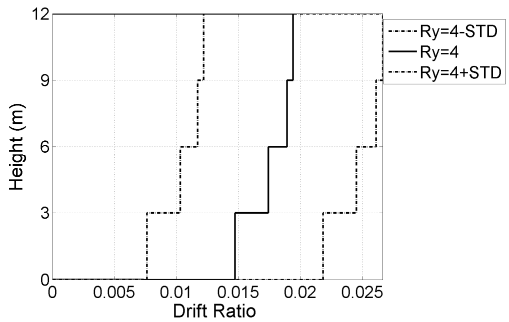

Figure B.42. Mean storey drift ratio diagram and ±1 standard deviation of four storey wall $R_y = 4.0$

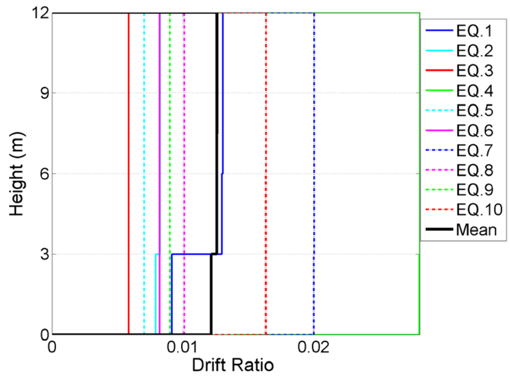

Figure B.43. Storey cumulative plastic drift ratio diagrams - four storey wall $R_y = 4.0$

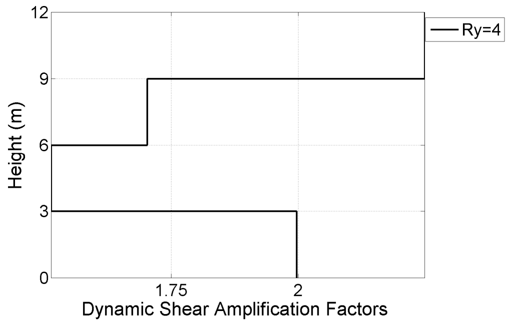

Figure B.44. Storey dynamic shear amplification factor diagrams - four storey wall $R_y = 4.0$

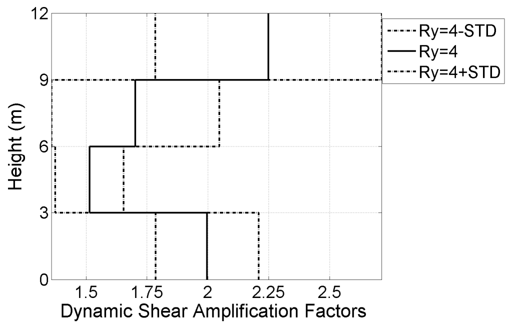

Figure B.45. Mean dynamic shear amplification factor diagram and ±1 standard deviation of four storey wall $R_y = 4.0$

B.1.4 Four Storey Structural Wall (R_y = 5.0)

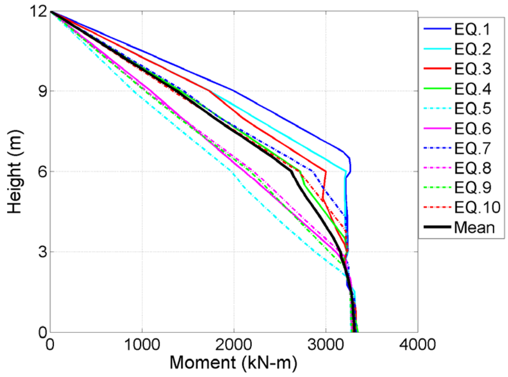

Figure B.46. Storey moment diagrams - four storey wall R_y = 5.0

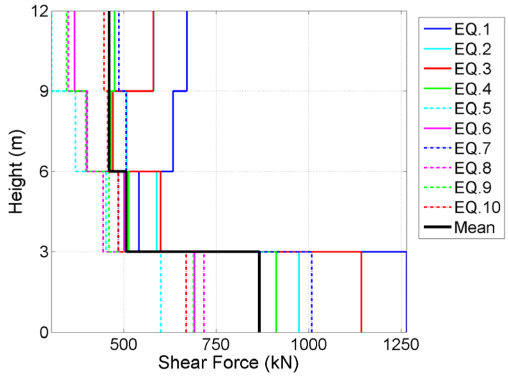

Figure B.48. Storey shear force diagrams - four storey wall R_y = 5.0

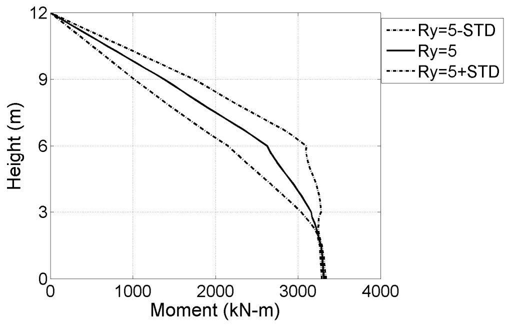

Figure B.47. Storey mean moment diagram and ±1 standard deviation of four storey wall R_y = 5.0

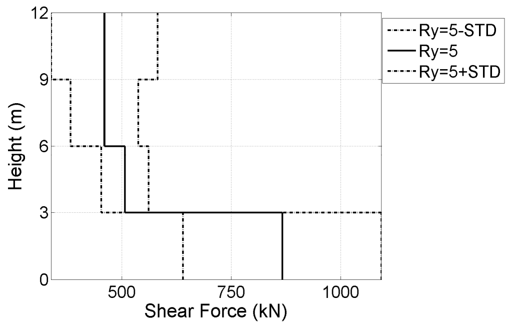

Figure B.49. Storey mean shear force diagram and ±1 standard deviation of four storey wall R_y = 5.0

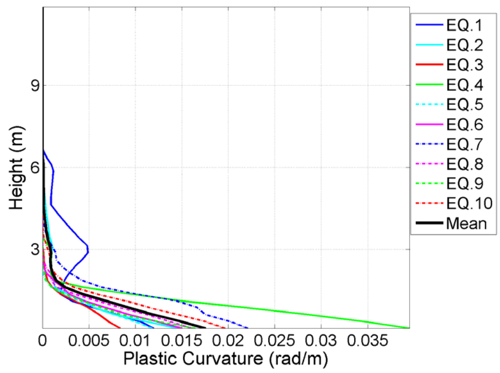

Figure B.50. Storey plastic curvature diagrams - four storey wall $R_y = 5.0$

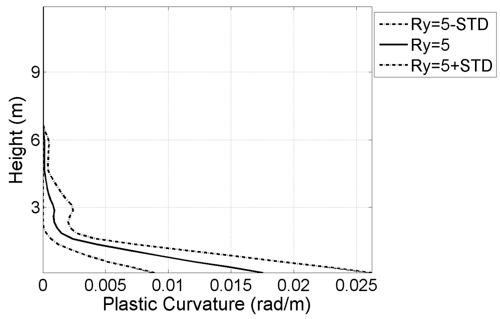

Figure B.51. Storey mean plastic curvature diagram and ±1 standard deviation of four storey wall $R_y = 5.0$

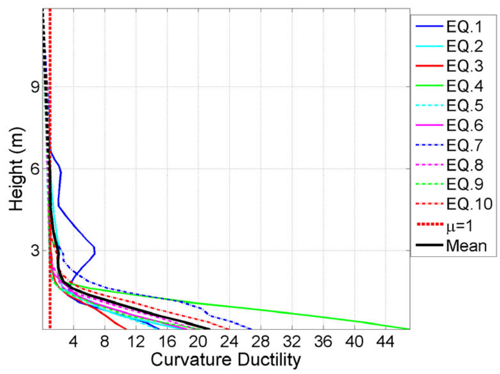

Figure B.52. Storey curvature ductility diagrams - four storey wall $R_y = 5.0$

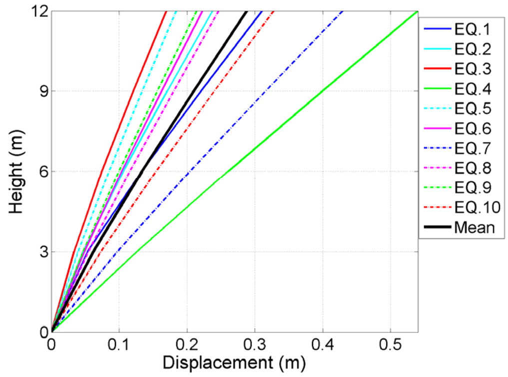

Figure B.53. Storey displacement diagrams - four storey wall $R_y = 5.0$

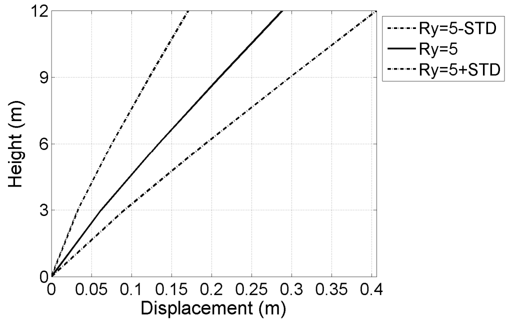

Figure B.54. Mean storey displacement diagram and ±1 standard deviation of four storey wall $R_y = 5.0$

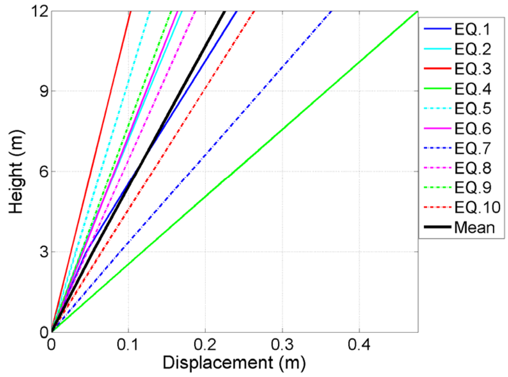

Figure B.55. Storey plastic displacement diagrams - four storey wall $R_y = 5.0$

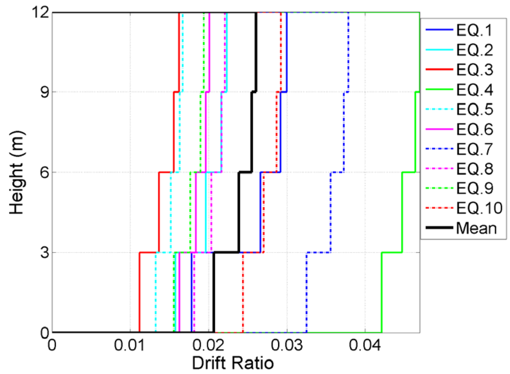

Figure B.56. Storey drift ratio diagrams - four storey wall $R_y = 5.0$

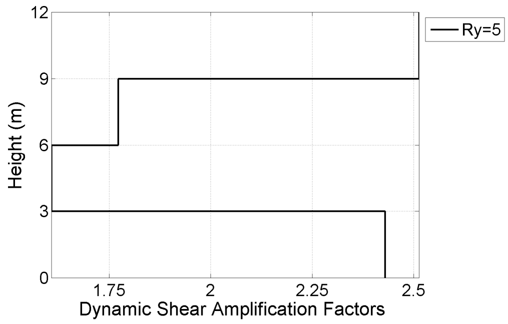

Figure B.59. Storey dynamic shear amplification factor diagrams - four storey wall $R_y = 5.0$

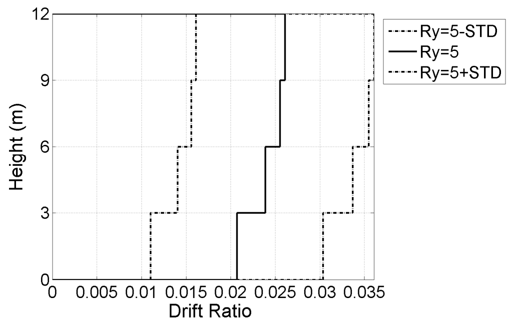

Figure B.57. Mean storey drift ratio diagram and ±1 standard deviation of four storey wall $R_y = 5.0$

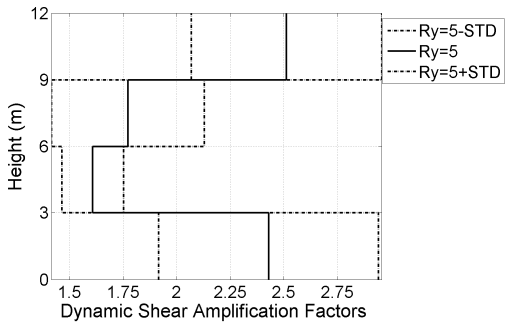

Figure B.60. Mean dynamic shear amplification factor diagram and ±1 standard deviation of four storey wall $R_y = 5.0$

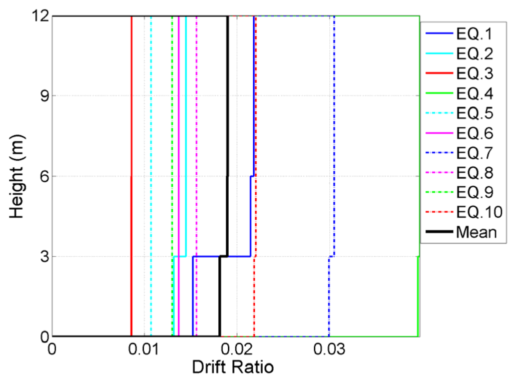

Figure B.58. Storey cumulative plastic drift ratio diagrams - four storey wall $R_y = 5.0$

B.1.5 Four Storey Structural Wall (R_y = 6.0)

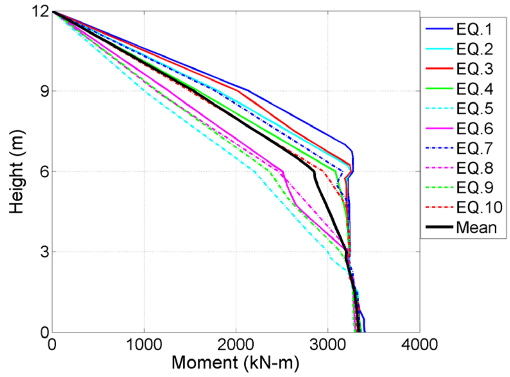

Figure B.61. Storey moment diagrams - four storey wall R_y = 6.0

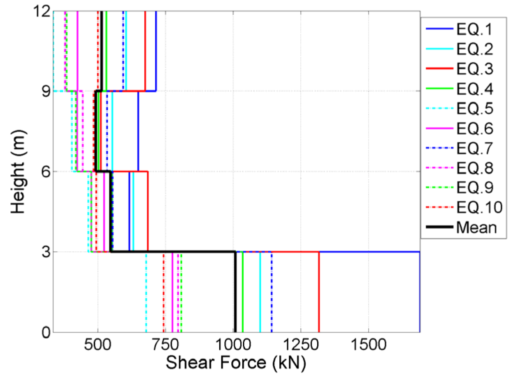

Figure B.63. Storey shear force diagrams - four storey wall R_y = 6.0

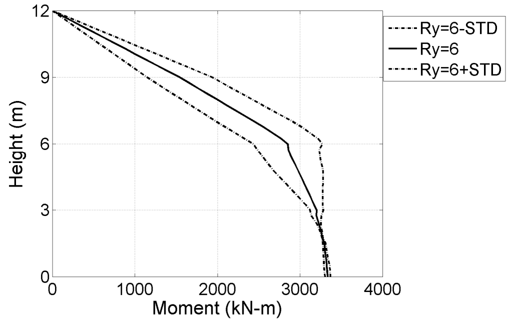

Figure B.62. Storey mean moment diagram and ±1 standard deviation of four storey wall R_y = 6.0

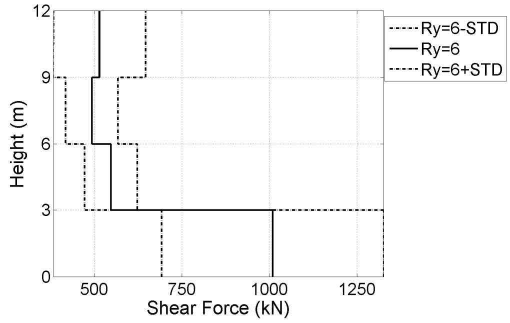

Figure B.64. Storey mean shear force diagram and ±1 standard deviation of four storey wall R_y = 6.0

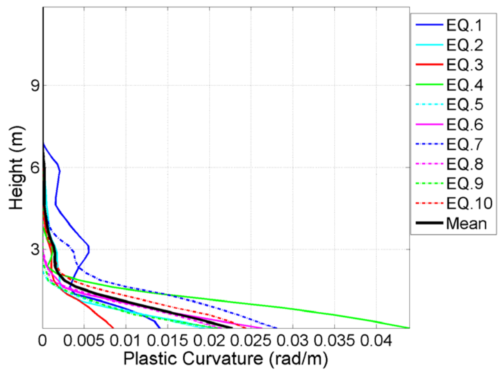

Figure B.65. Storey plastic curvature diagrams - four storey wall $R_y = 6.0$

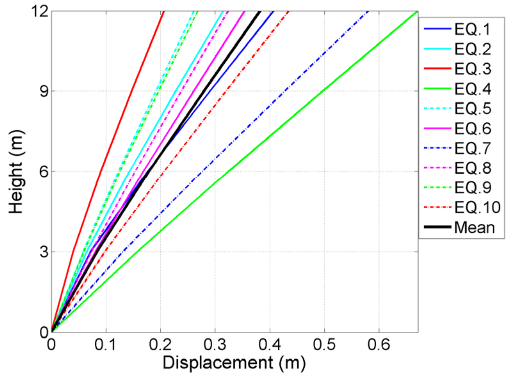

Figure B.68. Storey displacement diagrams - four storey wall $R_y = 6.0$

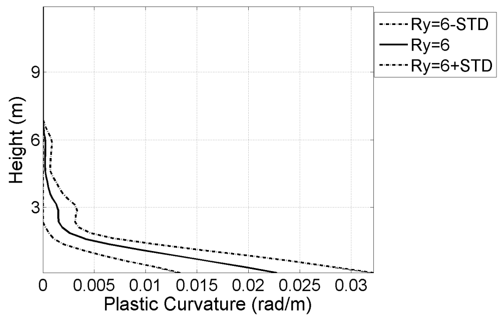

Figure B.66. Storey mean plastic curvature diagram and ±1 standard deviation of four storey wall $R_y = 6.0$

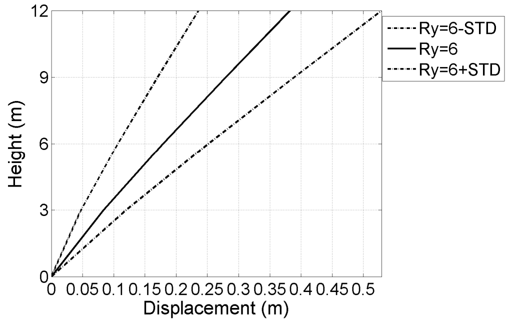

Figure B.69. Mean storey displacement diagram and ±1 standard deviation of four storey wall $R_y = 6.0$

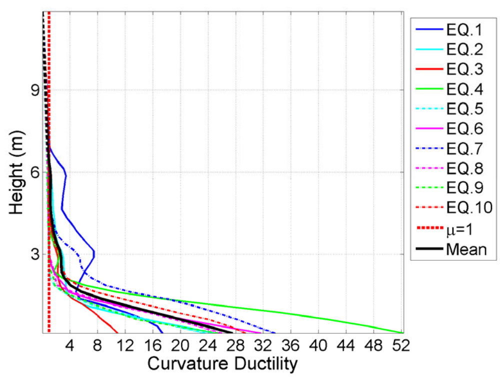

Figure B.67. Storey curvature ductility diagrams - four storey wall $R_y = 6.0$

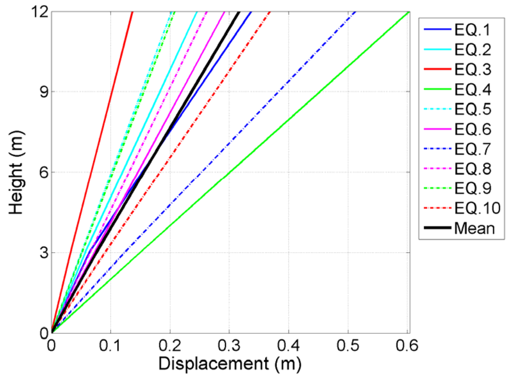

Figure B.70. Storey plastic displacement diagrams - four storey wall $R_y = 6.0$

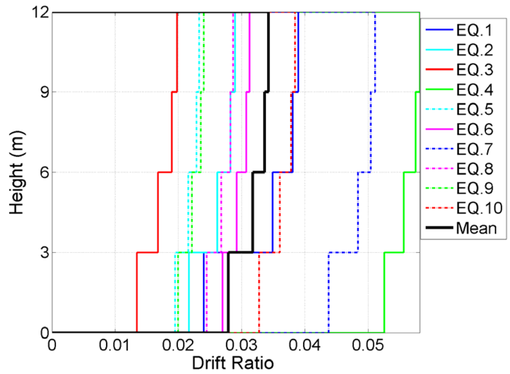

Figure B.71. Storey drift ratio diagrams - four storey wall $R_y = 6.0$

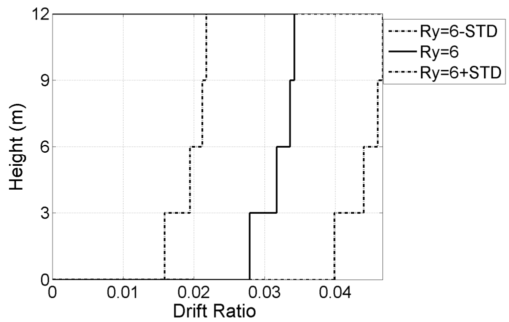

Figure B.72. Mean storey drift ratio diagram and ±1 standard deviation of four storey wall $R_y = 6.0$

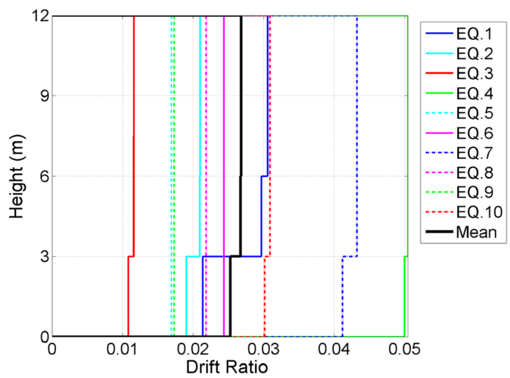

Figure B.73. Storey cumulative plastic drift ratio diagrams - four storey wall $R_y = 6.0$

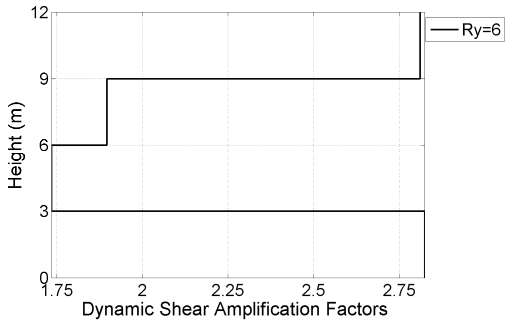

Figure B.74. Storey dynamic shear amplification factor diagrams - four storey wall $R_y = 6.0$

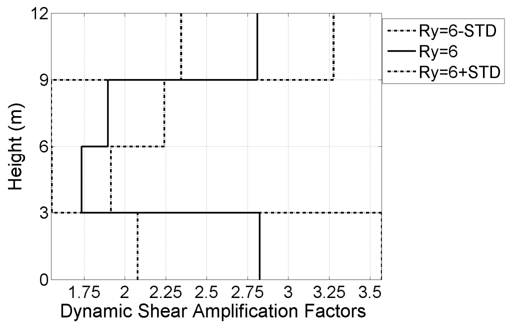

Figure B.75. Mean dynamic shear amplification factor diagram and ±1 standard deviation of four storey wall $R_y = 6.0$

B.1.6 Four Storey Structural Wall (Mean and ±1 standard deviation)

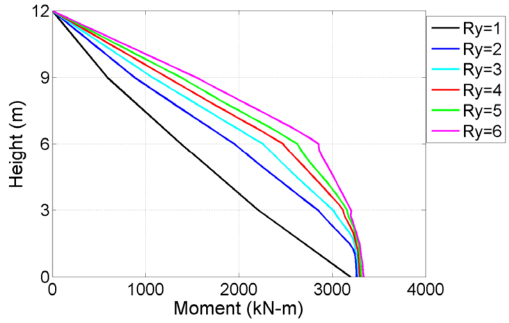

Figure B.76. Storey moment diagrams - four storey wall

R_y = 1.0, 2.0, 3.0, 4.0, 5.0, 6.0

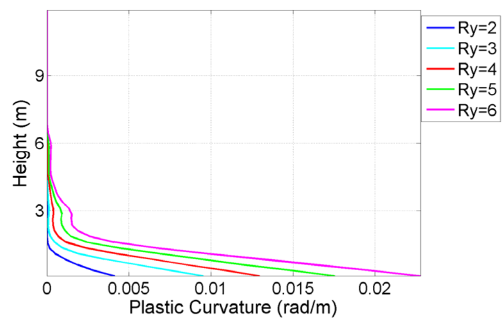

Figure B.78. Storey plastic curvature diagrams - four storey wall

R_y = 2.0, 3.0, 4.0, 5.0, 6.0

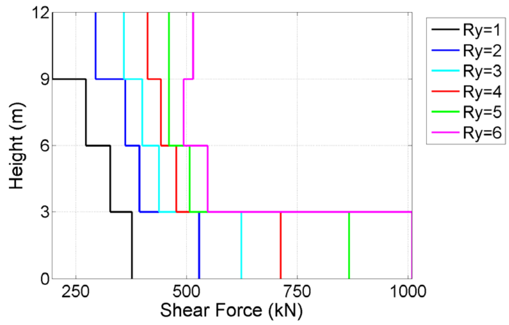

Figure B.77. Storey shear force diagrams - four storey wall

R_y = 1.0, 2.0, 3.0, 4.0, 5.0, 6.0

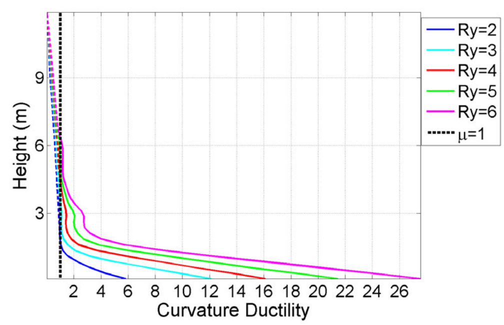

Figure B.79. Storey curvature ductility diagrams - four storey wall

R_y = 2.0, 3.0, 4.0, 5.0, 6.0

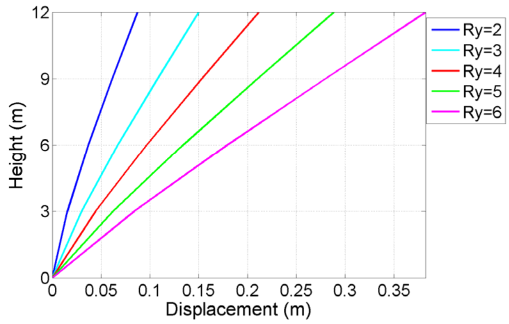

Figure B.80. Storey displacement diagrams - four storey wall $R_y = 2.0, 3.0, 4.0, 5.0, 6.0$

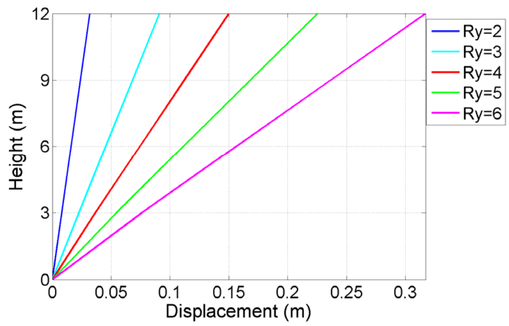

Figure B.81. Storey plastic displacement diagrams - four storey wall $R_y = 2.0, 3.0, 4.0, 5.0, 6.0$

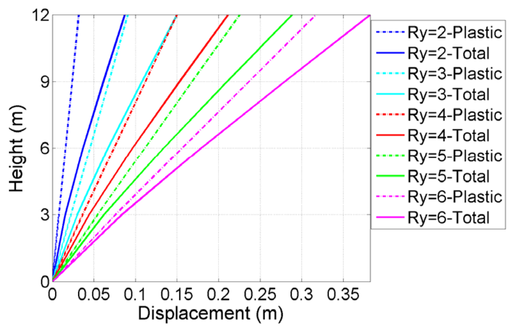

Figure B.82. Storey total displacement - plastic displacement comparison diagrams - four storey wall $R_y = 2.0, 3.0, 4.0, 5.0, 6.0$

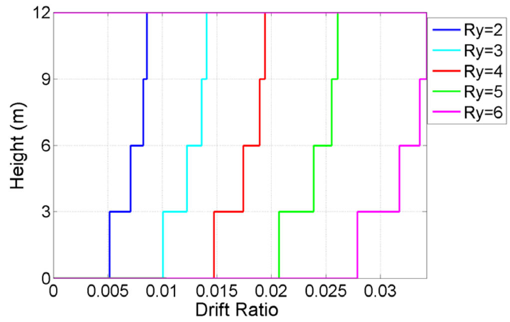

Figure B.83. Storey drift ratio diagrams - four storey wall $R_y = 2.0, 3.0, 4.0, 5.0, 6.0$

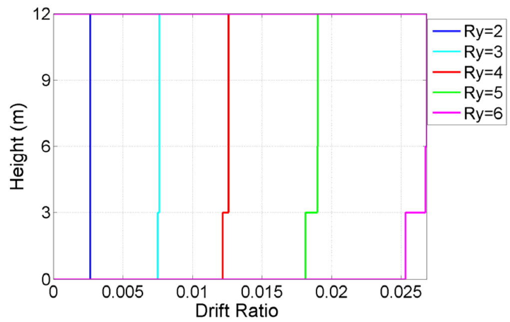

Figure B.84. Storey cumulative plastic drift ratio diagrams - four storey wall $R_y = 2.0, 3.0, 4.0, 5.0, 6.0$

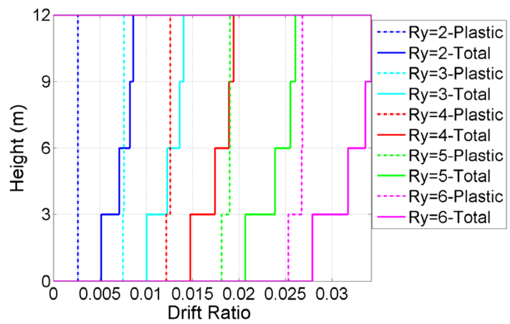

Figure B.85. Storey drift ratio - cumulative plastic drift ratio comparison diagrams - four storey wall $R_y = 2.0, 3.0, 4.0, 5.0, 6.0$

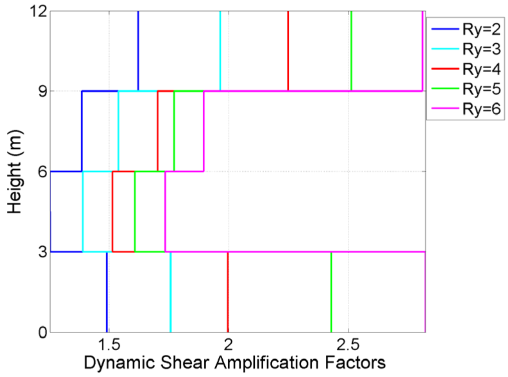

Figure B.86. Storey dynamic shear amplification factor diagrams - four storey wall R_y = 2.0, 3.0, 4.0, 5.0, 6.0

B.2.1 Eight Storey Structural Wall (R_y =2.0)

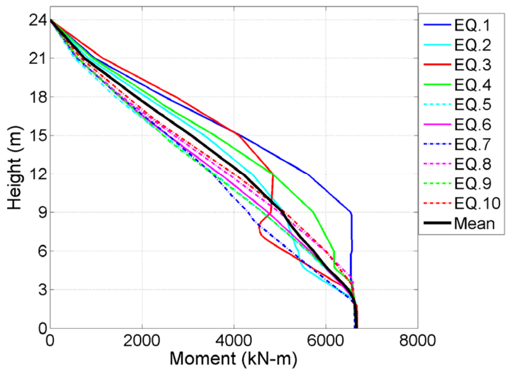

Figure B.87. Storey moment diagrams - eight storey wall R_y = 2.0

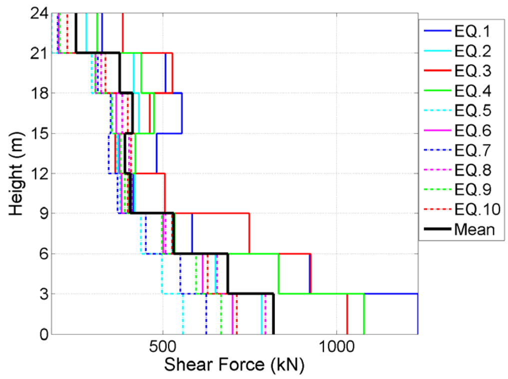

Figure B.89. Storey shear force diagrams - eight storey wall R_y = 2.0

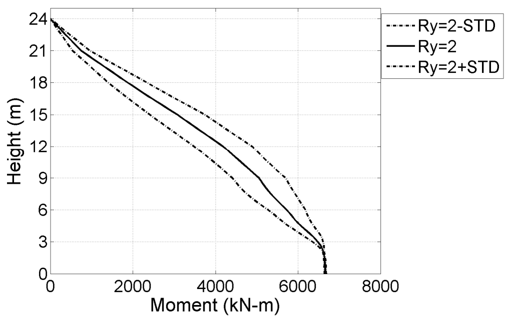

Figure B.88. Storey mean moment diagram and ±1 standard deviation of eight storey wall R_y =2

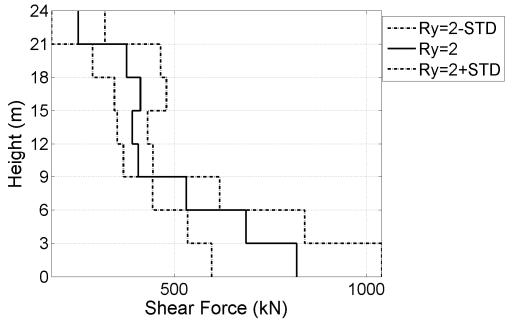

Figure B.90. Storey mean shear force diagram and ±1 standard deviation of eight storey wall R_y = 2.0

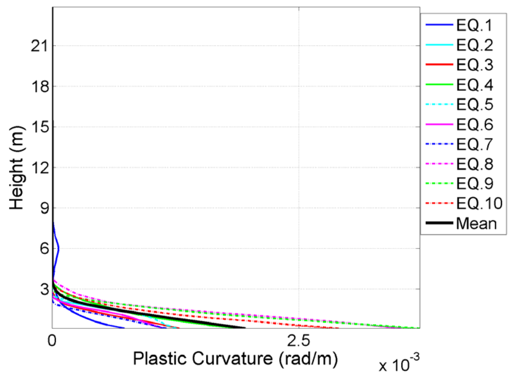

Figure B.91. Storey plastic curvature diagrams - eight storey wall $R_y = 2.0$

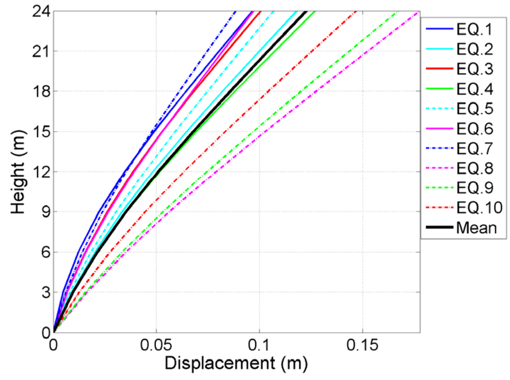

Figure B.94 . Storey displacement diagrams - eight storey wall $R_y = 2.0$

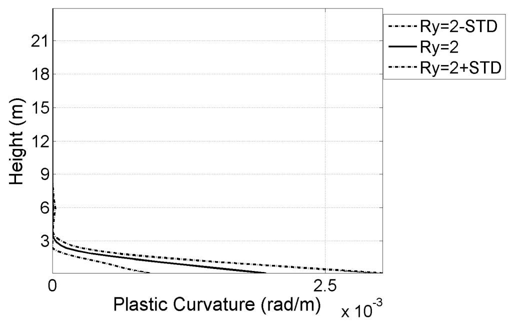

Figure B.92. Storey mean plastic curvature diagram and ±1 standard deviation of eight storey wall $R_y = 2.0$

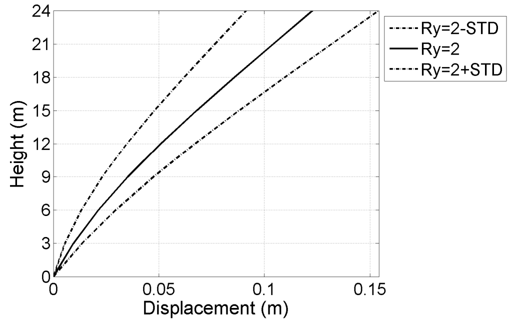

Figure B.95. Mean storey displacement diagram and ±1 standard deviation of eight storey wall $R_y = 2.0$

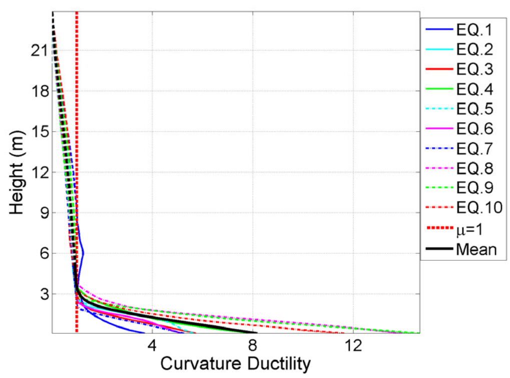

Figure B.93. Storey curvature ductility diagrams - eight storey wall $R_y = 2.0$

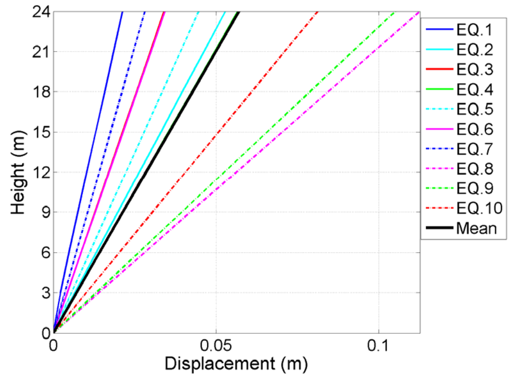

Figure B.96. Storey plastic displacement diagrams - eight storey wall $R_y = 2.0$

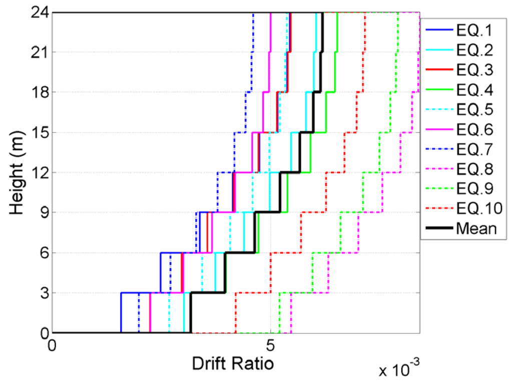

Figure B.97. Storey drift ratio diagrams - eight storey wall $R_y = 2.0$

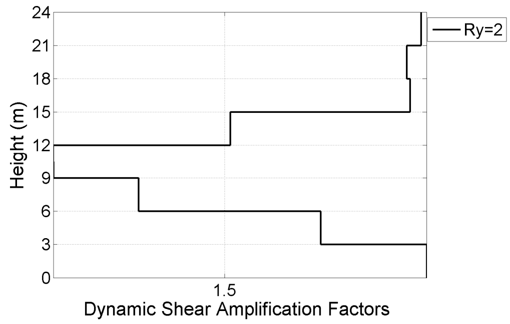

Figure B.100. Storey dynamic shear amplification factor diagrams - eight storey wall $R_y = 2.0$

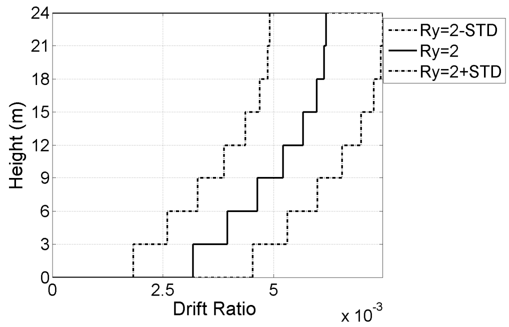

Figure B.98. Mean storey drift ratio diagram and ±1 standard deviation of eight storey wall $R_y = 2.0$

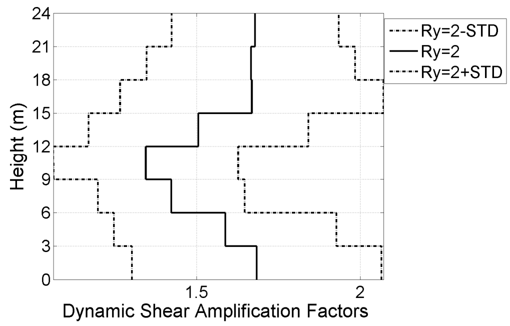

Figure B.101. Mean dynamic shear amplification factor diagram and ±1 standard deviation of eight storey wall $R_y = 2.0$

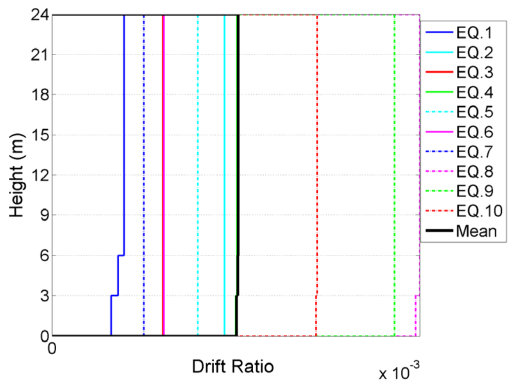

Figure B.99. Storey cumulative plastic drift ratio diagrams - eight storey wall $R_y = 2.0$

B.2.2 Eight Storey Structural Wall (R_y = 3.0)

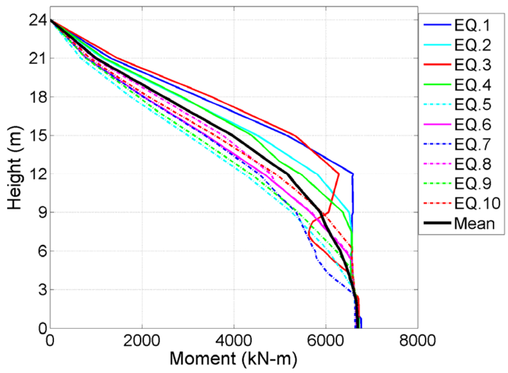

Figure B.102. Storey moment diagrams - eight storey wall R_y = 3.0

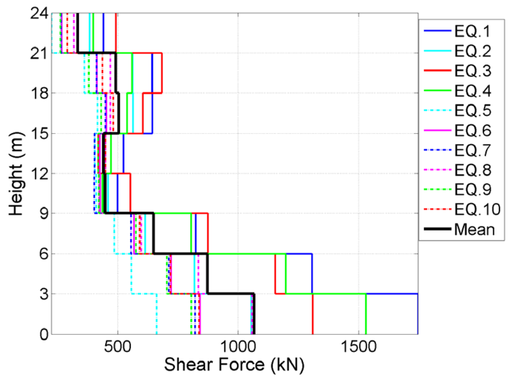

Figure B.104. Storey shear force diagrams - eight storey wall R_y = 3.0

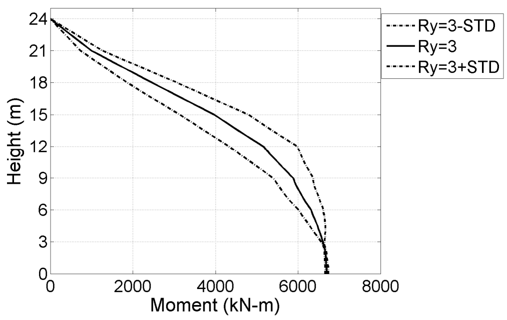

Figure B.103. Storey mean moment diagram and ±1 standard deviation of eight storey wall R_y = 3.0

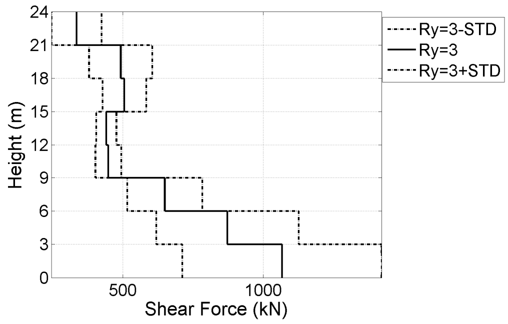

Figure B.105. Storey mean shear force diagram and ±1 standard deviation of eight storey wall R_y = 3.0

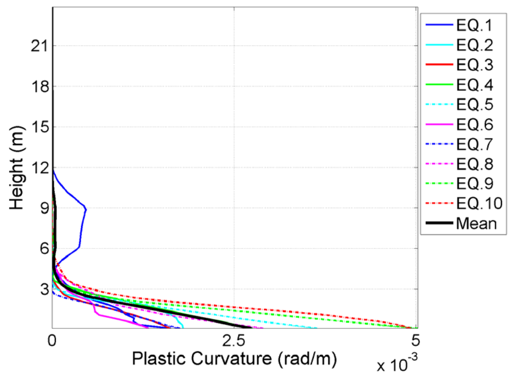

Figure B.106. Storey plastic curvature diagrams - eight storey wall $R_y = 3.0$

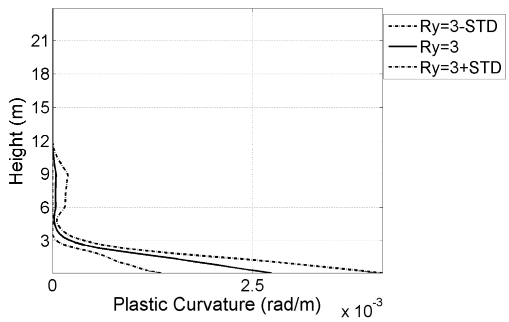

Figure B.107. Storey mean plastic curvature diagram and ±1 standard deviation of eight storey wall $R_y = 3.0$

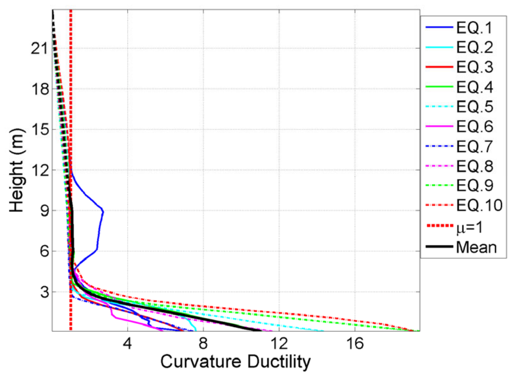

Figure B.108. Storey curvature ductility diagrams - eight storey wall $R_y = 3.0$

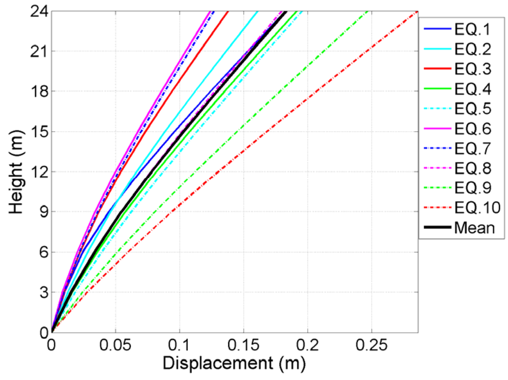

Figure B.109. Storey displacement diagrams - eight storey wall $R_y = 3.0$

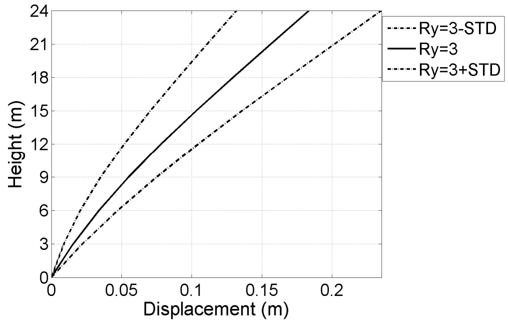

Figure B.110. Mean storey displacement diagram and ±1 standard deviation of eight storey wall $R_y = 3.0$

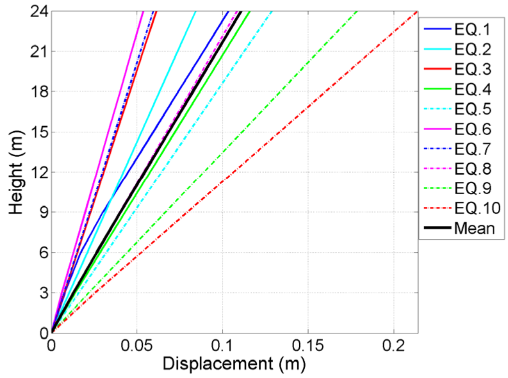

Figure B.111. Storey plastic displacement diagrams - eight storey wall $R_y = 3.0$

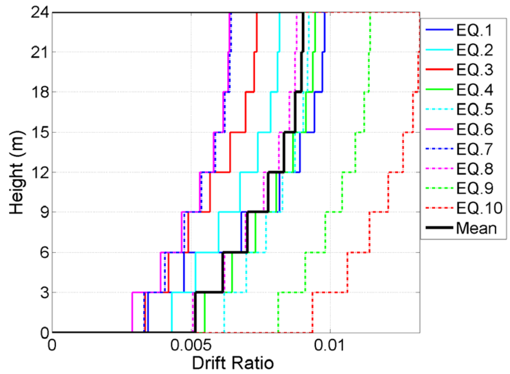

Figure B.112. Storey drift ratio diagrams - eight storey wall $R_y = 3.0$

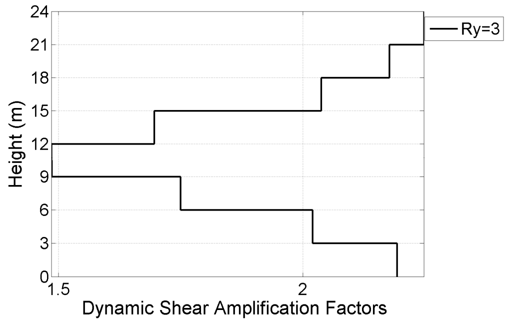

Figure B.115. Storey dynamic shear amplification factor diagrams - eight storey wall $R_y = 3.0$

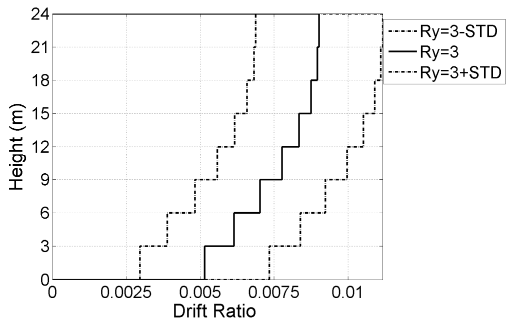

Figure B.113. Mean storey drift ratio diagram and ±1 standard deviation of eight storey wall $R_y = 3.0$

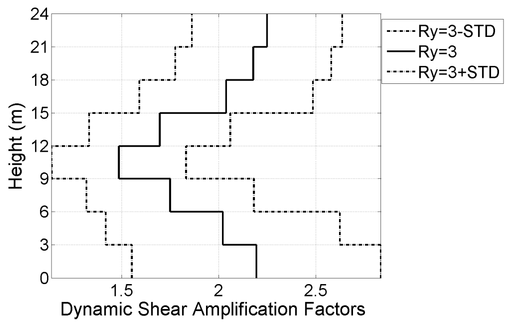

Figure B.116. Mean dynamic shear amplification factor diagram and ±1 standard deviation of eight storey wall $R_y = 3.0$

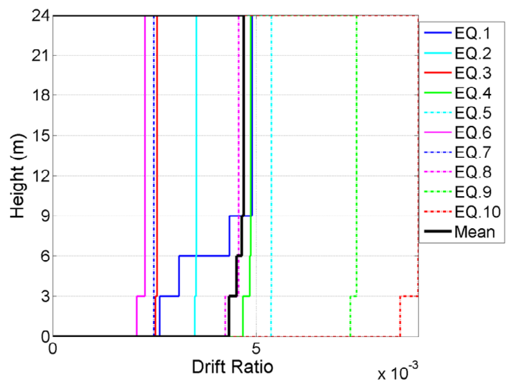

Figure B.114. Storey cumulative plastic drift ratio diagrams - eight storey wall $R_y = 3.0$

B.2.3 Eight Storey Structural Wall ($R_y = 4.0$)

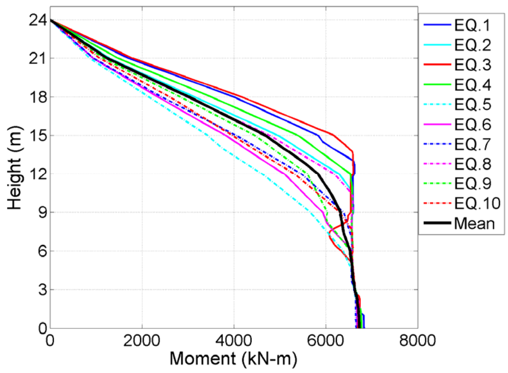

Figure B.117. Storey moment diagrams - eight storey wall $R_y = 4.0$

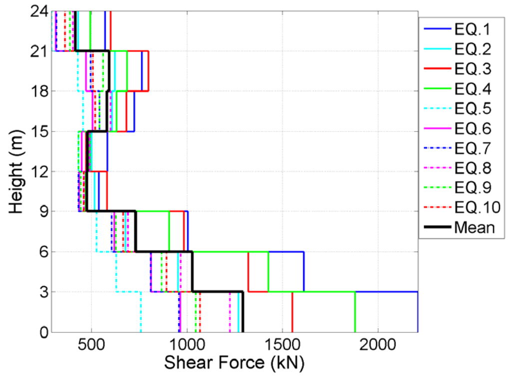

Figure B.119. Storey shear force diagrams - eight storey wall $R_y = 4.0$

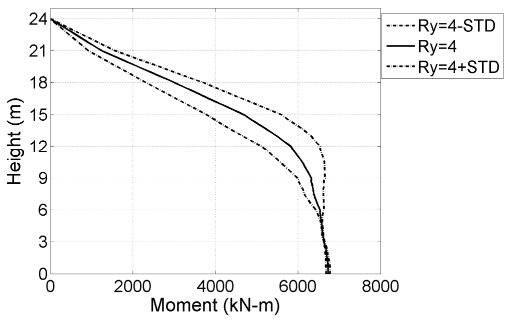

Figure B.118. Storey mean moment diagram and ±1 standard deviation of eight storey wall $R_y = 4.0$

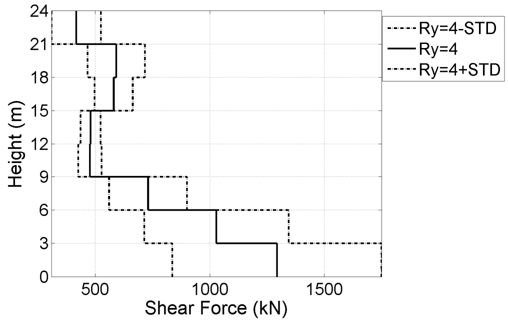

Figure B.120. Storey mean shear force diagram and ±1 standard deviation of eight storey wall $R_y = 4.0$

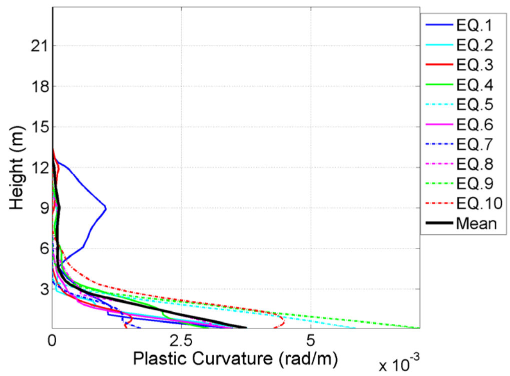

Figure B.121. Storey plastic curvature diagrams - eight storey wall $R_y = 4.0$

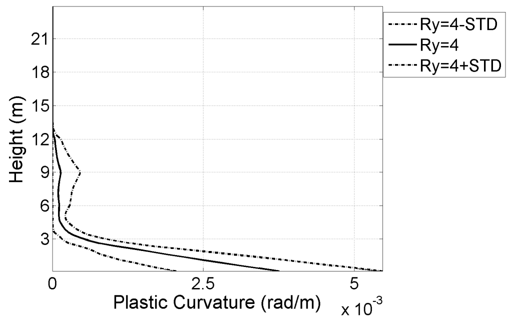

Figure B.122. Storey mean plastic curvature diagram and ±1 standard deviation of eight storey wall $R_y = 4.0$

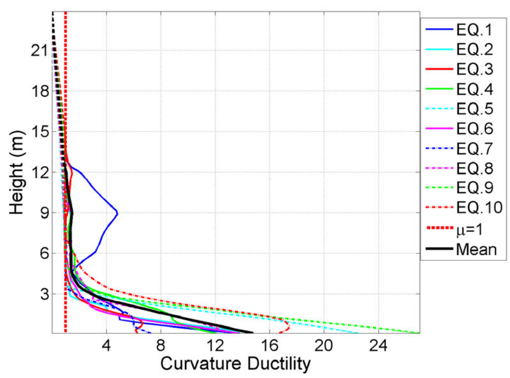

Figure B.123. Storey curvature ductility diagrams - eight storey wall $R_y = 4.0$

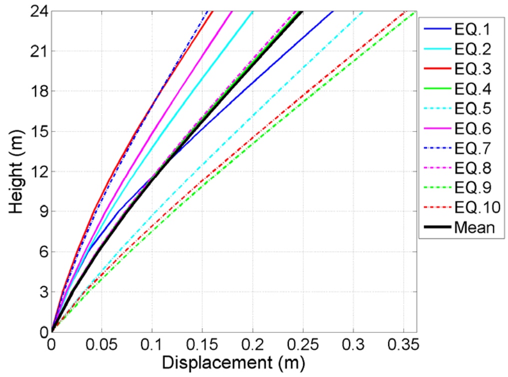

Figure B.124. Storey displacement diagrams - eight storey wall $R_y = 4.0$

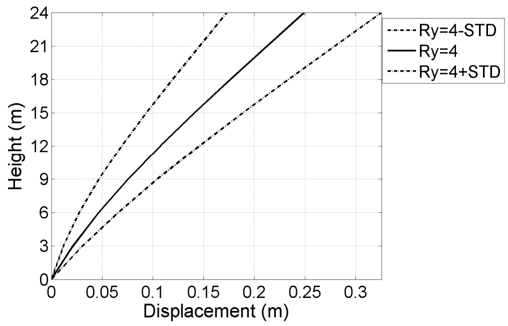

Figure B.125. Mean storey displacement diagram and ±1 standard deviation of eight storey wall $R_y = 4.0$

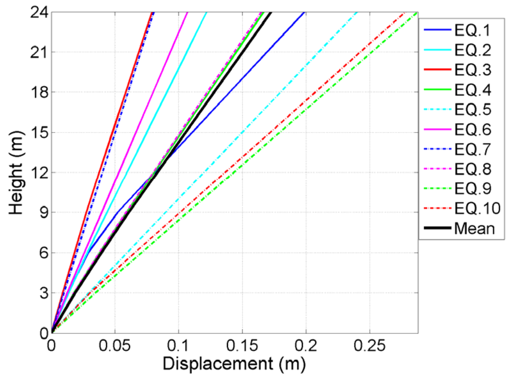

Figure B.126. Storey plastic displacement diagrams - eight storey wall $R_y = 4.0$

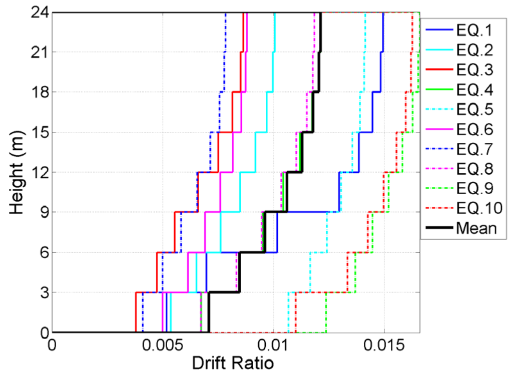

FigureB.127. Storey drift ratio diagrams - eight storey wall $R_y = 4.0$

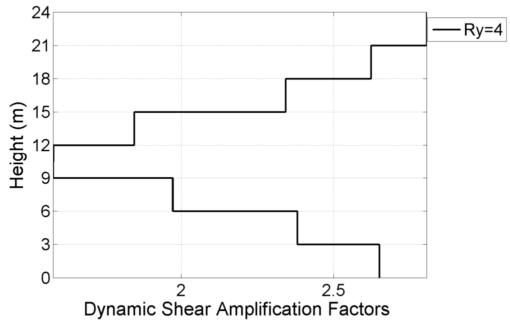

Figure B.130. Storey dynamic shear amplification factor diagrams - eight storey wall $R_y = 4.0$

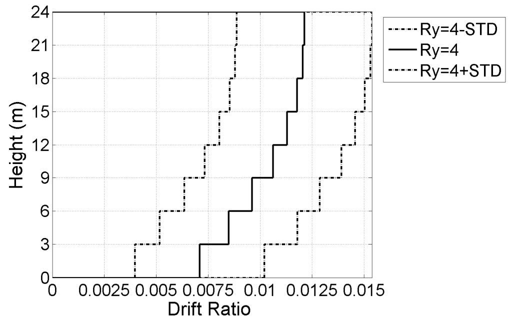

Figure B.128. Mean storey drift ratio diagram and ±1 standard deviation of eight storey wall $R_y = 4.0$

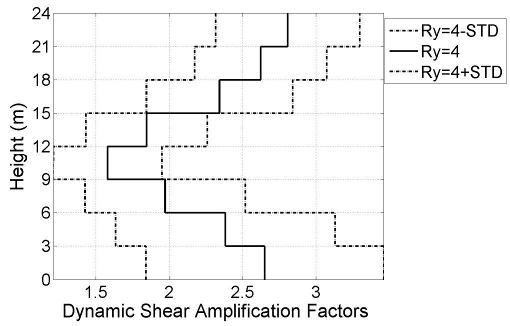

Figure B.131. Mean dynamic shear amplification factor diagram and ±1 standard deviation of eight storey wall $R_y = 4.0$

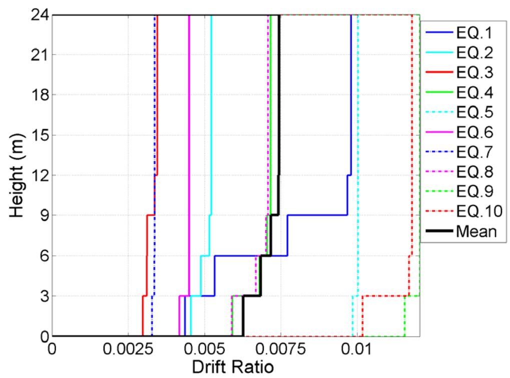

Figure B.129. Storey cumulative plastic drift ratio diagrams - eight storey wall $R_y = 4.0$

B.2.4 Eight Storey Structural Wall (R_y = 5.0)

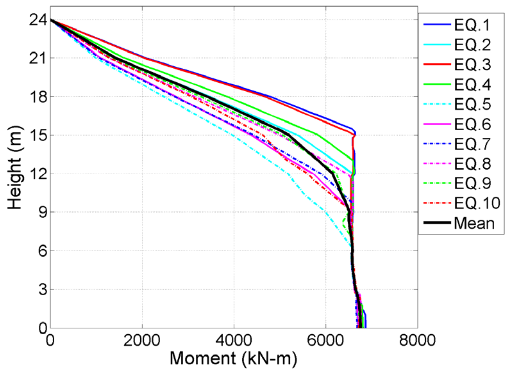

Figure B.132. Storey moment diagrams - eight storey wall R_y = 5.0

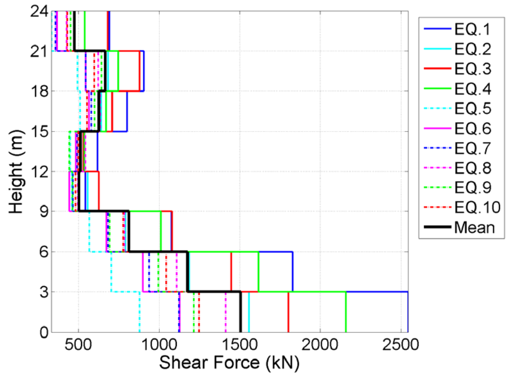

Figure B.134. Storey shear force diagrams - eight storey wall R_y = 5.0

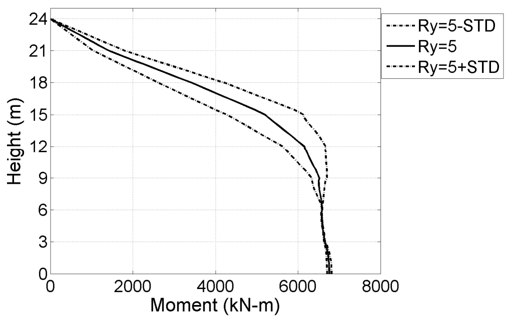

Figure B.133 . Storey mean moment diagram and ±1 standard deviation of eight storey wall R_y = 5.0

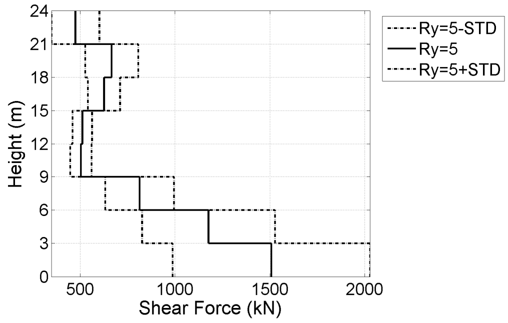

Figure B.135. Storey mean shear force diagram and ±1 standard deviation of eight storey wall R_y = 5.0

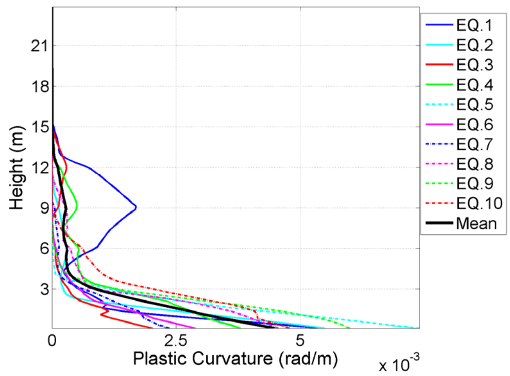

Figure B.136. Storey plastic curvature diagrams - eight storey wall $R_y = 5.0$

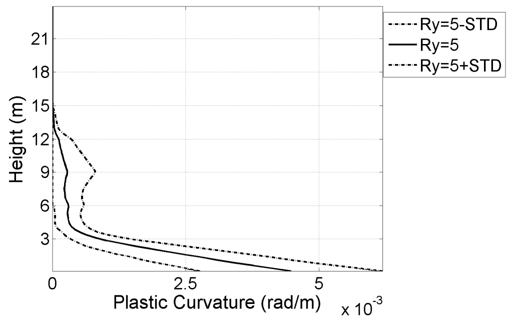

Figure B.137. Storey mean plastic curvature diagram and ±1 standard deviation of eight storey wall $R_y = 5.0$

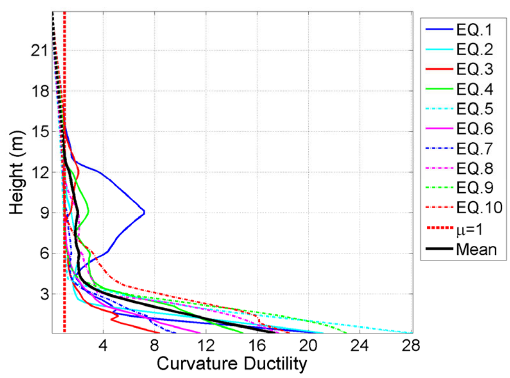

Figure B.138.Storey curvature ductility diagrams - eight storey wall $R_y = 5.0$

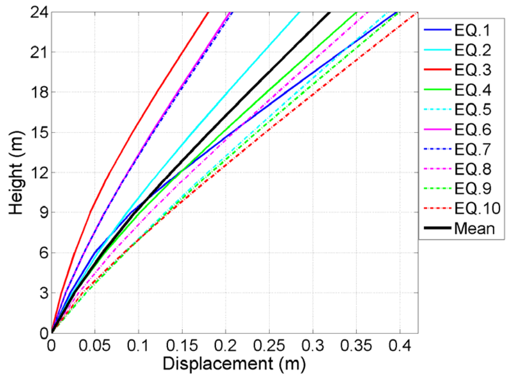

Figure B.139. Storey displacement diagrams - eight storey wall $R_y = 5.0$

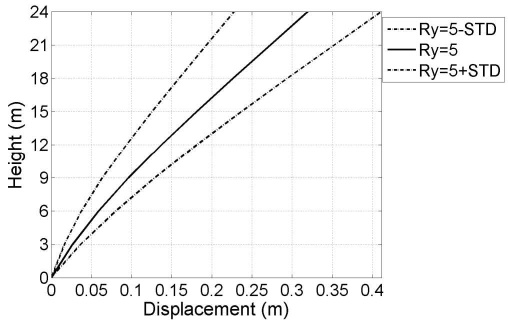

Figure B.140. Mean storey displacement diagram and ±1 standard deviation of eight storey wall $R_y = 5.0$

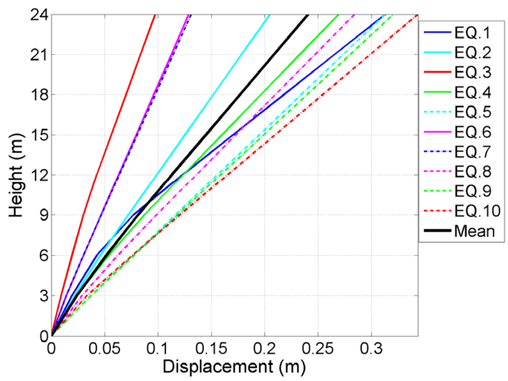

Figure B.141. Storey plastic displacement diagrams - eight storey wall $R_y = 5.0$

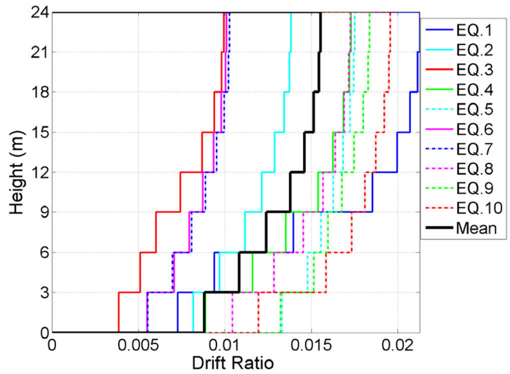

Figure B.142. Storey drift ratio diagrams - eight storey wall $R_y = 5.0$

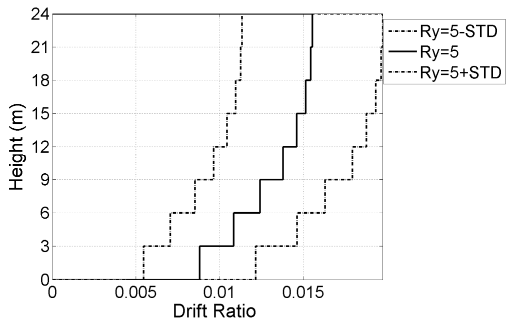

Figure B.143. Mean storey drift ratio diagram and ±1 standard deviation of eight storey wall $R_y = 5.0$

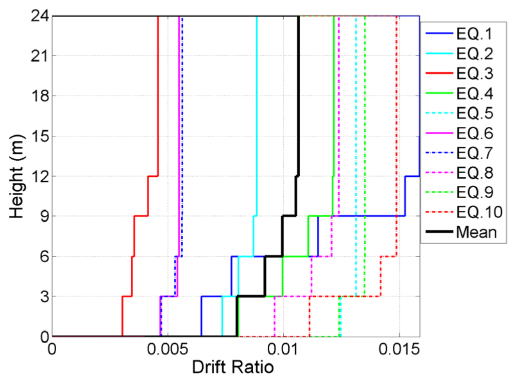

Figure B.144. Storey cumulative plastic drift ratio diagrams - eight storey wall $R_y = 5.0$

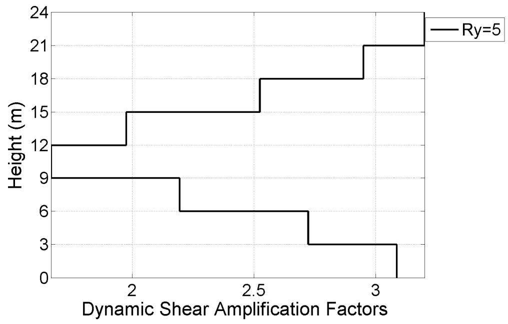

Figure B.145. Storey dynamic shear amplification factor diagrams - eight storey wall $R_y = 5.0$

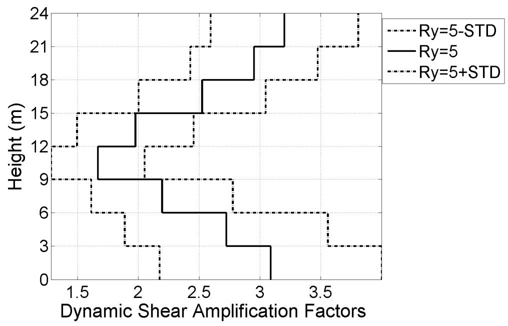

Figure B.146. Mean dynamic shear amplification factor diagram and ±1 standard deviation of eight storey wall $R_y = 5.0$

B.2.5 Eight Storey Structural Wall (R_y = 6.0)

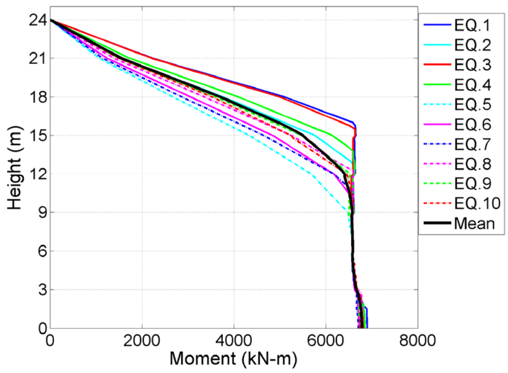

Figure B.147. Storey moment diagrams - eight storey wall R_y = 6.0

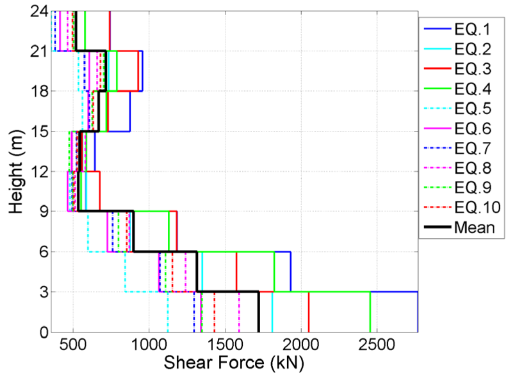

Figure B.149. Storey shear force diagrams - eight storey wall R_y = 6.0

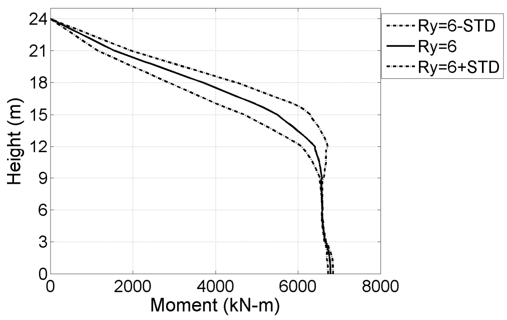

Figure B.148. Storey mean moment diagram and ±1 standard deviation of eight storey wall R_y = 6.0

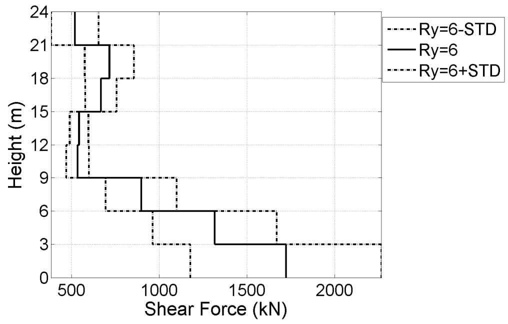

Figure B.150. Storey mean shear force diagram and ±1 standard deviation of eight storey wall R_y = 6.0

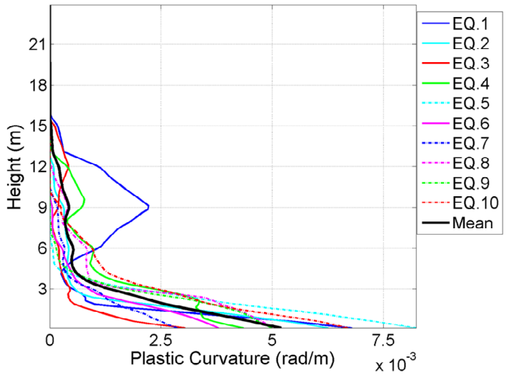

Figure B.151. Storey plastic curvature diagrams - eight storey wall $R_y = 6.0$

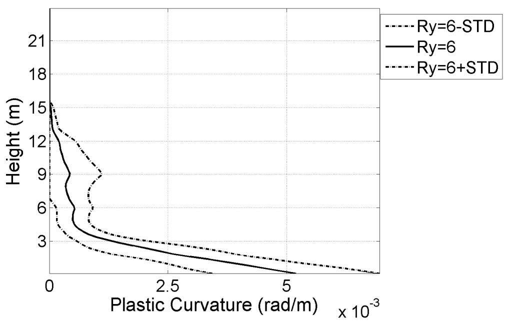

Figure B.152. Storey mean plastic curvature diagram and ±1 standard deviation of eight storey wall $R_y = 6.0$

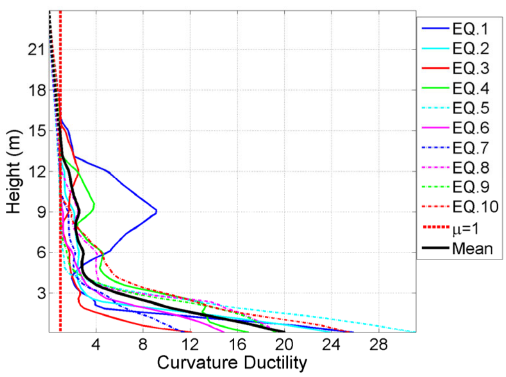

Figure B.153.Storey curvature ductility diagrams - eight storey wall $R_y = 6.0$

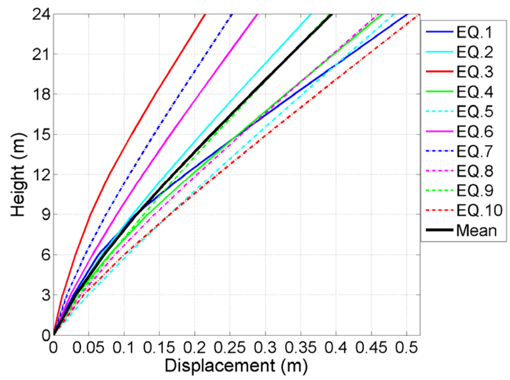

Figure B.154. Storey displacement diagrams - eight storey wall $R_y = 6.0$

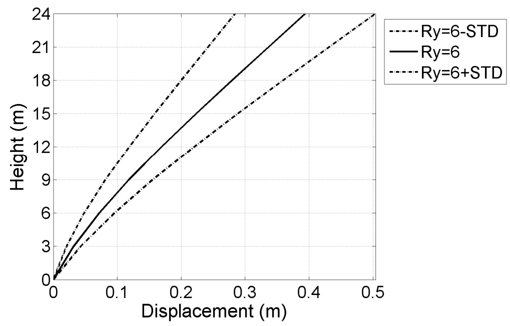

Figure B.155. Mean storey displacement diagram and ±1 standard deviation of eight storey wall $R_y = 6.0$

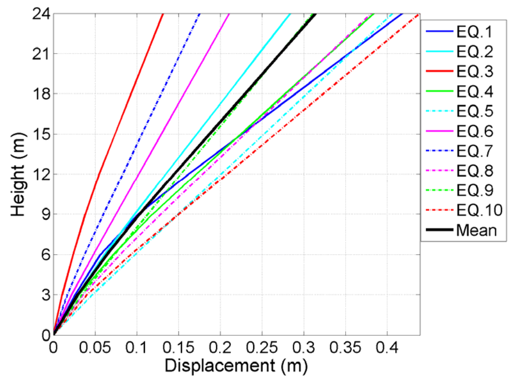

Figure B.156. Storey plastic displacement diagrams - eight storey wall $R_y = 6.0$

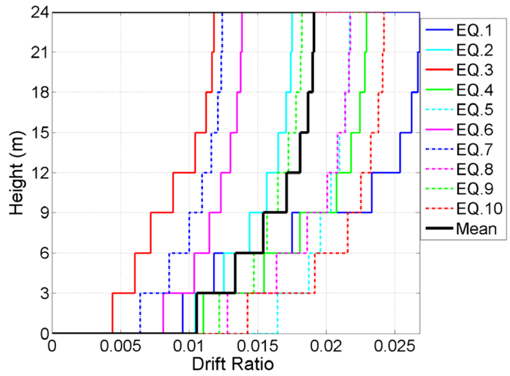

Figure B.157. Storey drift ratio diagrams - eight storey wall $R_y = 6.0$

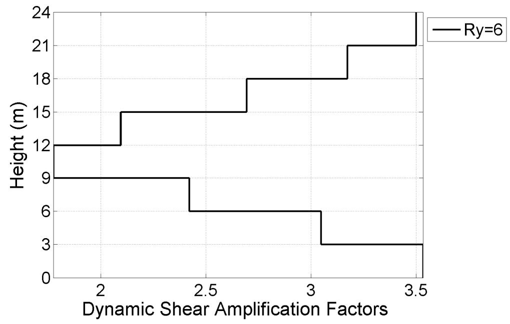

Figure B.160. Storey dynamic shear amplification factor diagrams - eight storey wall $R_y = 6.0$

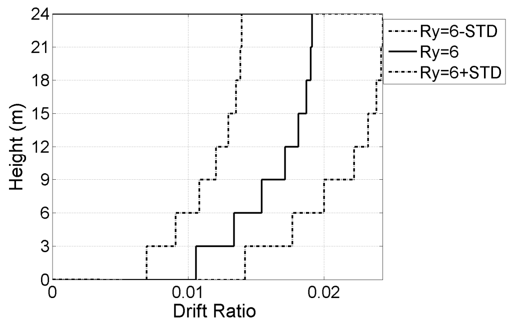

Figure B.158. Mean storey drift ratio diagram and ±1 standard deviation of eight storey wall $R_y = 6.0$

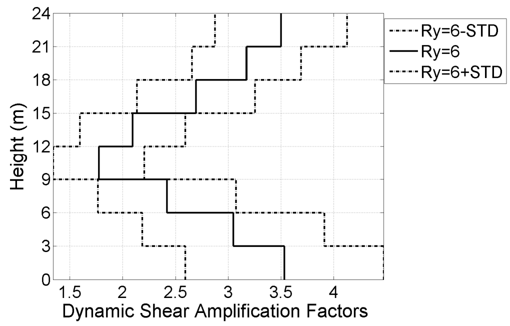

Figure B.161. Mean dynamic shear amplification factor diagram and ±1 standard deviation of eight storey wall $R_y = 6.0$

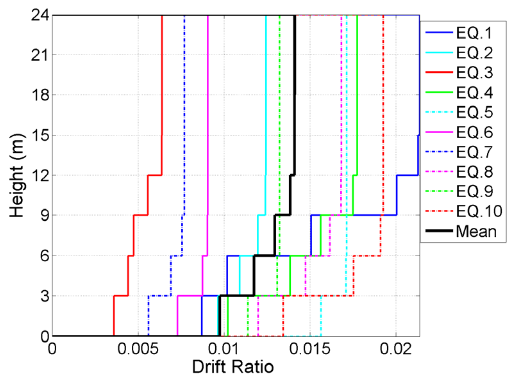

Figure B.159. Storey cumulative plastic drift ratio diagrams - eight storey wall $R_y = 6.0$

B.2.6 Eight Storey Structural Wall (Mean and ±1 standard deviation)

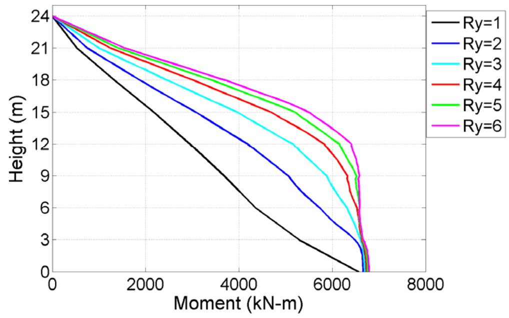

Figure B.162. Storey moment diagrams - eight storey wall

R_y = 1.0, 2.0, 3.0, 4.0, 5.0, 6.0

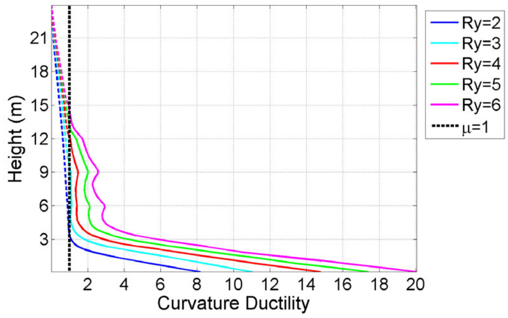

Figure B.164. Storey plastic curvature diagrams - eight storey wall

R_y = 2.0, 3.0, 4.0, 5.0, 6.0

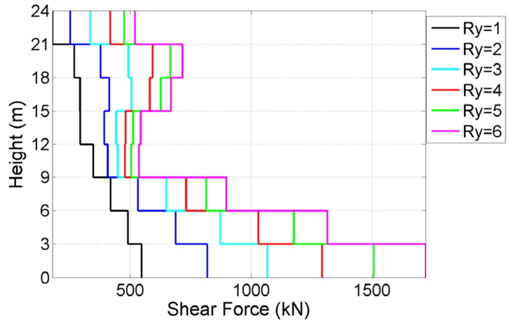

Figure B.163. Storey shear force diagrams - eight storey wall

R_y = 1.0, 2.0, 3.0, 4.0, 5.0, 6.0

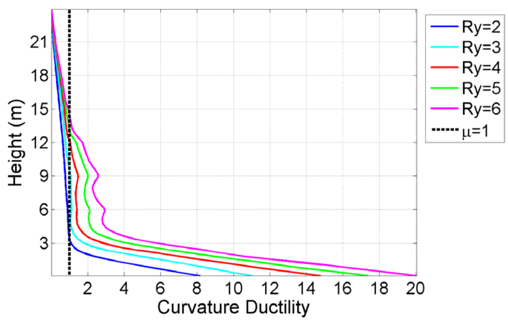

Figure B.165.Storey curvature ductility diagrams - eight storey wall

R_y = 2.0, 3.0, 4.0, 5.0, 6.0

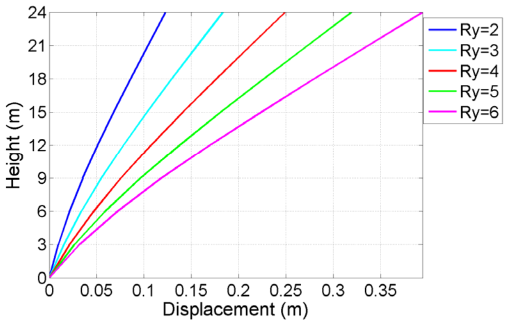

Figure B.166. Storey displacement diagrams - eight storey wall R_y = 2.0, 3.0, 4.0, 5.0, 6.0

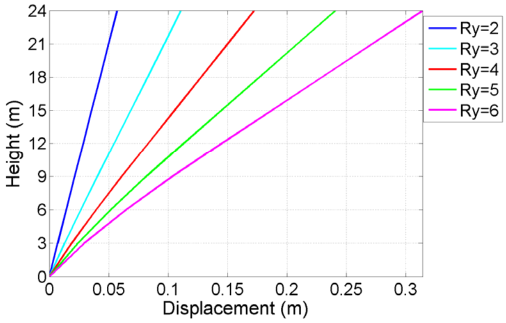

Figure B.167. Storey plastic displacement diagrams - eight storey wall R_y = 2.0, 3.0, 4.0, 5.0, 6.0

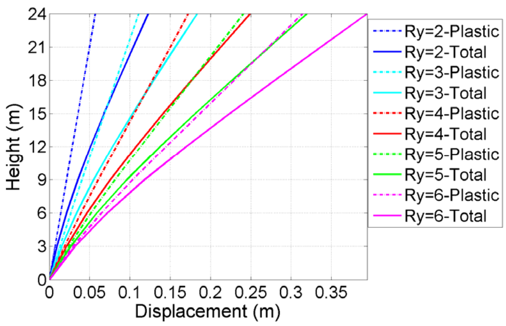

Figure B.168. Storey total displacement - plastic displacement comparison diagrams - eight storey wall R_y = 2.0, 3.0, 4.0, 5.0, 6.0

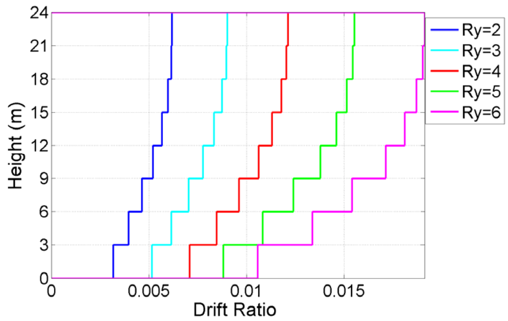

Figure B.169. Storey drift ratio diagrams - eight storey wall R_y = 2.0, 3.0, 4.0, 5.0, 6.0

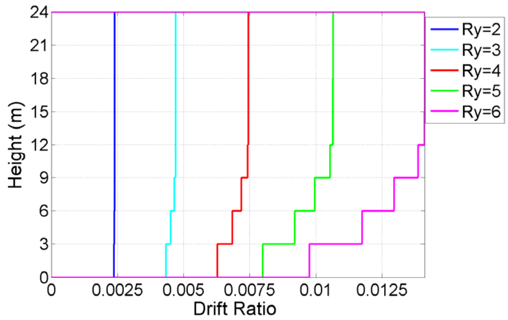

Figure B.170. Storey cumulative plastic drift ratio diagrams - eight storey wall R_y = 2.0, 3.0, 4.0, 5.0, 6.0

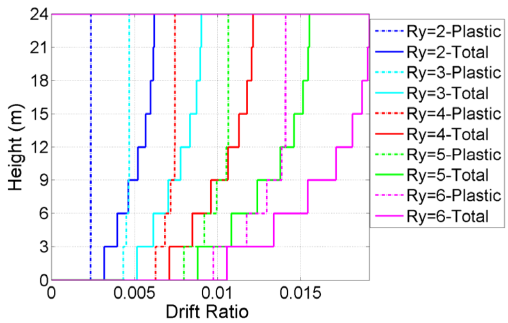

Figure B.171. Storey drift ratio - cumulative plastic drift ratio comparison diagrams - eight storey wall R_y = 2.0, 3.0, 4.0, 5.0, 6.0

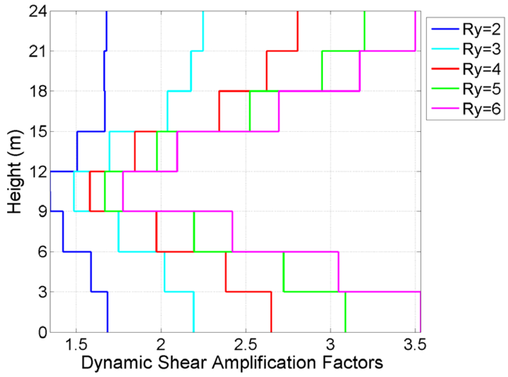

Figure B.172. Storey dynamic shear amplification factor diagrams - eight storey wall R_y = 2.0, 3.0, 4.0, 5.0, 6.0

B.3.1 Twelve Storey Structural Wall (R_y = 2.0)

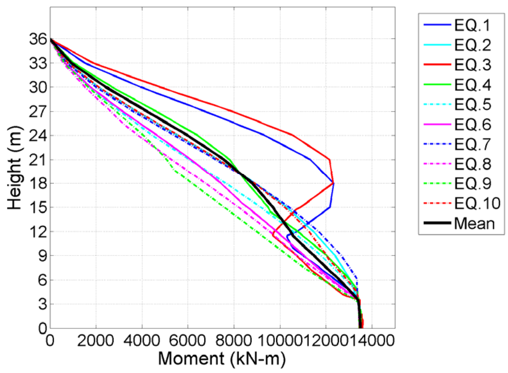

Figure B.173. Storey moment diagrams - twelve storey wall R_y =2

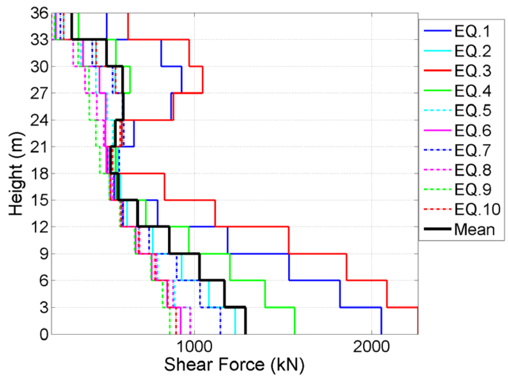

Figure B.175. Storey shear force diagrams - twelve storey wall R_y = 2.0

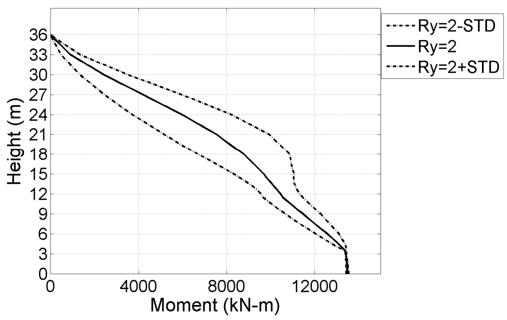

Figure B.174. Storey mean moment diagram and ±1 standard deviation of twelve storey wall R_y =2

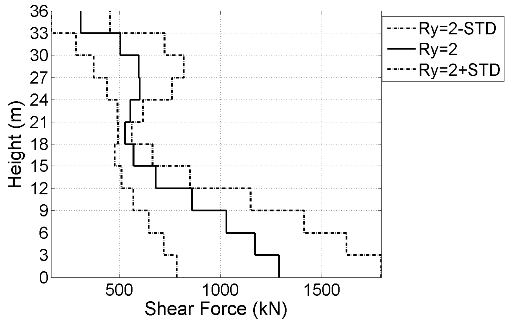

Figure B.176. Storey mean shear force diagram and ±1 standard deviation of twelve storey wall R_y = 2.0

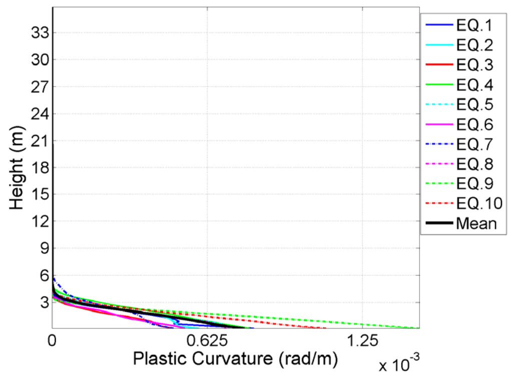

Figure B.177. Storey plastic curvature diagrams - twelve storey wall $R_y = 2.0$

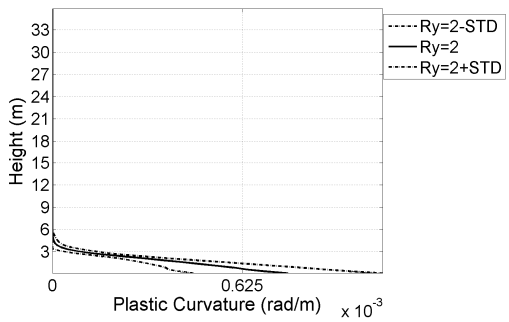

Figure B.178. Storey mean plastic curvature diagram and ±1 standard deviation of twelve storey wall $R_y = 2.0$

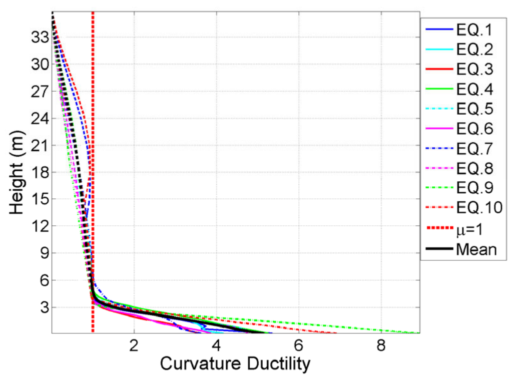

Figure B.179. Storey curvature ductility diagrams - twelve storey wall $R_y = 2.0$

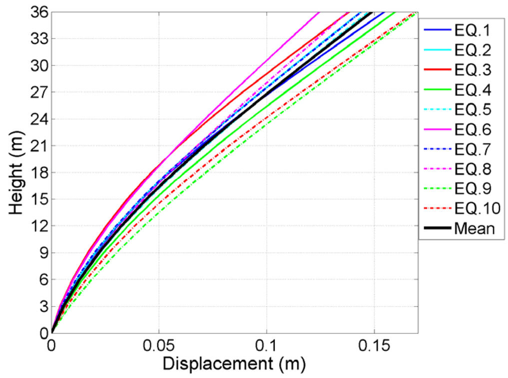

Figure B.180. Storey displacement diagrams - twelve storey wall $R_y = 2.0$

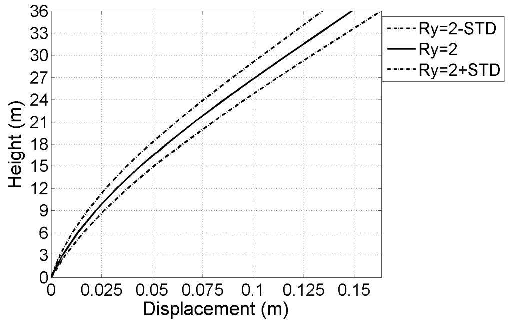

Figure B.181. Mean storey displacement diagram and ±1 standard deviation of twelve storey wall $R_y = 2.0$

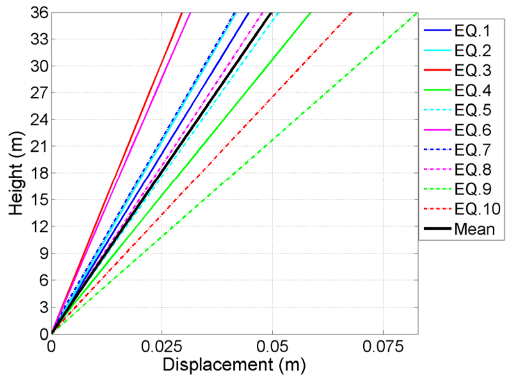

Figure B.182. Storey plastic displacement diagrams - twelve storey wall $R_y = 2.0$

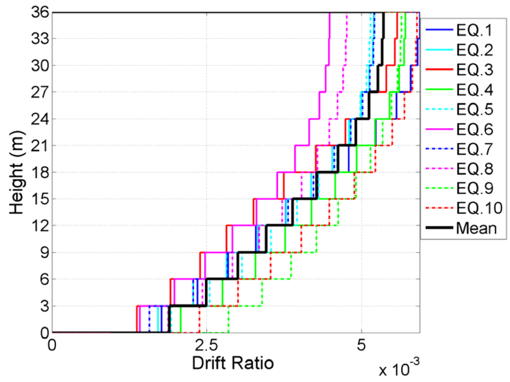

Figure B.183. Storey drift ratio diagrams - twelve storey wall $R_y = 2.0$

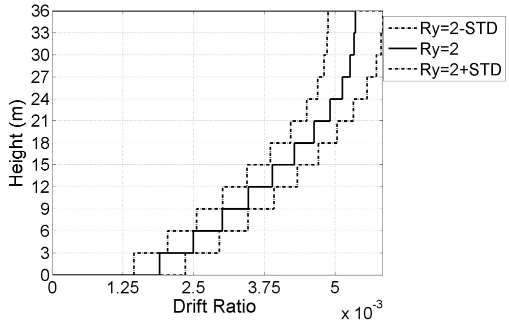

Figure B.184. Mean storey drift ratio diagram and ±1 standard deviation of twelve storey wall $R_y = 2.0$

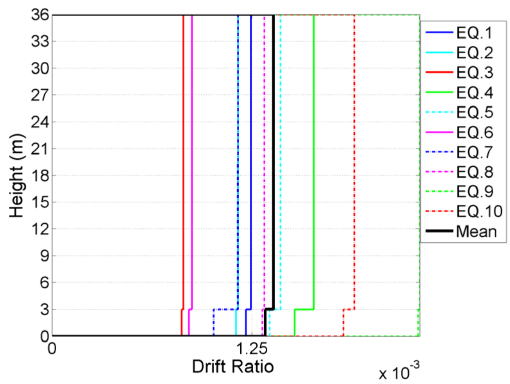

Figure B.185. Storey cumulative plastic drift ratio diagrams - twelve storey wall $R_y = 2.0$

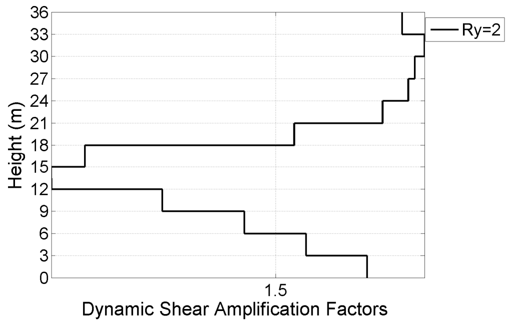

Figure B.186. Storey dynamic shear amplification factor diagrams - twelve storey wall $R_y = 2.0$

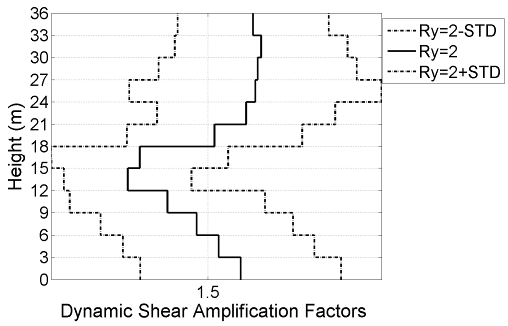

Figure B.187. Mean dynamic shear amplification factor diagram and ±1 standard deviation of twelve storey wall $R_y = 2.0$

B.3.2 Twelve Storey Structural Wall (R_y = 3.0)

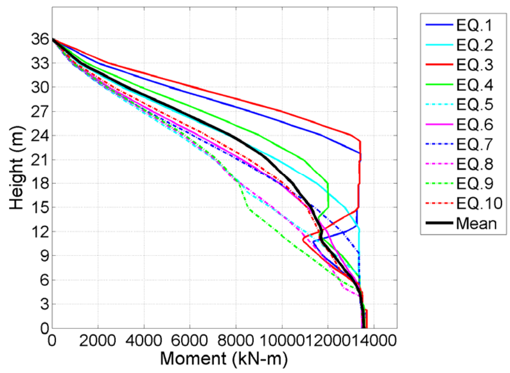

Figure B.188. Storey moment diagrams - twelve storey wall R_y = 3.0

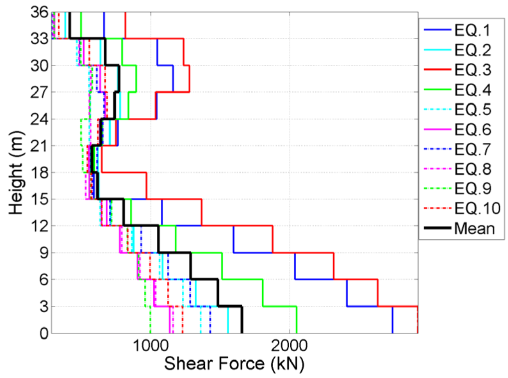

Figure B.190. Storey shear force diagrams - twelve storey wall R_y = 3.0

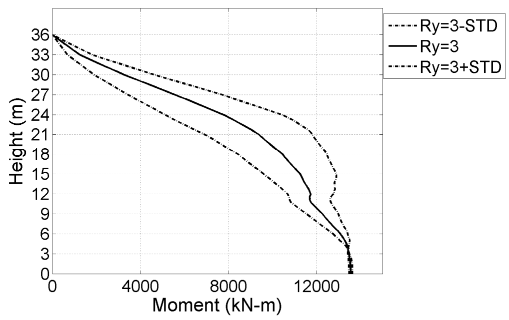

Figure B.189. Storey mean moment diagram and ±1 standard deviation of twelve storey wall R_y = 3.0

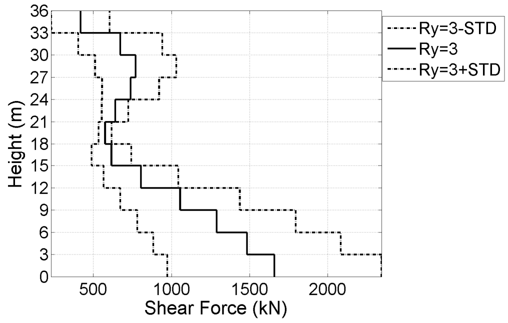

Figure B.191. Storey mean shear force diagram and ±1 standard deviation of twelve storey wall R_y = 3.0

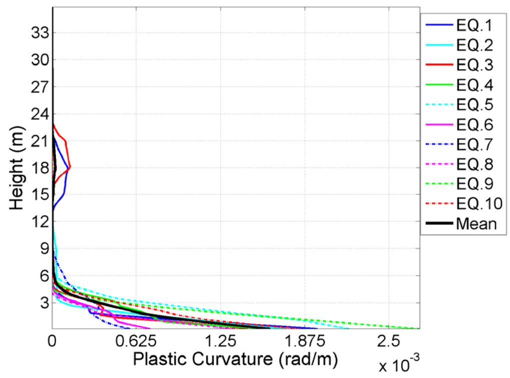

Figure B.192. Storey plastic curvature diagrams - twelve storey wall $R_y = 3.0$

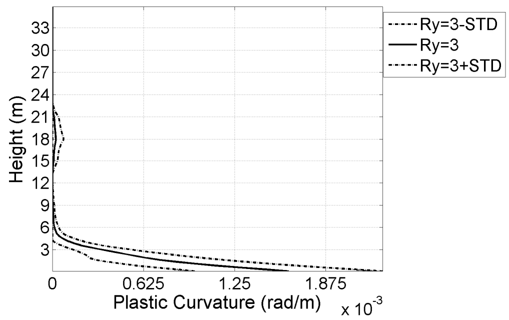

Figure B.193. Storey mean plastic curvature diagram and ±1 standard deviation of twelve storey wall $R_y = 3.0$

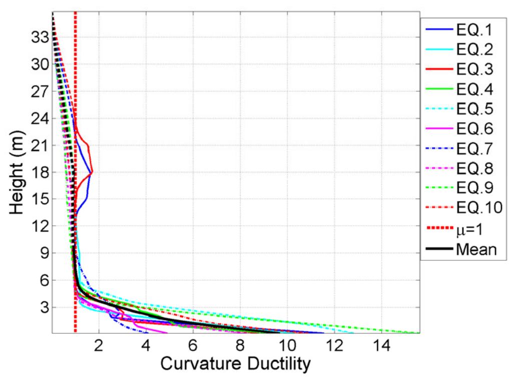

Figure B.194. Storey curvature ductility diagrams - twelve storey wall $R_y = 3.0$

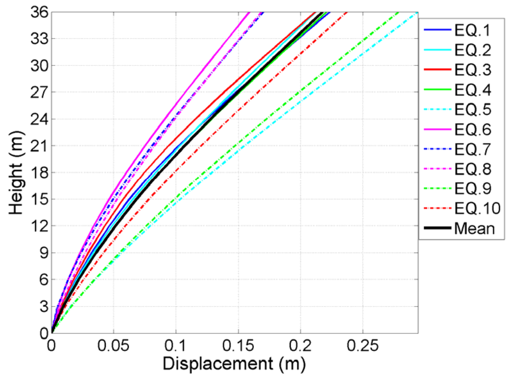

Figure B.195. Storey displacement diagrams - twelve storey wall $R_y = 3.0$

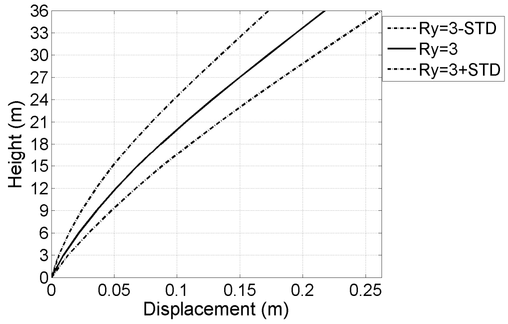

Figure B.196. Mean storey displacement diagram and ±1 standard deviation of twelve storey wall $R_y = 3.0$

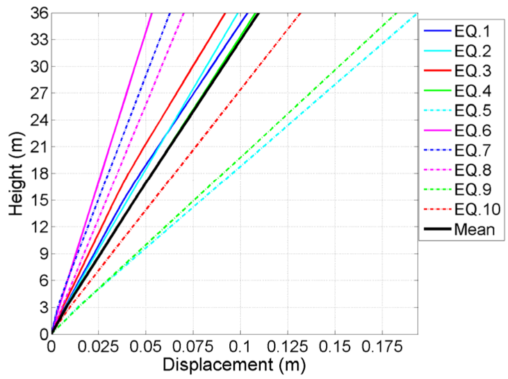

Figure B.197. Storey plastic displacement diagrams - twelve storey wall $R_y = 3.0$

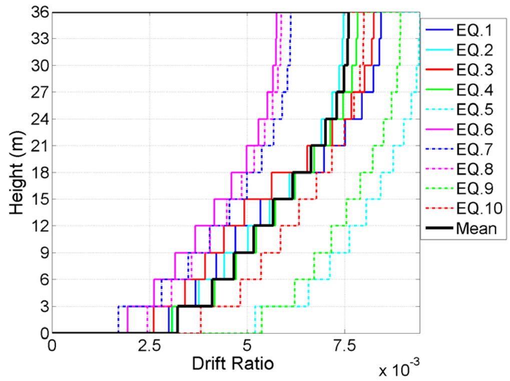

Figure B.198. Storey drift ratio diagrams - twelve storey wall $R_y = 3.0$

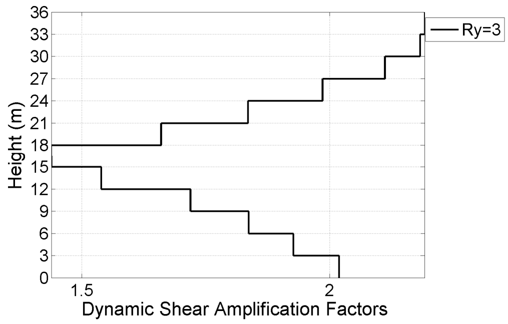

Figure B.201. Storey dynamic shear amplification factor diagrams - twelve storey wall $R_y = 3.0$

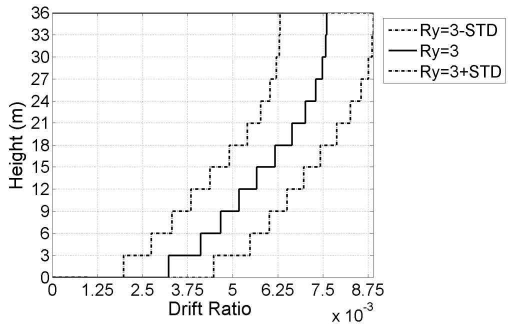

Figure B.199. Mean storey drift ratio diagram and ±1 standard deviation of twelve storey wall $R_y = 3.0$

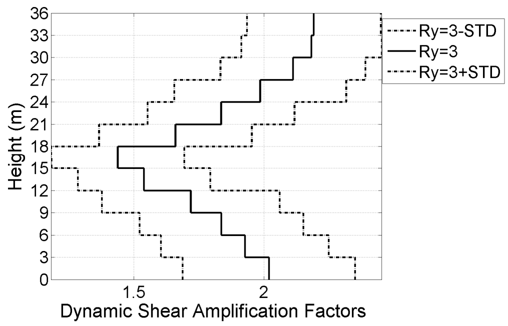

Figure B.202. Mean dynamic shear amplification factor diagram and ±1 standard deviation of twelve storey wall $R_y = 3.0$

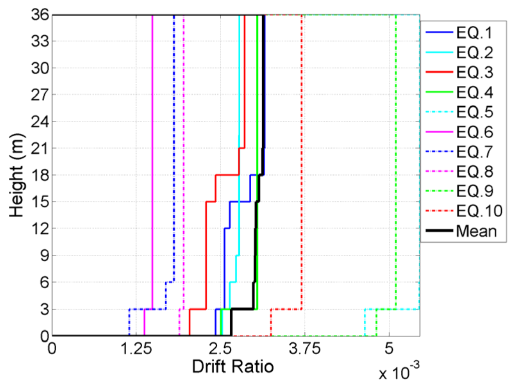

Figure B.200. Storey cumulative plastic drift ratio diagrams - twelve storey wall $R_y = 3.0$

B.3.3 Twelve Storey Structural Wall (R_y = 4.0)

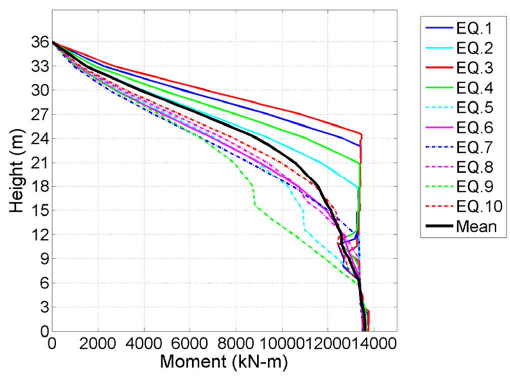

Figure B.203. Storey moment diagrams - twelve storey wall R_y = 4.0

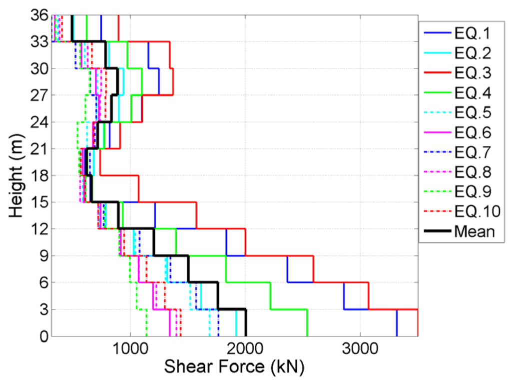

Figure B.205. Storey shear force diagrams - twelve storey wall R_y = 4.0

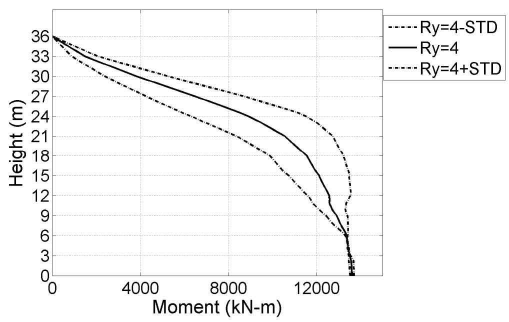

Figure B.204. Storey mean moment diagram and ±1 standard deviation of twelve storey wall R_y = 4.0

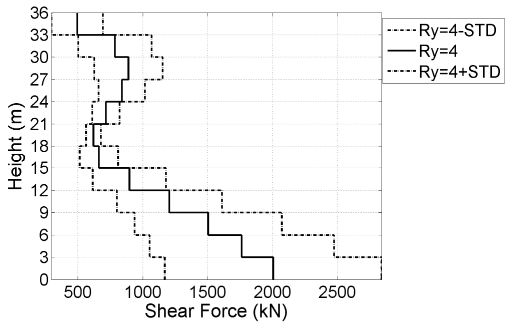

Figure B.206. Storey mean shear force diagram and ±1 standard deviation of twelve storey wall R_y = 4.0

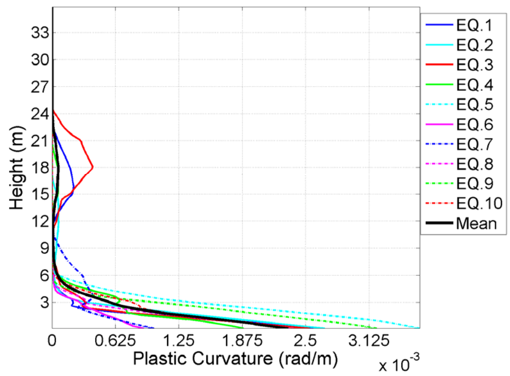

Figure B.207. Storey plastic curvature diagrams - twelve storey wall $R_y = 4.0$

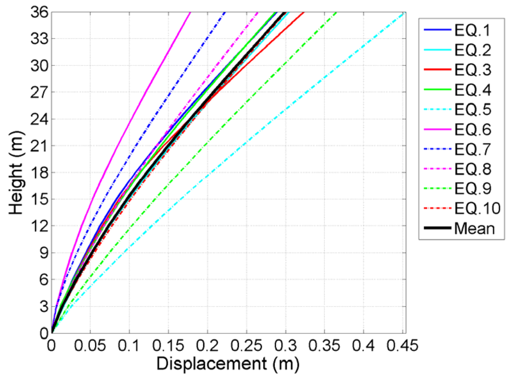

Figure B.210. Storey displacement diagrams - twelve storey wall $R_y = 4.0$

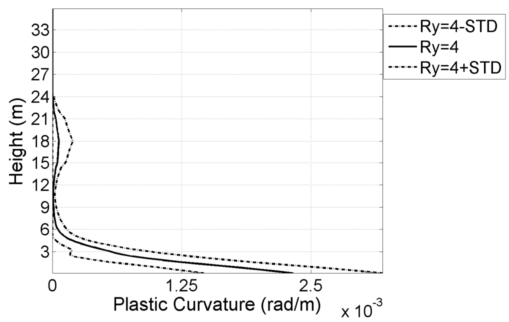

Figure B.208. Storey mean plastic curvature diagram and ±1 standard deviation of twelve storey wall $R_y = 4.0$

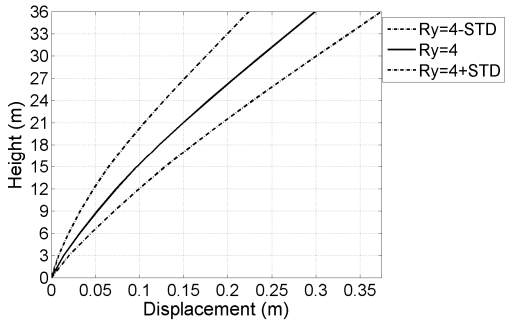

Figure B.211. Mean storey displacement diagram and ±1 standard deviation of twelve storey wall $R_y = 4.0$

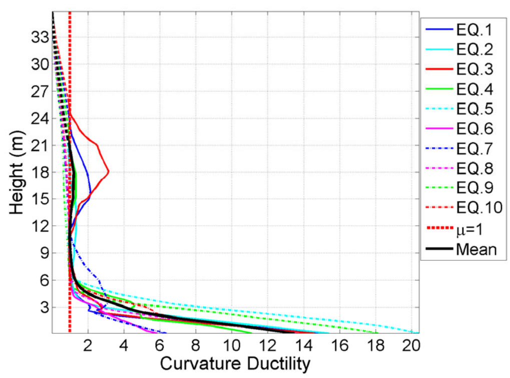

Figure B.209. Storey curvature ductility diagrams - twelve storey wall $R_y = 4.0$

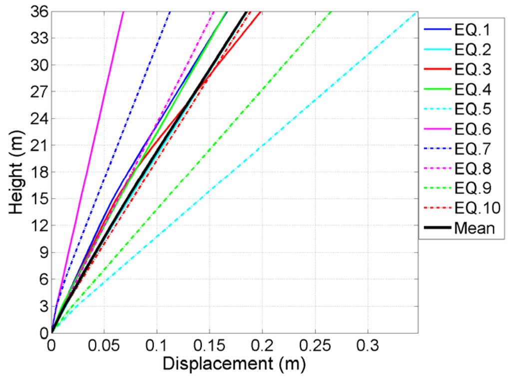

Figure B.212. Storey plastic displacement diagrams - twelve storey wall $R_y = 4.0$

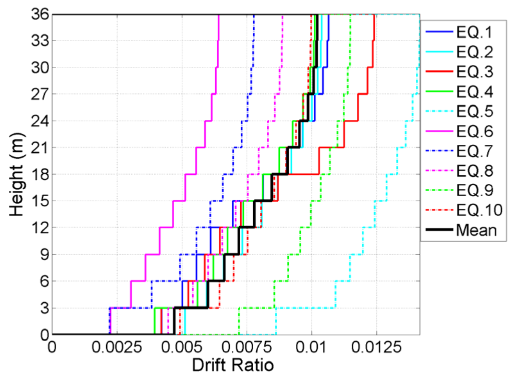

Figure B.213. Storey drift ratio diagrams - twelve storey wall $R_y = 4.0$

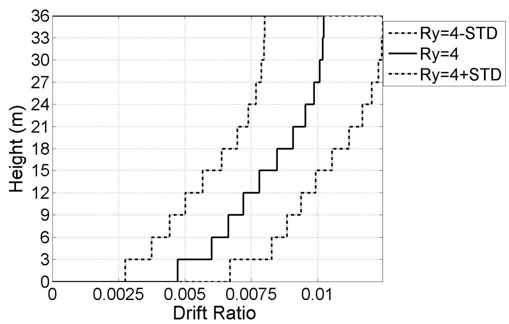

Figure B.214. Mean storey drift ratio diagram and ±1 standard deviation of twelve storey wall $R_y = 4.0$

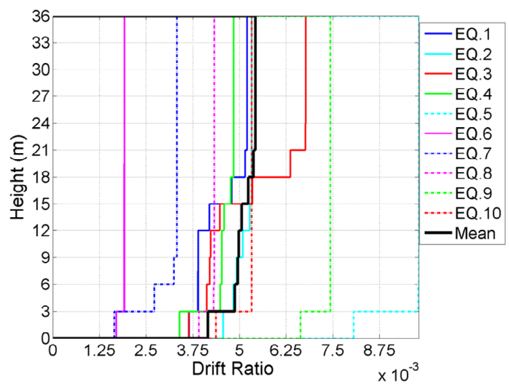

Figure B.215. Storey cumulative plastic drift ratio diagrams - twelve storey wall $R_y = 4.0$

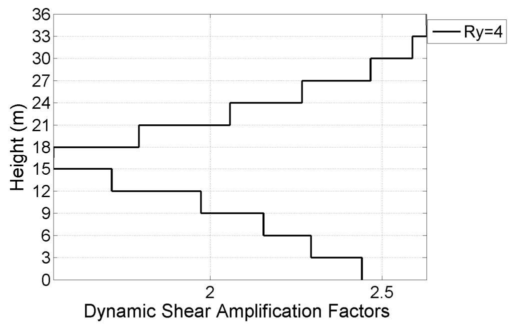

Figure B.216. Storey dynamic shear amplification factor diagrams - twelve storey wall $R_y = 4.0$

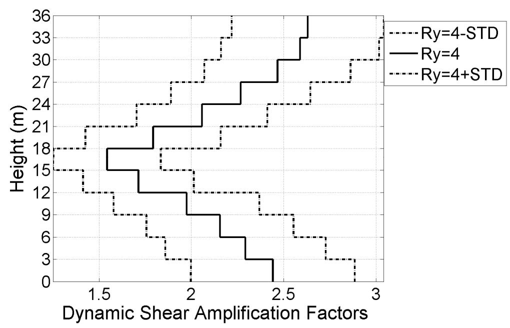

Figure B.217. Mean dynamic shear amplification factor diagram and ±1 standard deviation of twelve storey wall $R_y = 4.0$

B.3.4 Twelve Storey Structural Wall (R_y = 5.0)

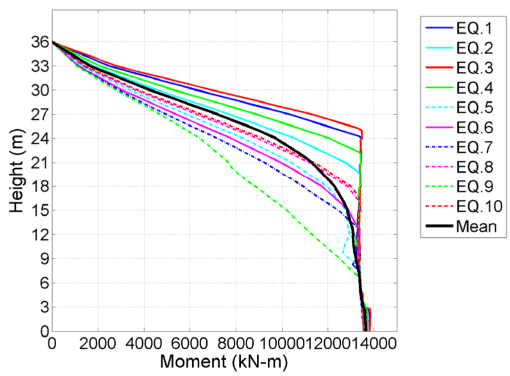

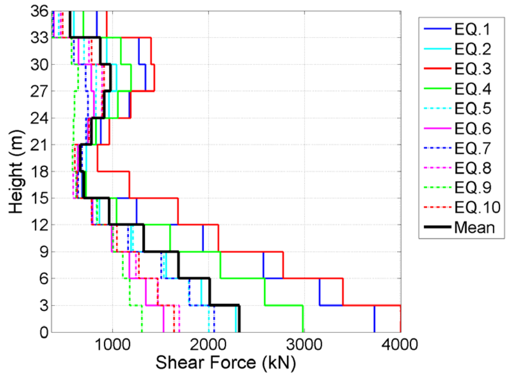

Figure B.218. Storey moment diagrams - twelve storey wall R_y = 5.0

Figure B.220. Storey shear force diagrams - twelve storey wall R_y = 5.0

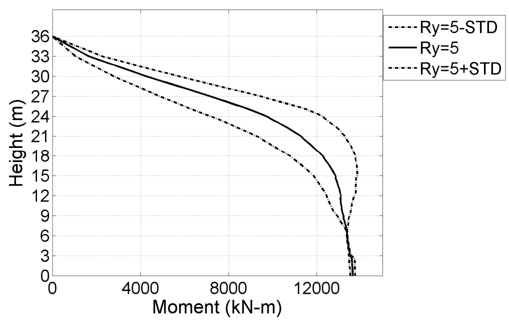

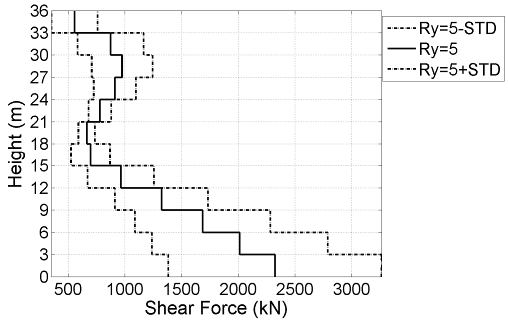

Figure B.219. Storey mean moment diagram and ±1 standard deviation of twelve storey wall R_y = 5.0

Figure B.221. Storey mean shear force diagram and ±1 standard deviation of twelve storey wall R_y = 5.0

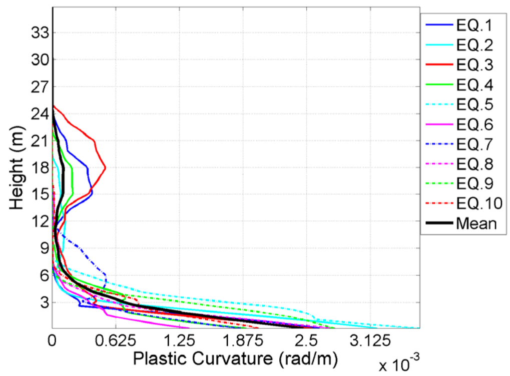

Figure B.222. Storey plastic curvature diagrams - twelve storey wall $R_y = 5.0$

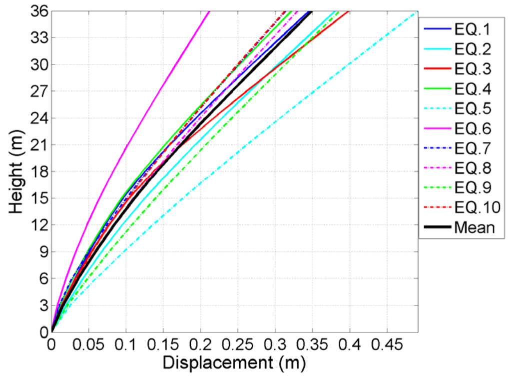

Figure B.225. Storey displacement diagrams - twelve storey wall $R_y = 5.0$

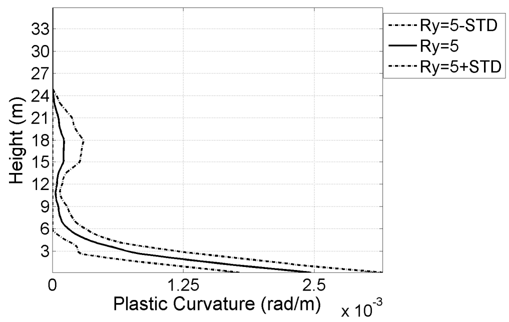

Figure B.223. Storey mean plastic curvature diagram and ±1 standard deviation of twelve storey wall $R_y = 5.0$

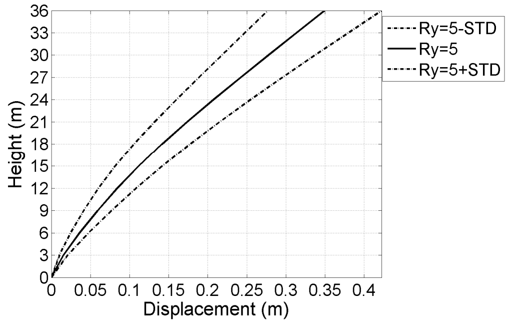

Figure B.226. Mean storey displacement diagram and ±1 standard deviation of twelve storey wall $R_y = 5.0$

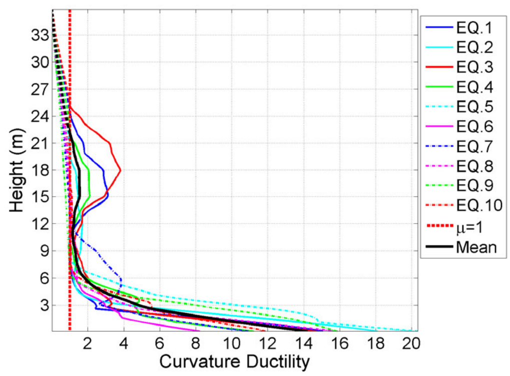

Figure B.224. Storey curvature ductility diagrams - twelve storey wall $R_y = 5.0$

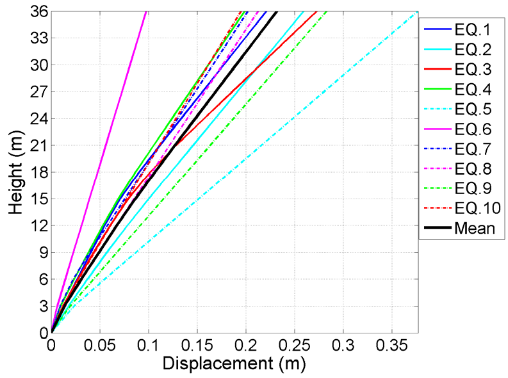

Figure B.227. Storey plastic displacement diagrams - twelve storey wall $R_y = 5.0$

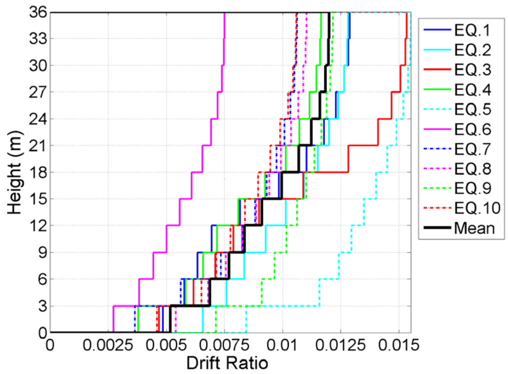

Figure B.228. Storey drift ratio diagrams - twelve storey wall $R_y = 5.0$

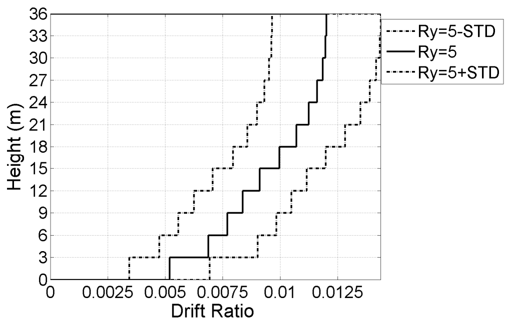

Figure B.229. Mean storey drift ratio diagram and ±1 standard deviation of twelve storey wall $R_y = 5.0$

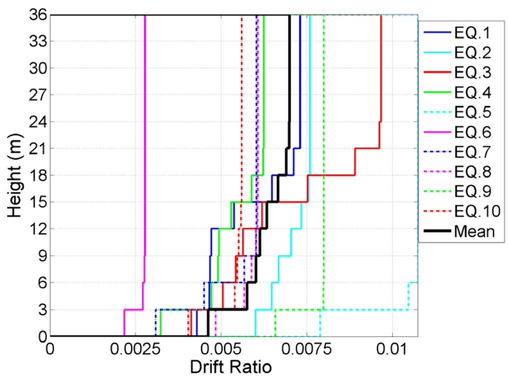

Figure B.230. Storey cumulative plastic drift ratio diagrams - twelve storey wall $R_y = 5.0$

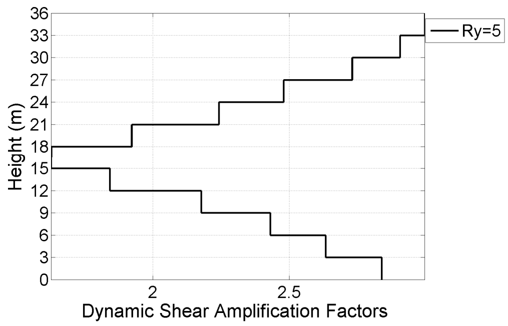

Figure B.231. Storey dynamic shear amplification factor diagrams - twelve storey wall $R_y = 5.0$

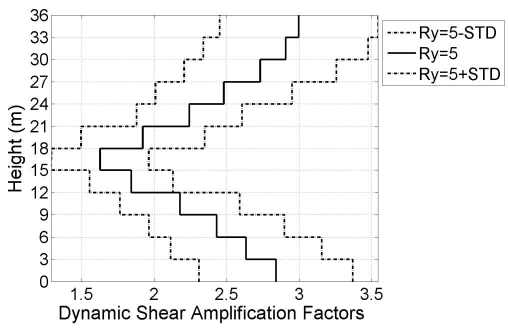

Figure B.232. Mean dynamic shear amplification factor diagram and ±1 standard deviation of twelve storey wall $R_y = 5.0$

B.3.5 Twelve Storey Structural Wall (R_y = 6.0)

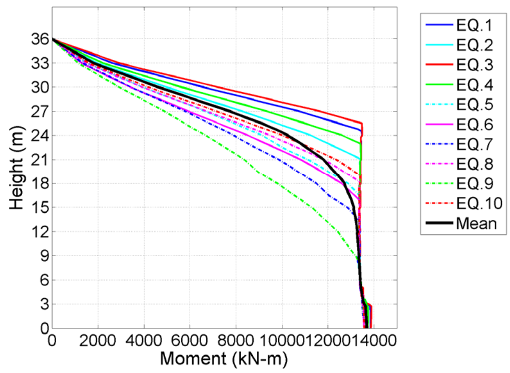

Figure B.233. Storey moment diagrams - twelve storey wall R_y = 6.0

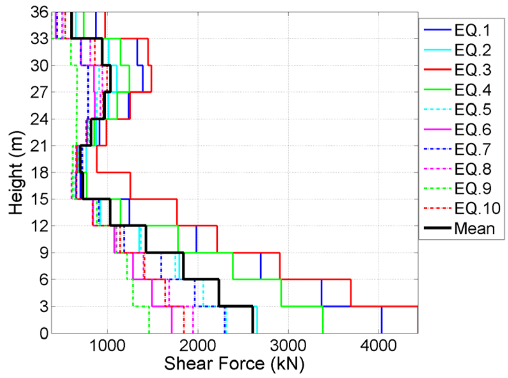

Figure B.235. Storey shear force diagrams - twelve storey wall R_y = 6.0

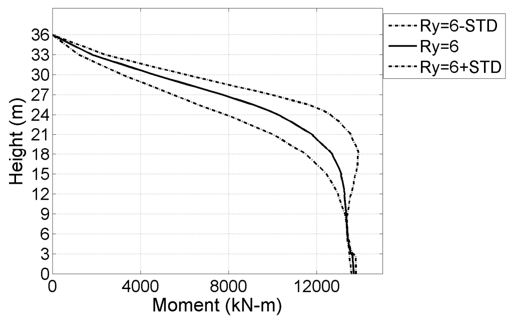

Figure B.234. Storey mean moment diagram and ±1 standard deviation of twelve storey wall R_y = 6.0

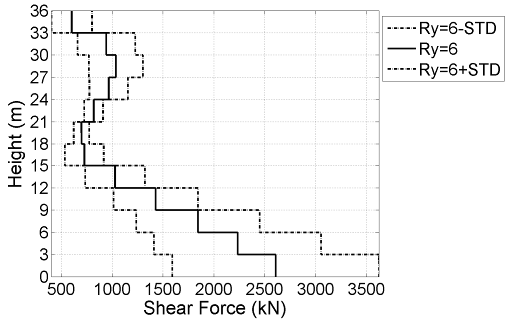

Figure B.236. Storey mean shear force diagram and ±1 standard deviation of twelve storey wall R_y = 6.0

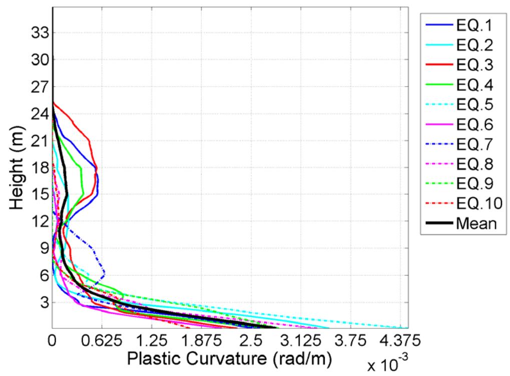

Figure B.237. Storey plastic curvature diagrams - twelve storey wall $R_y = 6.0$

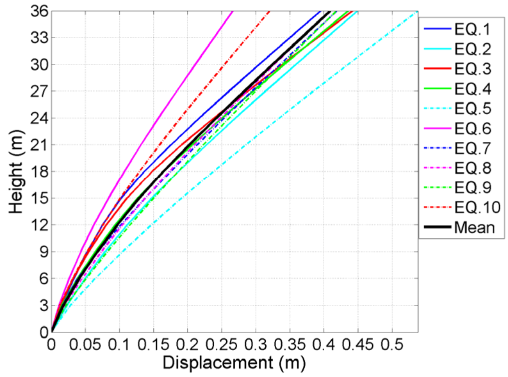

Figure B.240. Storey displacement diagrams - twelve storey wall $R_y = 6.0$

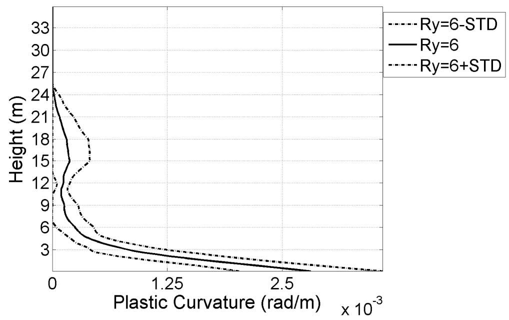

Figure B.238. Storey mean plastic curvature diagram and ±1 standard deviation of twelve storey wall $R_y = 6.0$

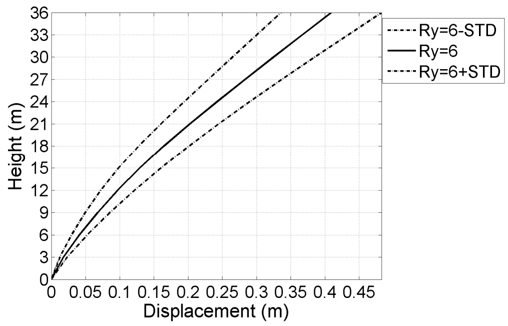

Figure B.241. Mean storey displacement diagram and ±1 standard deviation of twelve storey wall $R_y = 6.0$

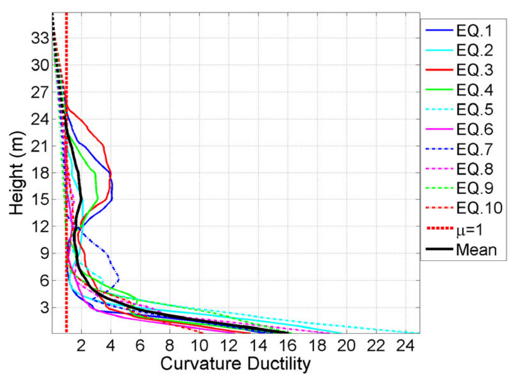

Figure B.239. Storey curvature ductility diagrams - twelve storey wall $R_y = 6.0$

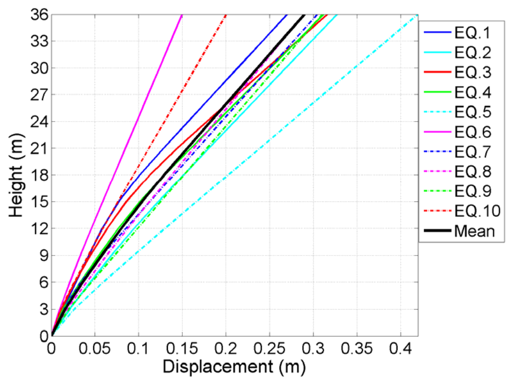

Figure B.242. Storey plastic displacement diagrams - twelve storey wall $R_y = 6.0$

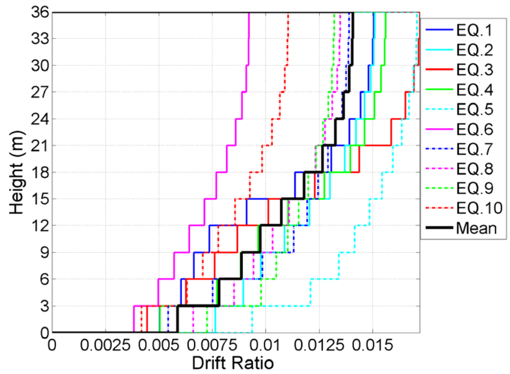

Figure B.243. Storey drift ratio diagrams - twelve storey wall $R_y = 6.0$

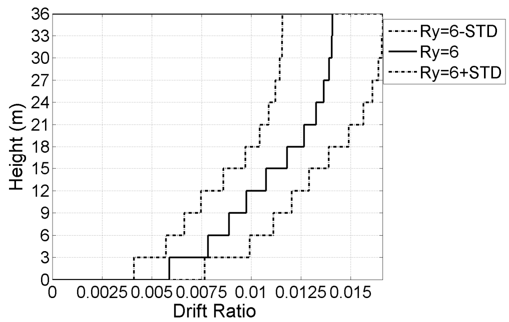

Figure B.244. Mean storey drift ratio diagram and ±1 standard deviation of twelve storey wall $R_y = 6.0$

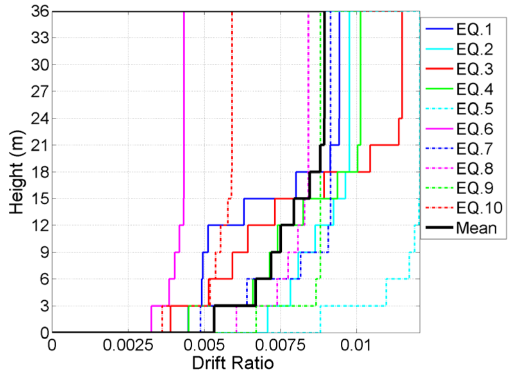

Figure B.245. Storey cumulative plastic drift ratio diagrams - twelve storey wall $R_y = 6.0$

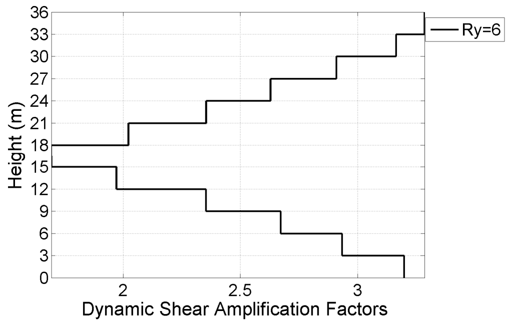

Figure B.246. Storey dynamic shear amplification factor diagrams - twelve storey wall $R_y = 6.0$

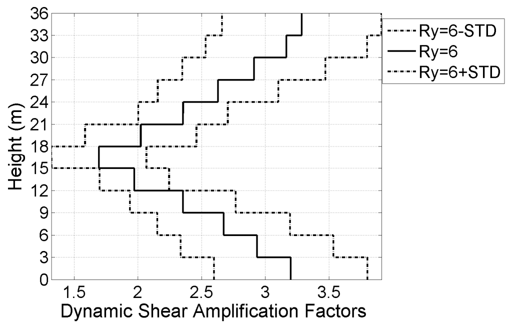

Figure B.247. Mean dynamic shear amplification factor diagram and ±1 standard deviation of twelve storey wall $R_y = 6.0$

B.3.6 Twelve Storey Structural Wall (Mean and ±1 standard deviation)

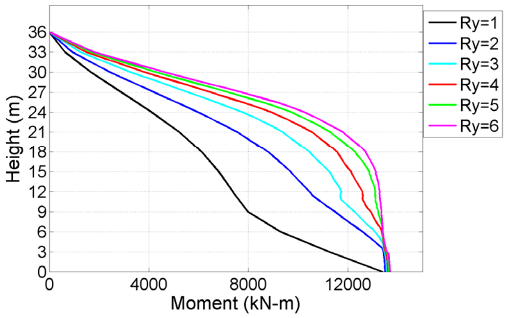

Figure B.248. Storey moment diagrams - twelve storey wall

R_y = 1.0, 2.0, 3.0, 4.0, 5.0, 6.0

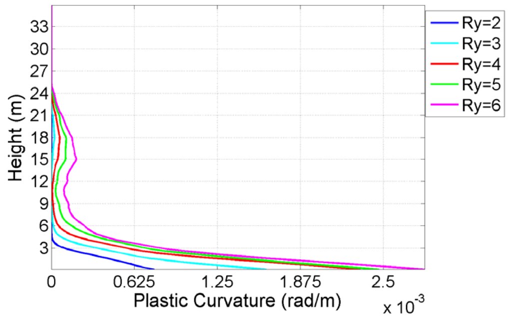

Figure B.250. Storey plastic curvature diagrams - twelve storey wall

R_y = 2.0, 3.0, 4.0, 5.0, 6.0

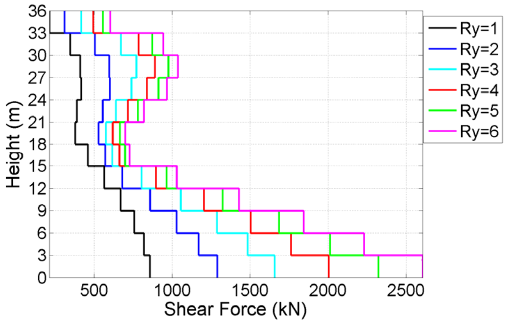

Figure B.249. Storey shear force diagrams - twelve storey wall

R_y = 1.0, 2.0, 3.0, 4.0, 5.0, 6.0

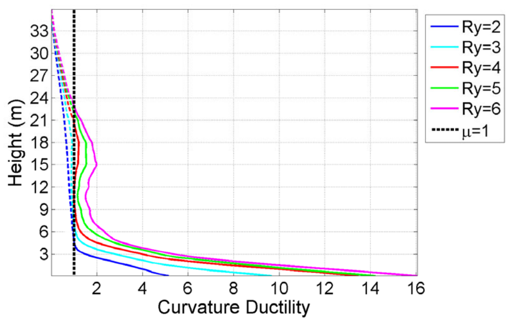

Figure B.251. Storey curvature ductility diagrams - twelve storey wall

R_y = 2.0, 3.0, 4.0, 5.0, 6.0

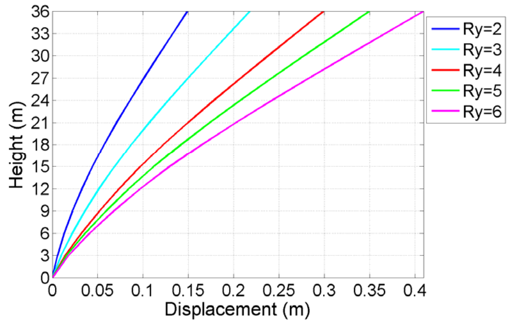

Figure B.252. Storey displacement diagrams - twelve storey wall R_y = 2.0, 3.0, 4.0, 5.0, 6.0

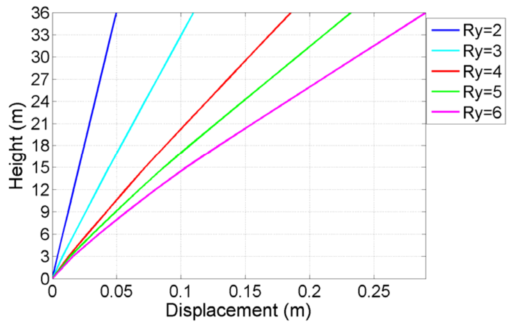

Figure B.253. Storey plastic displacement diagrams - twelve storey wall R_y = 2.0, 3.0, 4.0, 5.0, 6.0

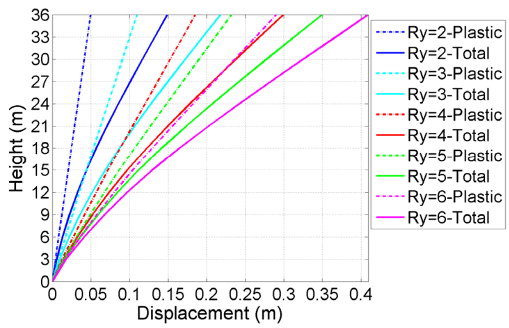

Figure B.254. Storey total displacement - plastic displacement comparison diagrams - twelve storey wall R_y = 2.0, 3.0, 4.0, 5.0, 6.0

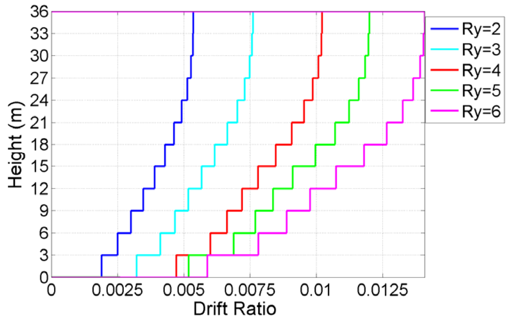

Figure B.255. Storey drift ratio diagrams - twelve storey wall R_y = 2.0, 3.0, 4.0, 5.0, 6.0

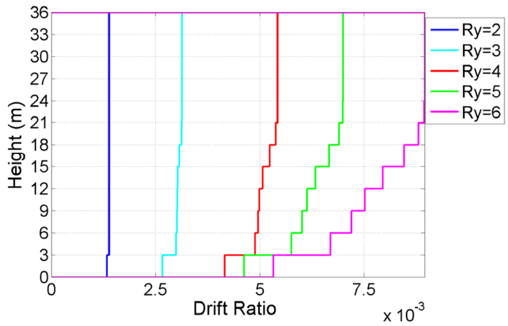

Figure B.256. Storey cumulative plastic drift ratio diagrams - twelve storey wall R_y = 2.0, 3.0, 4.0, 5.0, 6.0

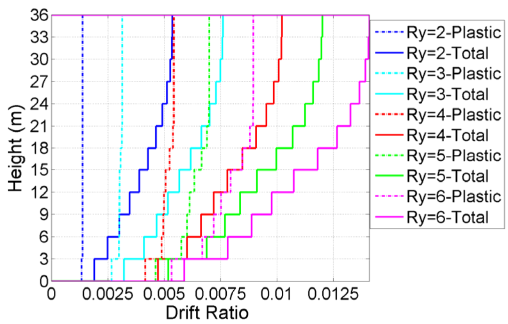

Figure B.257. Storey drift ratio - cumulative plastic drift ratio comparison diagrams - twelve storey wall R_y = 2.0, 3.0, 4.0, 5.0, 6.0

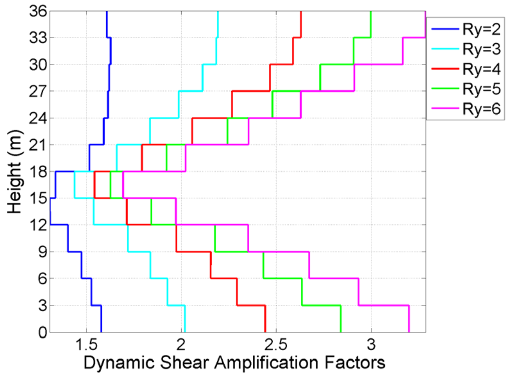

Figure B.258. Storey dynamic shear amplification factor diagrams - twelve storey wall R_y = 2.0, 3.0, 4.0, 5.0, 6.0

B.4.1 Sixteen Storey Structural Wall (R_y =2.0)

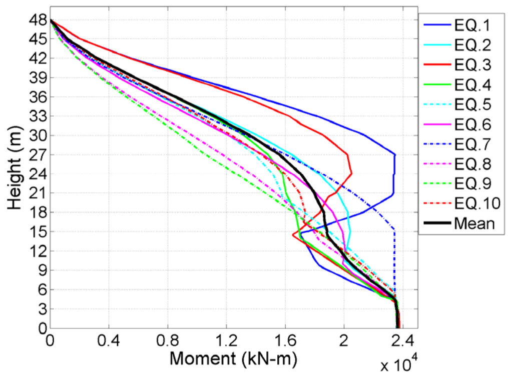

Figure B.259. Storey moment diagrams - sixteen storey wall R_y = 2.0

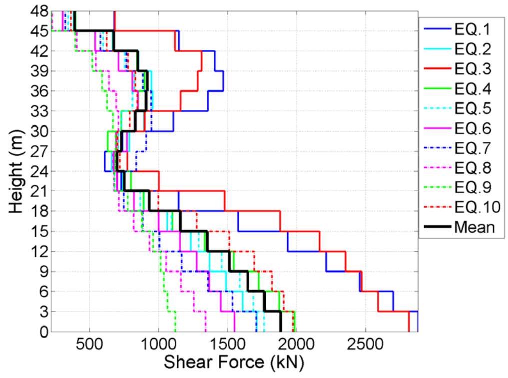

Figure B.261. Storey shear force diagrams - sixteen storey wall R_y = 2.0

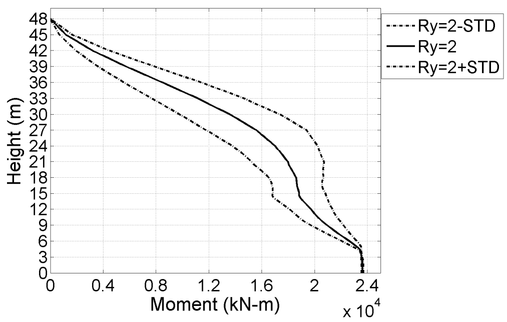

Figure B.260. Storey mean moment diagram and ±1 standard deviation of sixteen storey wall R_y = 2.0

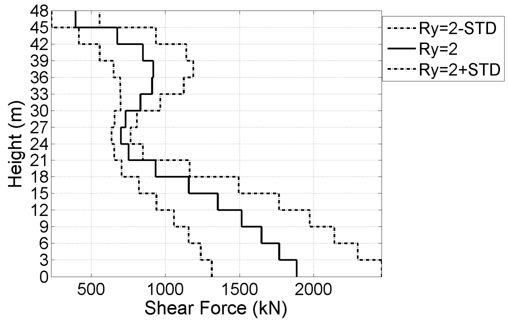

Figure B.262. Storey mean shear force diagram and ±1 standard deviation of sixteen storey wall R_y = 2.0

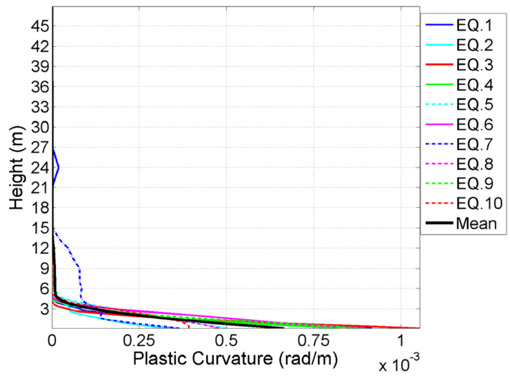

Figure B.263. Storey plastic curvature diagrams - sixteen storey wall $R_y = 2.0$

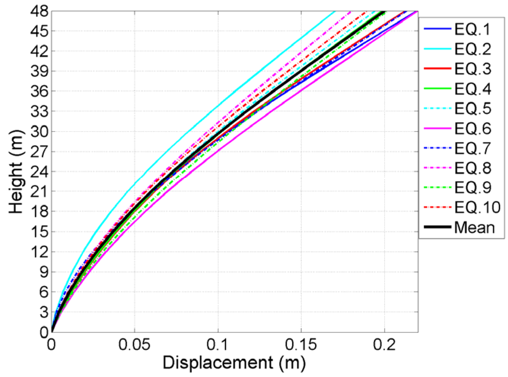

Figure B.266. Storey displacement diagrams - sixteen storey wall $R_y = 2.0$

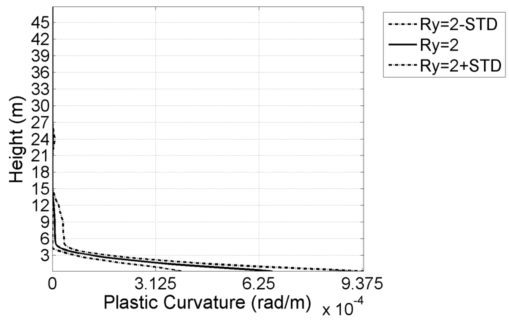

Figure B.264. Storey mean plastic curvature diagram and ±1 standard deviation of sixteen storey wall $R_y = 2.0$

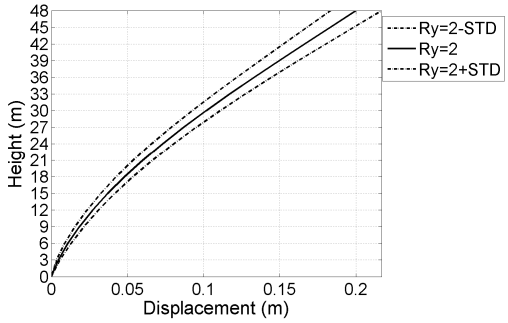

Figure B.267. Mean storey displacement diagram and ±1 standard deviation of sixteen storey wall $R_y = 2.0$

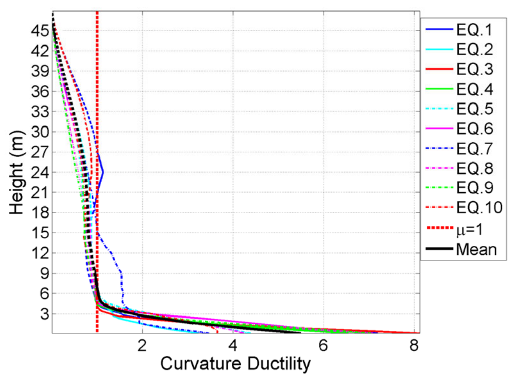

Figure B.265. Storey curvature ductility diagrams - sixteen storey wall $R_y = 2.0$

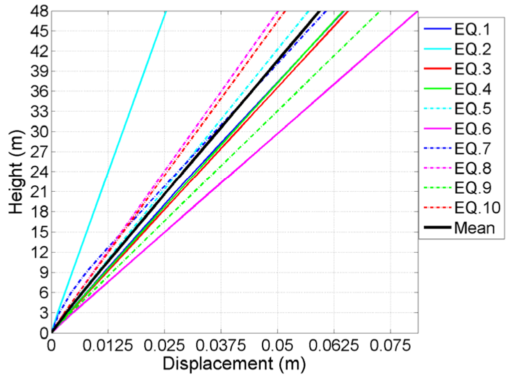

Figure B.268. Storey plastic displacement diagrams - sixteen storey wall $R_y = 2.0$

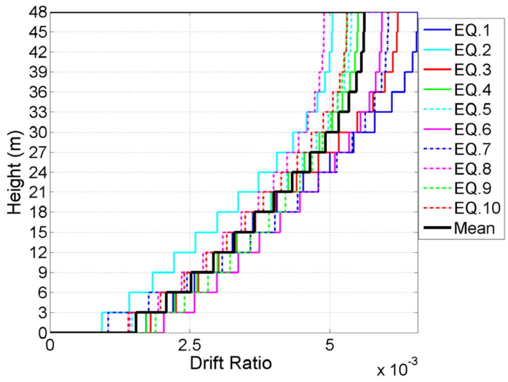

Figure B.269. Storey drift ratio diagrams - sixteen storey wall $R_y = 2.0$

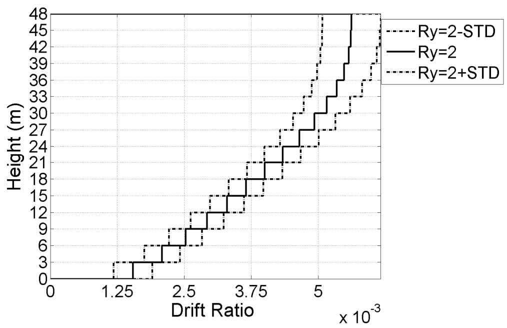

Figure B.270. Mean storey drift ratio diagram and ±1 standard deviation of sixteen storey wall $R_y = 2.0$

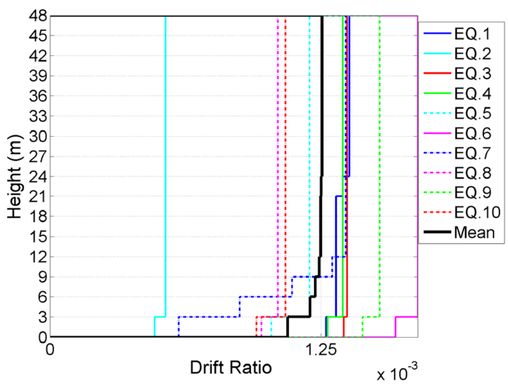

Figure B.271. Storey cumulative plastic drift ratio diagrams - sixteen storey wall $R_y = 2.0$

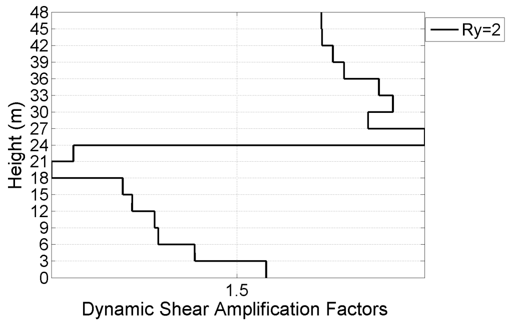

Figure B.272. Storey dynamic shear amplification factor diagrams - sixteen storey wall $R_y = 2.0$

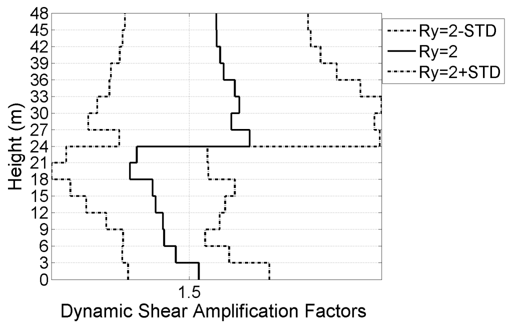

Figure B.273. Mean dynamic shear amplification factor diagram and ±1 standard deviation of sixteen storey wall $R_y = 2.0$

B.4.2 Sixteen Storey Structural Wall (R_y = 3.0)

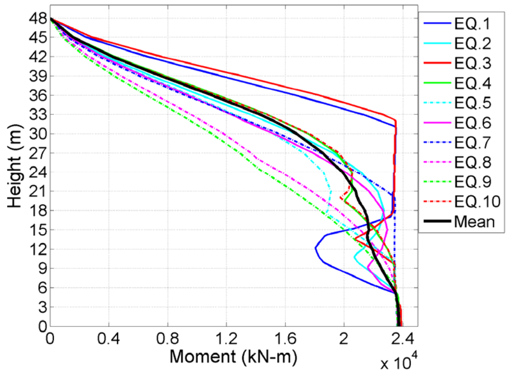

Figure B.274. Storey moment diagrams - sixteen storey wall R_y = 3.0

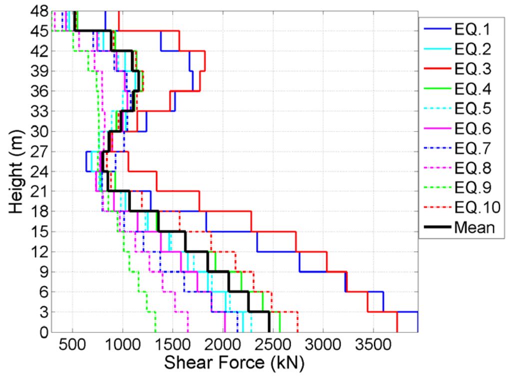

Figure B.276. Storey shear force diagrams - sixteen storey wall R_y = 3.0

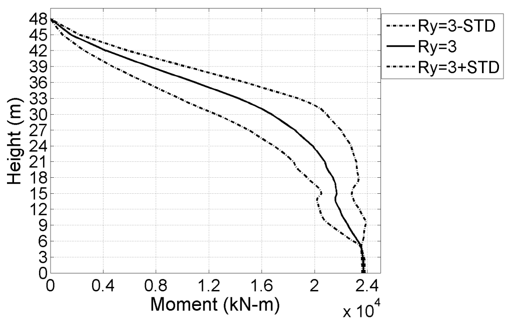

Figure B.275. Storey mean moment diagram and ±1 standard deviation of sixteen storey wall R_y = 3.0

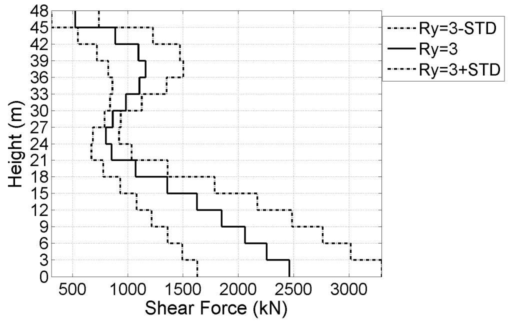

Figure B.277. Storey mean shear force diagram and ±1 standard deviation of sixteen storey wall R_y = 3.0

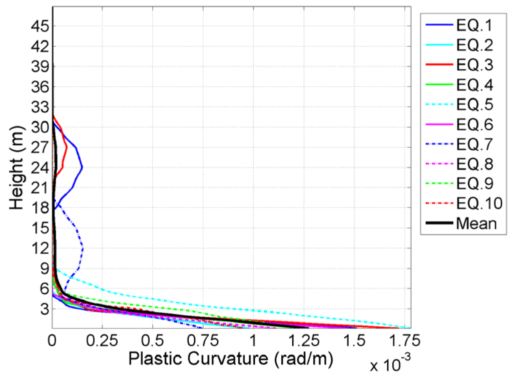

Figure B.278. Storey plastic curvature diagrams - sixteen storey wall $R_y = 3.0$

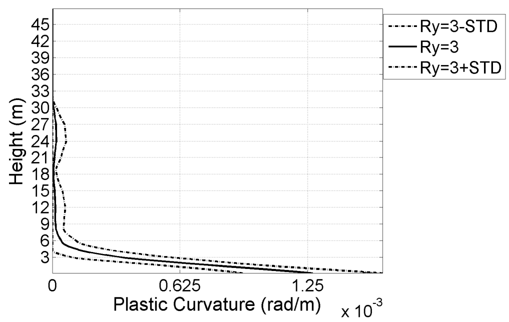

Figure B.279. Storey mean plastic curvature diagram and ±1 standard deviation of sixteen storey wall $R_y = 3.0$

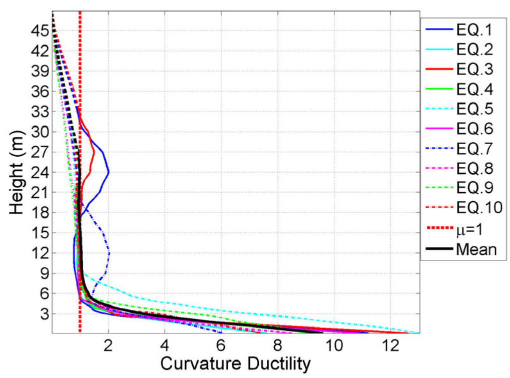

Figure B.280. Storey curvature ductility diagrams - sixteen storey wall $R_y = 3.0$

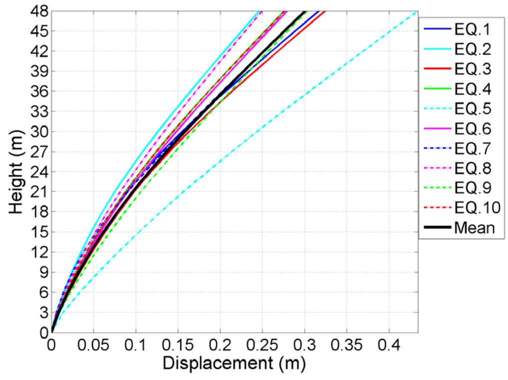

Figure B.281. Storey displacement diagrams - sixteen storey wall $R_y = 3.0$

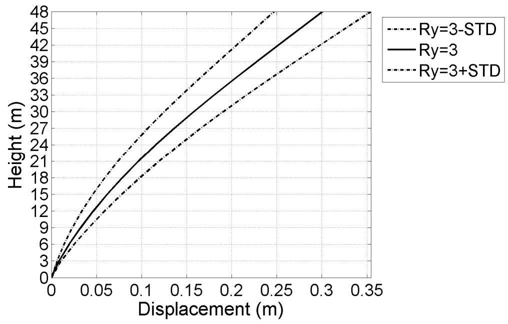

Figure B.282. Mean storey displacement diagram and ±1 standard deviation of sixteen storey wall $R_y = 3.0$

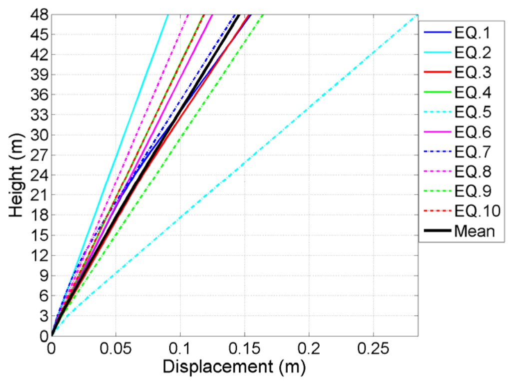

Figure B.283. Storey plastic displacement diagrams - sixteen storey wall $R_y = 3.0$

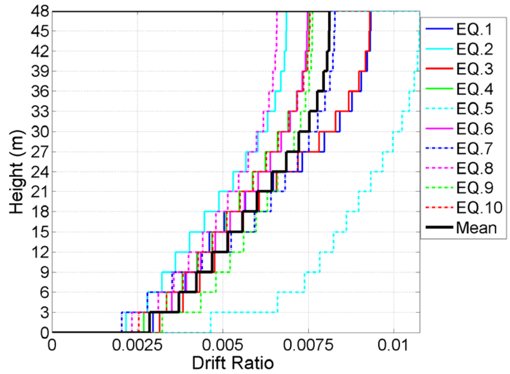

Figure B.284. Storey drift ratio diagrams - sixteen storey wall $R_y = 3.0$

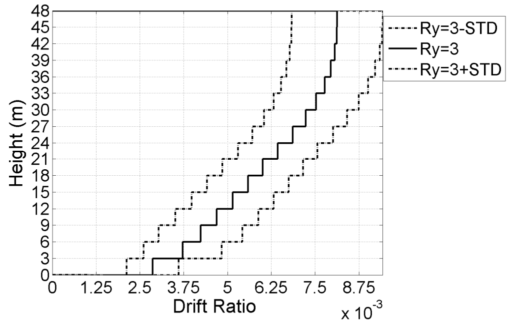

Figure B.285. Mean storey drift ratio diagram and ±1 standard deviation of sixteen storey wall $R_y = 3.0$

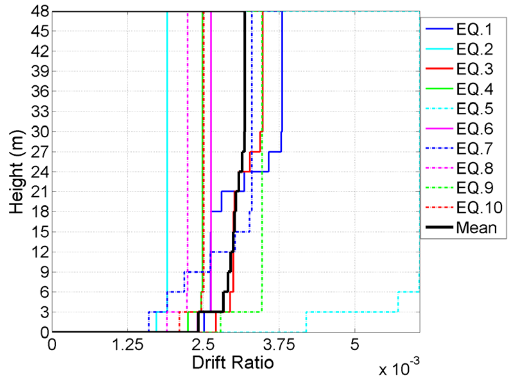

Figure B.286. Storey cumulative plastic drift ratio diagrams - sixteen storey wall $R_y = 3.0$

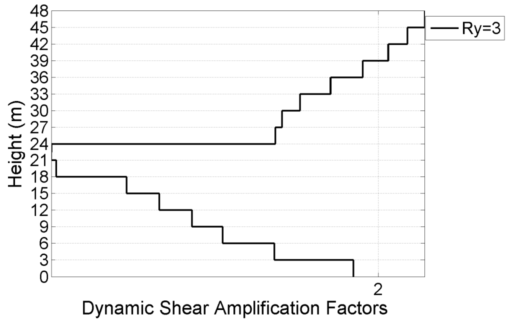

Figure B.287. Storey dynamic shear amplification factor diagrams - sixteen storey wall $R_y = 3.0$

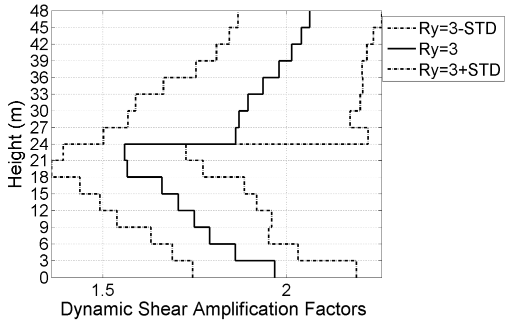

Figure B.288. Mean dynamic shear amplification factor diagram and ±1 standard deviation of storey sixteen storey wall $R_y = 3.0$

B.4.3 Sixteen Storey Structural Wall (R_y = 4.0)

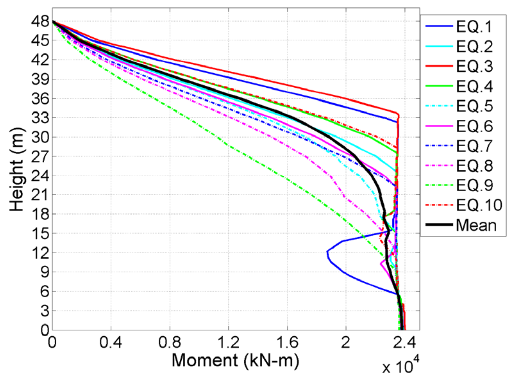

Figure B.289. Storey moment diagrams - sixteen storey wall R_y = 4.0

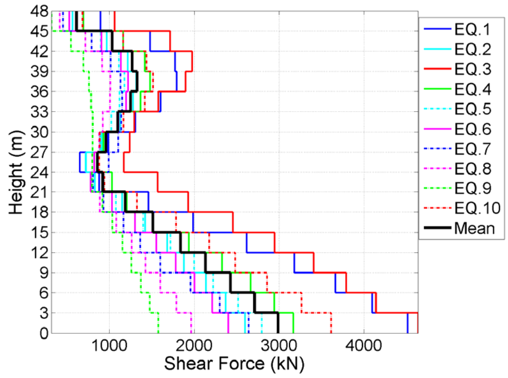

Figure B.291. Storey shear force diagrams - sixteen storey wall R_y = 4.0

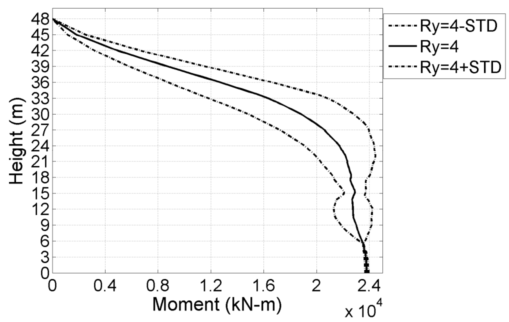

Figure B.290. Storey mean moment diagram and ±1 standard deviation of sixteen storey wall R_y = 4.0

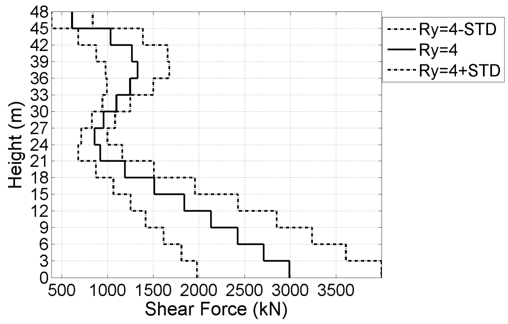

Figure B.292. Storey mean shear force diagram and ±1 standard deviation of sixteen storey wall R_y = 4.0

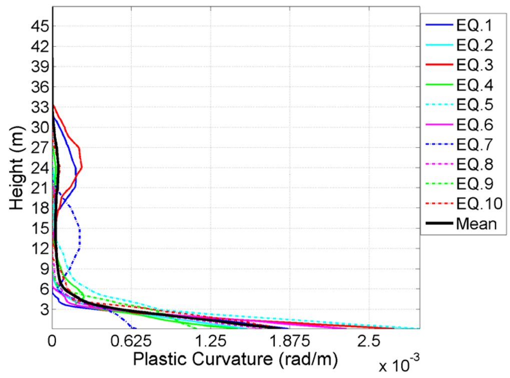

Figure B.293. Storey plastic curvature diagrams - sixteen storey wall $R_y = 4.0$

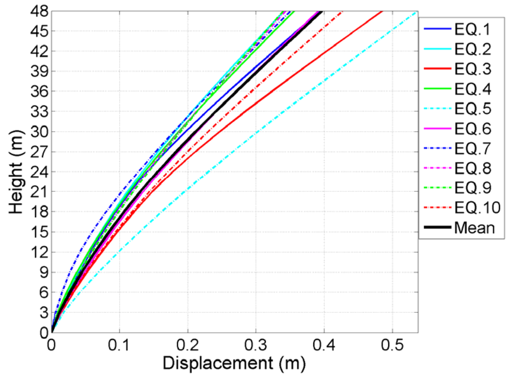

Figure B.296. Storey displacement diagrams - sixteen storey wall $R_y = 4.0$

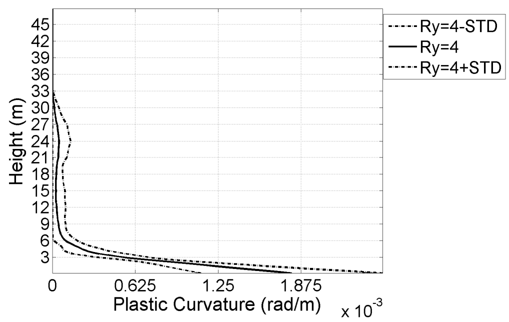

Figure B.294. Storey mean plastic curvature diagram and ±1 standard deviation of sixteen storey wall $R_y = 4.0$

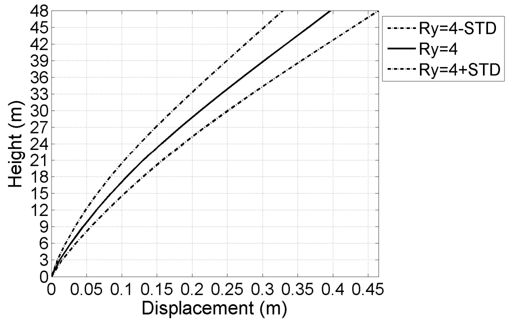

Figure B.297. Mean storey displacement diagram and ±1 standard deviation of sixteen storey wall $R_y = 4.0$

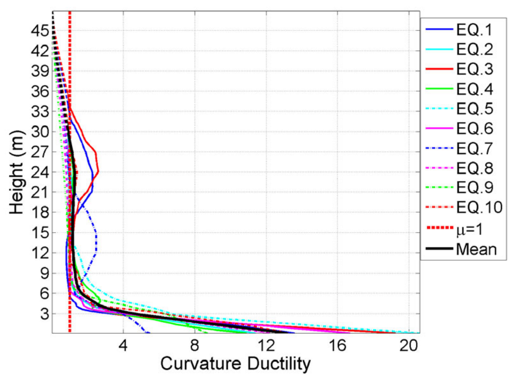

Figure B.295. Storey curvature ductility diagrams - sixteen storey wall $R_y = 4.0$

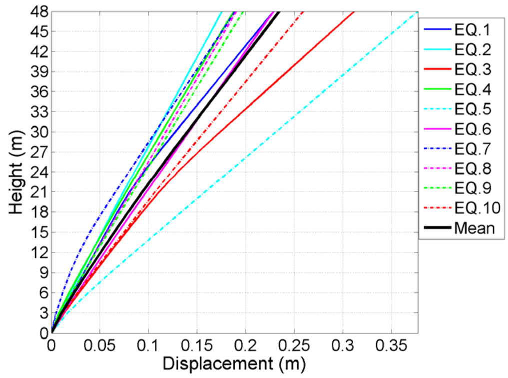

Figure B.298. Storey plastic displacement diagrams - sixteen storey wall $R_y = 4.0$

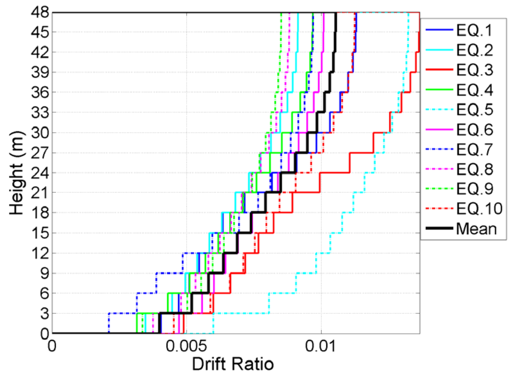

Figure B.299. Storey drift ratio diagrams - sixteen storey wall $R_y = 4.0$

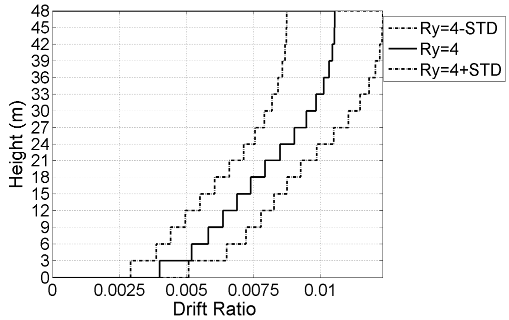

Figure B.300. Mean storey drift ratio diagram and ±1 standard deviation of sixteen storey wall $R_y = 4.0$

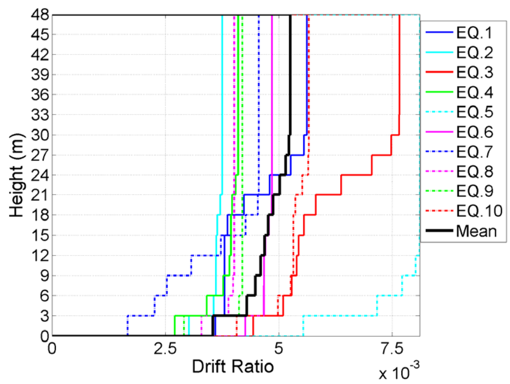

Figure B.301. Storey cumulative plastic drift ratio diagrams - sixteen storey wall $R_y = 4.0$

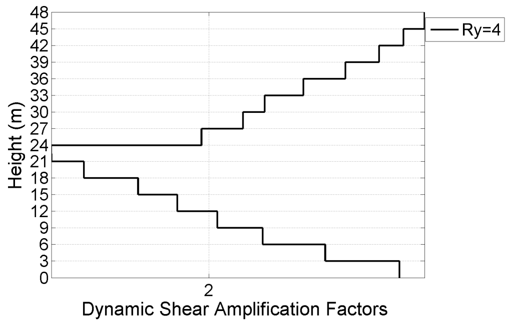

Figure B.302. Storey dynamic shear amplification factor diagrams - sixteen storey wall $R_y = 4.0$

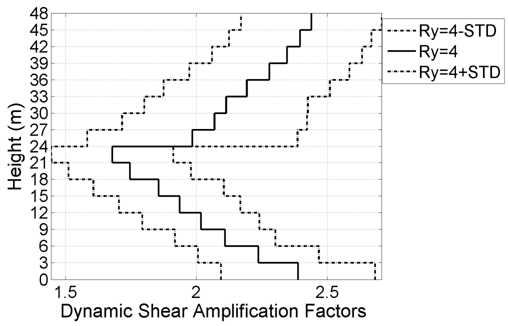

Figure B.303. Mean dynamic shear amplification factor diagram and ±1 standard deviation of sixteen storey wall $R_y = 4.0$

B.4.4 Sixteen Storey Structural Wall (R_y = 5.0)

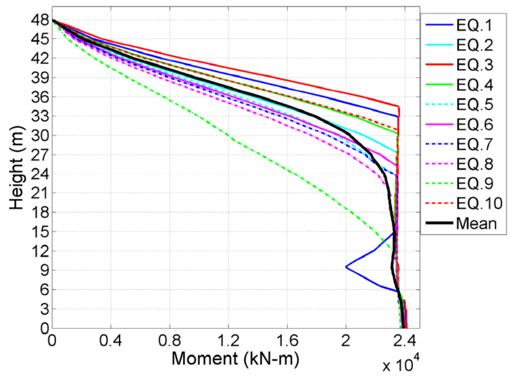

Figure B.304. Storey moment diagrams - sixteen storey wall R_y = 5.0

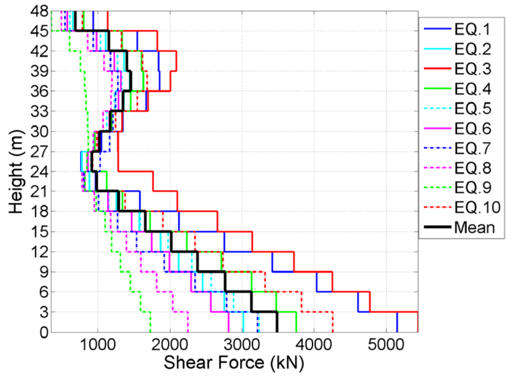

Figure B.306. Storey shear force diagrams - sixteen storey wall R_y = 5.0

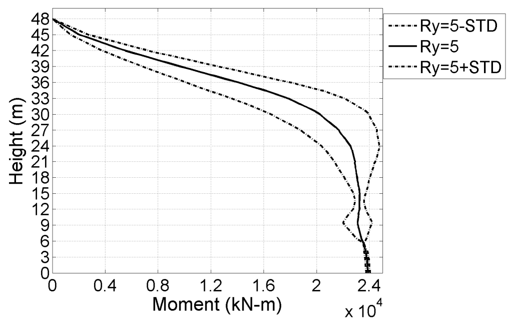

Figure B.305. Storey mean moment diagram and ±1 standard deviation of sixteen storey wall R_y = 5.0

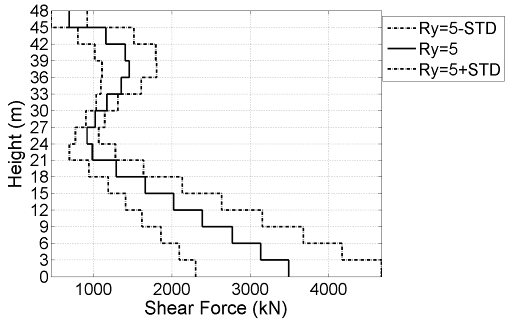

Figure B.307. Storey mean shear force diagram and ±1 standard deviation of sixteen storey wall R_y = 5.0

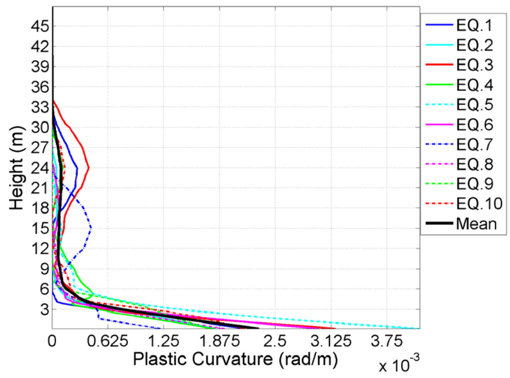

Figure B.308. Storey plastic curvature diagrams - sixteen storey wall $R_y = 5.0$

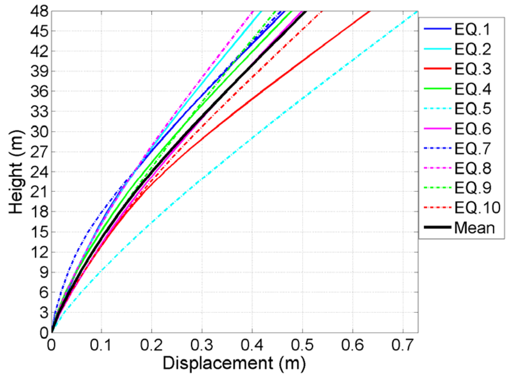

Figure B.311. Storey displacement diagrams - sixteen storey wall $R_y = 5.0$

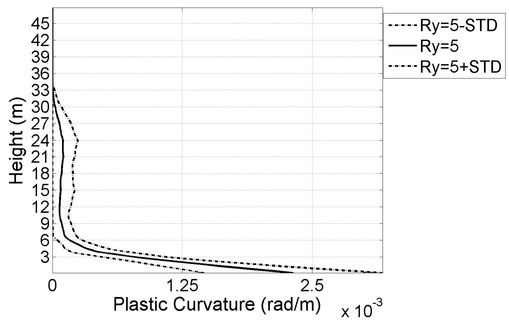

Figure B.309. Storey mean plastic curvature diagram and ±1 standard deviation of sixteen storey wall $R_y = 5.0$

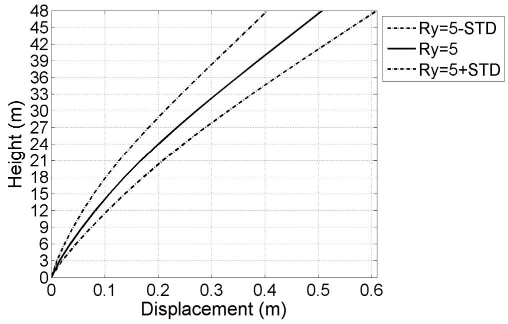

Figure B.312. Mean storey displacement diagram and ±1 standard deviation of sixteen storey wall $R_y = 5.0$

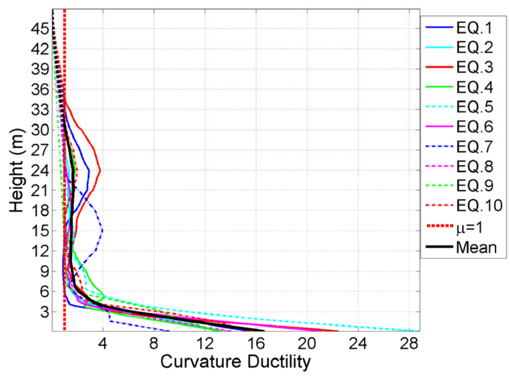

Figure B.310. Storey curvature ductility diagrams - sixteen storey wall $R_y = 5.0$

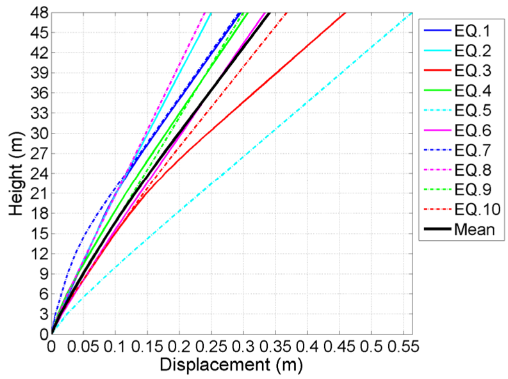

Figure B.313. Storey plastic displacement diagrams - sixteen storey wall $R_y = 5.0$

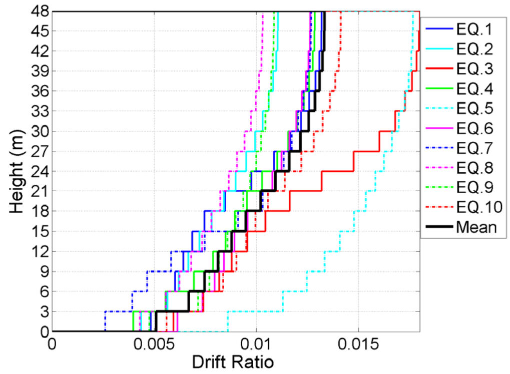

Figure B.314. Storey drift ratio diagrams - sixteen storey wall $R_y = 5.0$

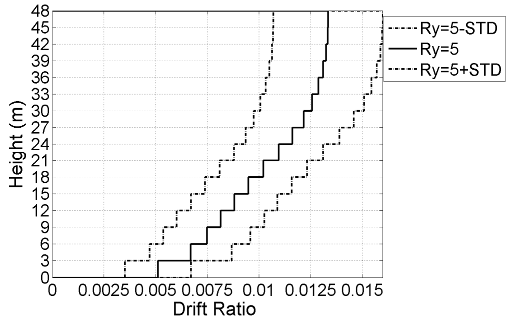

Figure B.315. Mean storey drift ratio diagram and ±1 standard deviation of sixteen storey wall $R_y = 5.0$

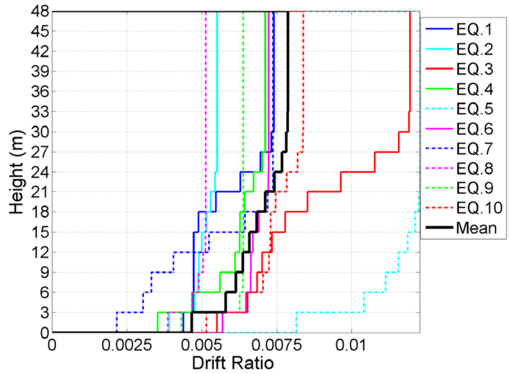

Figure B.316. Storey cumulative plastic drift ratio diagrams - sixteen storey wall $R_y = 5.0$

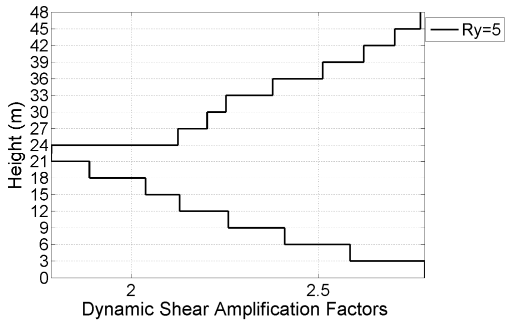

Figure B.317. Storey dynamic shear amplification factor diagrams - sixteen storey wall $R_y = 5.0$

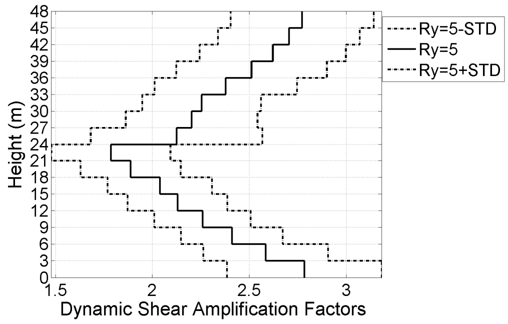

Figure B.318. Mean dynamic shear amplification factor diagram and ±1 standard deviation of sixteen storey wall $R_y = 5.0$

B.4.5. Sixteen Storey Structural Wall (Ry = 6.0)

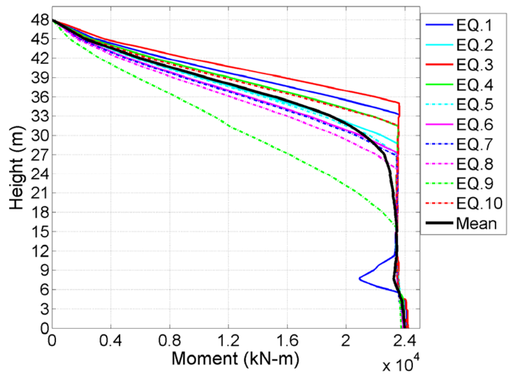

Figure B.319. Storey moment diagrams - sixteen storey wall $R_y = 6.0$

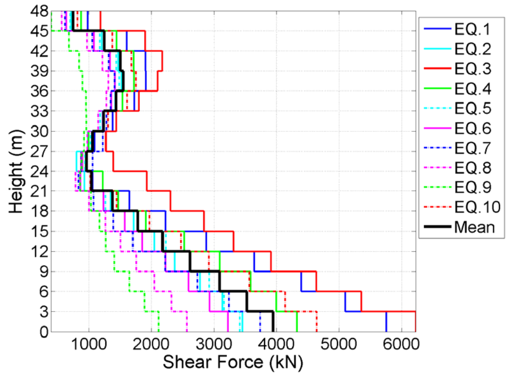

Figure B.321. Storey shear force diagrams - sixteen storey wall $R_y = 6.0$

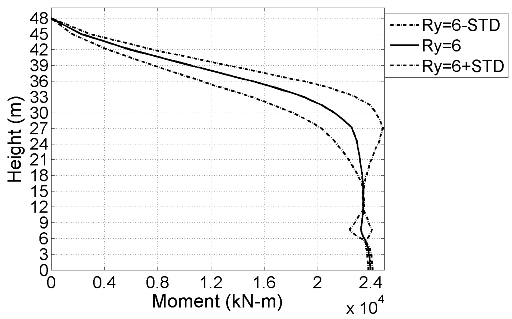

Figure B.320. Storey mean moment diagram and ±1 standard deviation of sixteen storey wall $R_y = 6.0$

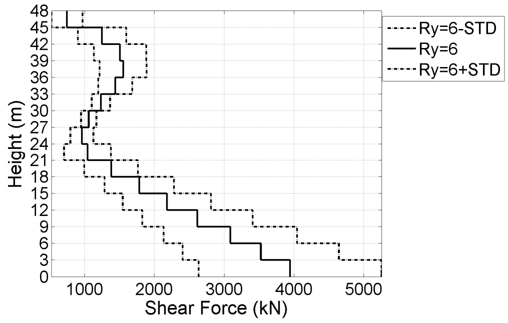

Figure B.322. Storey mean shear force diagram and ±1 standard deviation of sixteen storey wall $R_y = 6.0$

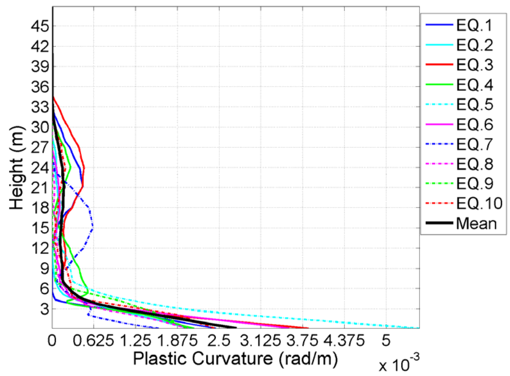

Figure B.323. Storey plastic curvature diagrams - sixteen storey wall $R_y = 6.0$

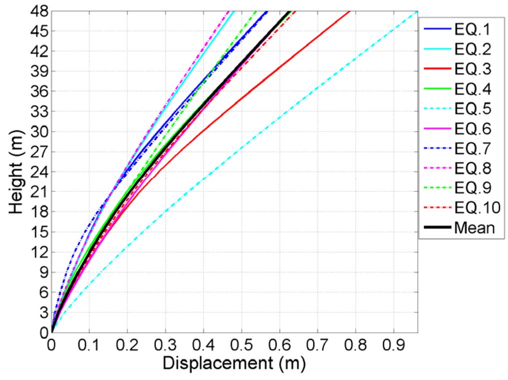

Figure B.326. Storey displacement diagrams - sixteen storey wall $R_y = 6.0$

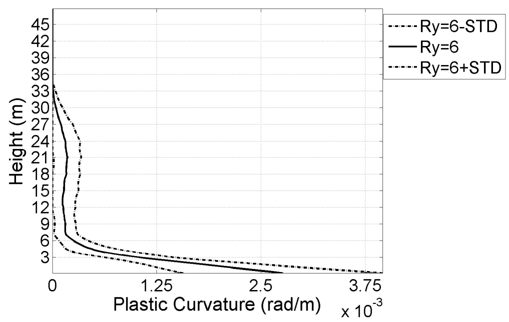

Figure B.324. Storey mean plastic curvature diagram and ±1 standard deviation of sixteen storey wall $R_y = 6.0$

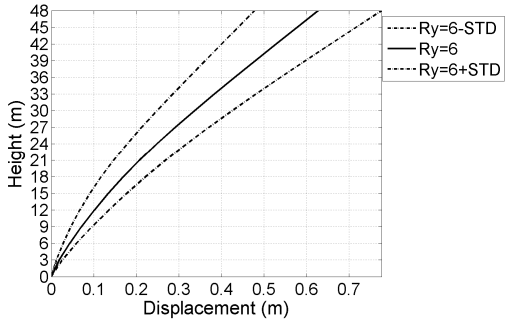

Figure B.327. Mean storey displacement diagram and ±1 standard deviation of sixteen storey wall $R_y = 6.0$

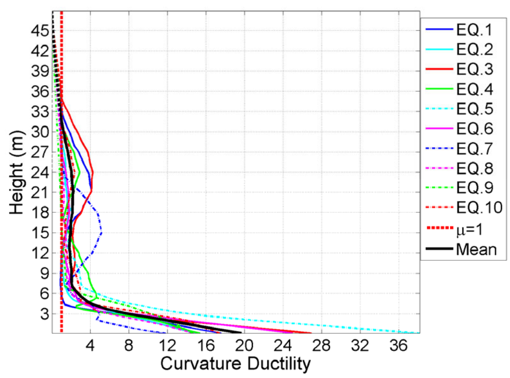

Figure B.325. Storey curvature ductility diagrams - sixteen storey wall $R_y = 6.0$

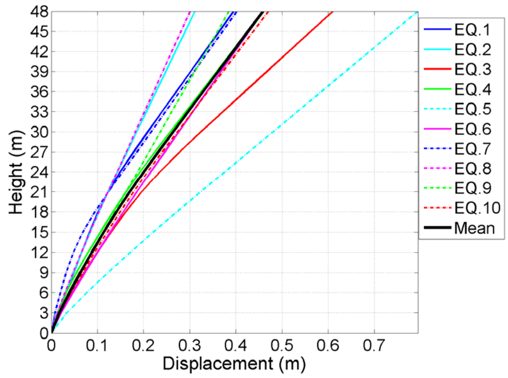

Figure B.328. Storey plastic displacement diagrams - sixteen storey wall $R_y = 6.0$

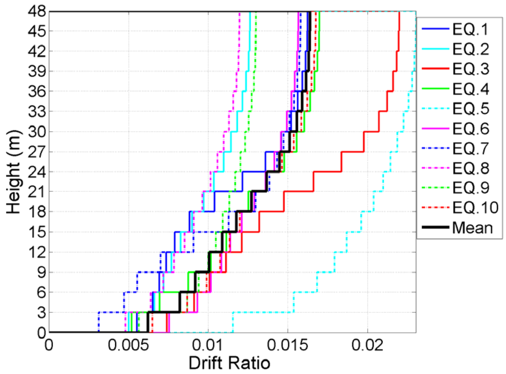

Figure B.329. Storey drift ratio diagrams - sixteen storey wall $R_y = 6.0$

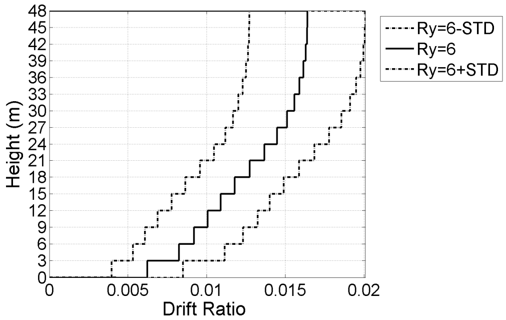

Figure B.330. Mean storey drift ratio diagram and ±1 standard deviation of sixteen storey wall $R_y = 6.0$

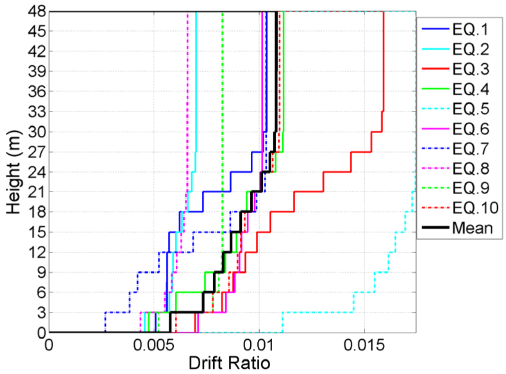

Figure B.331. Storey cumulative plastic drift ratio diagrams - sixteen storey wall $R_y = 6.0$

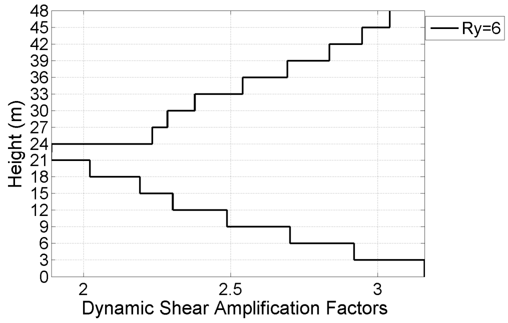

Figure B.332. Storey dynamic shear amplification factor diagrams - sixteen storey wall $R_y = 6.0$

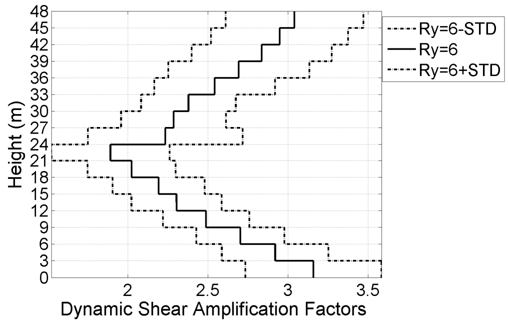

Figure B.333. Mean dynamic shear amplification factor diagram and ±1 standard deviation of sixteen storey wall $R_y = 6.0$

B.4.6 Sixteen Storey Structural Wall (Mean and ±1 standard deviation)

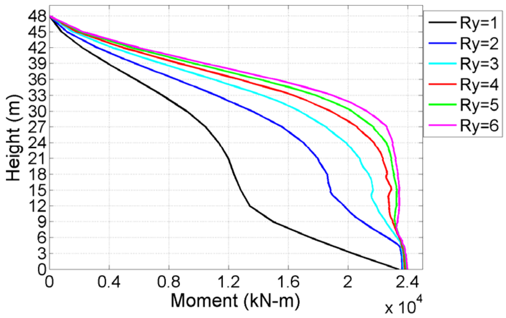

Figure B.334. Storey moment diagrams - sixteen storey wall

Ry = 1.0, 2.0, 3.0, 4.0, 5.0, 6.0

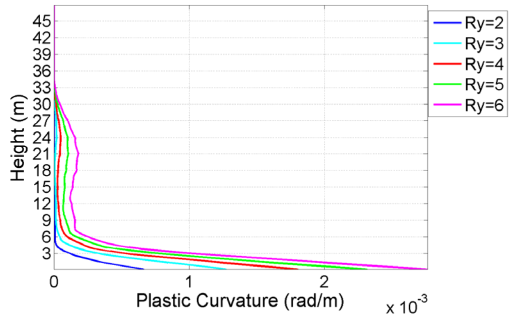

Figure B.336. Storey plastic curvature diagrams - sixteen storey wall

R_y = 2.0, 3.0, 4.0, 5.0, 6.0

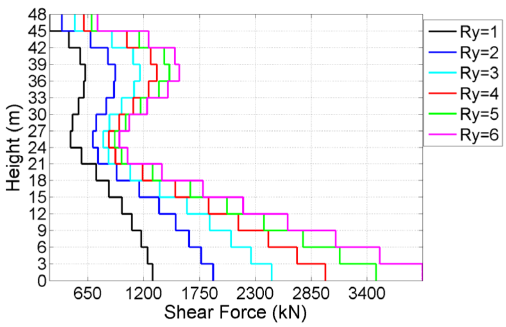

Figure B.335. Storey shear force diagrams - sixteen storey wall

R_y = 1.0, 2.0, 3.0, 4.0, 5.0, 6.0

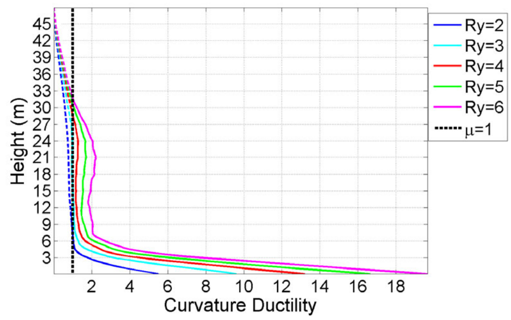

Figure B.337. Storey curvature ductility diagrams - sixteen storey wall

R_y = 2.0, 3.0, 4.0, 5.0, 6.0

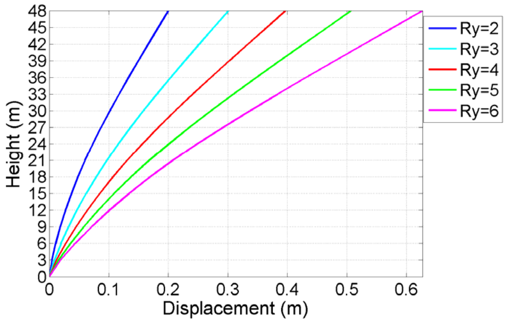

Figure B.338. Storey displacement diagrams - sixteen storey wall R_y = 2.0, 3.0, 4.0, 5.0, 6.0

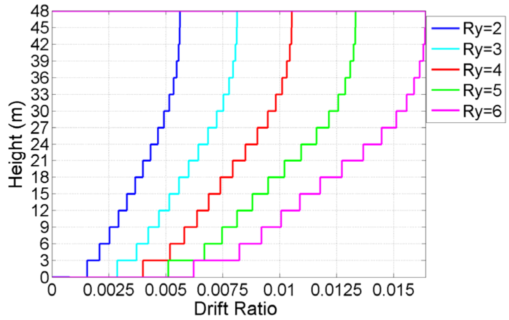

Figure B.341. Storey drift ratio diagrams - sixteen storey wall R_y = 2.0, 3.0, 4.0, 5.0, 6.0

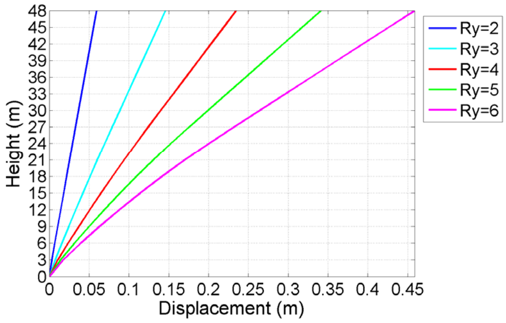

Figure B.339. Storey plastic displacement diagrams - sixteen storey wall R_y = 2.0, 3.0, 4.0, 5.0, 6.0

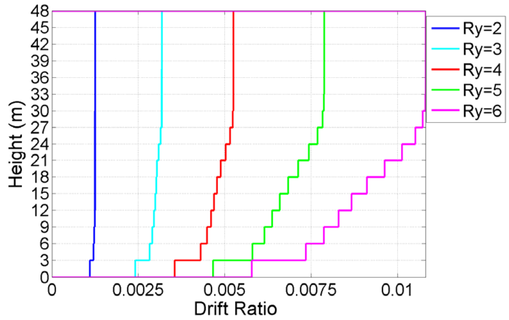

Figure B.342. Storey cumulative plastic drift ratio diagrams - sixteen storey wall R_y = 2.0, 3.0, 4.0, 5.0, 6.0

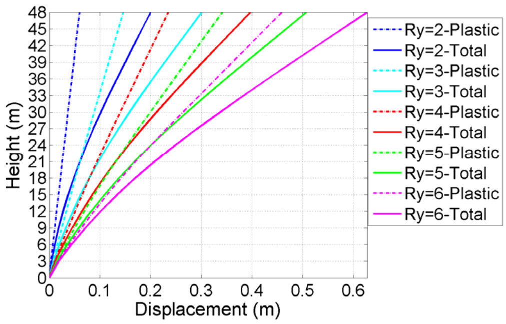

Figure B.340. Storey total displacement - plastic displacement comparison diagrams - sixteen storey wall R_y = 2.0, 3.0, 4.0, 5.0, 6.0

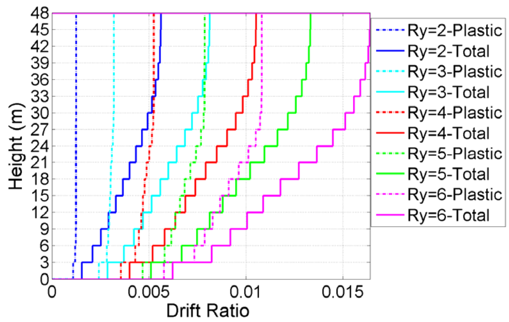

Figure B.343. Storey drift ratio - cumulative plastic drift ratio comparison diagrams - sixteen storey wall R_y = 2.0, 3.0, 4.0, 5.0, 6.0

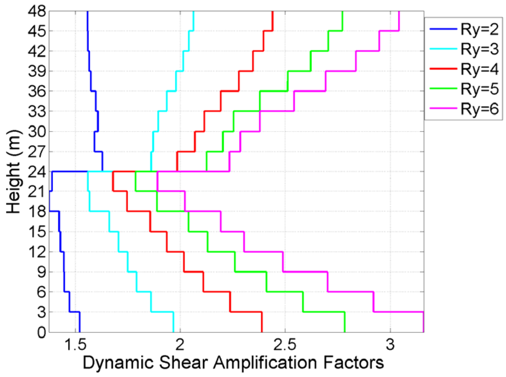

Figure B.344. Storey dynamic shear amplification factor diagrams - sixteen storey wall R_y = 2.0, 3.0, 4.0, 5.0, 6.0

REFERENCES

Blakeley, G., C. Cooney, .and M. Megget, 1975, "Seismic Shear Loading at Flexural Capacity in Cantilever Wall Structures", *Bulletin of the New Zealand National Society for Earthquake Engineering*, Vol. 8, No.4, pp. 278-290.

Celep, U.U., 2008, *Dynamic Shear Amplification in seismic Response of Structural Wall Systems*, PhD Dissertation, Boğaziçi University.

COSMOS, 1999-2007, *Cosmos Virtual Data Center*, http://db.cosmos-eq.org

CSI, 2007, "PERFORM 3D Non-linear Analysis and Performance Assessment of 3D Structures", Computers and Structures Inc., Berkeley, California, USA.

Derecho, A. and W. Corley, 1984, "Design Requirements for Structural Walls in Multistory Buildings", *Proceedings of Eighth World Conference on Earthquake Engineering*, San Francisco, California, July 1984, Vol. 5, pp. 541-548.

Eberhard, M. and M. Sözen, 1993, "Behavior Based Method to Determine Design Shear in Earthquake-Resistant Walls", *Journal of the Structural Division, American Society of Civil Engineers (ASCE)*, Vol. 119(2), pp. 619-640.

Eibl, J. and E. Keintzel, 1988, "Seismic Shear Forces in RC Cantilever Shear Walls", *Proceedings of Ninth World Conference on Earthquake Engineering*, Kyoto, Japan, 2 August-9 August 1991,Vol. VI, pp. VI/5-VI/10.

Filiatrault, A., D. D'Aronco and R. Tinawi, 1994, "Seismic Shear of Ductile Cantilever Walls: A Canadian Code Perspective", *Canadian Journal of Civil Engineering*, Vol. 21, pp. 363-376.

Gosh, S. and P. Markevicius, 1990, "Design of Earthquake Resistant Shearwalls to Prevent Shear Walls", *Proceedings of Fourth U.S. National Conference on Earthquake Engineering*, Palm Springs, California, 20 May-24 May 1990, Vol. 2, pp. 905-913.

Kabeyasawa, T., 1987, "Ultimate-state Design of Reinforced Concrete Wall-Frame Structures", *Proceedings of Pacific Conference on Earthquake Engineering*, Auckland, New Zealand, Vol. 4, pp. 431-440.

PEER, 2000, *PEER Strong Motion Database*, http://peer.berkeley.edu/smcat

Rutenberg, A. and E. Nsieri, 2006, "The Seismic Shear of Ductile Cantilever Wall Systems and the EC8 Provisions", *Bulletin of Earthquake Engineering*, Vol. 4, pp.1-21.

Senaviratna, K. and H. Krawinkler, 1994, "Strength and Displacement Demands for Seismic Design of Structural Walls", *Proceedings of Fifth U.S. National Conference on Earthquake Engineering*, Chicago, Illinois, 10 July-14 July 1994, Vol. II, pp.181-190.

Turkish Seismic Design Code, 2007, "Specification for Buildings to be Built on Seismic Areas", in Turkish, Ministry of Public Works and Settlement, Ankara, Turkey.

REFERENCES NOT CITED

Kappos, A.J. and P. Antoniadis, 2007, “A Contribution to Seismic Shear Design of R/C Walls in Dual Structures”, *Bulletin of Earthquake Engineering*, Vol. 5, pp. 443-466.